# DISSERTATION

Titel der Dissertation:

## Einfluss der Messgenauigkeit sowie der räumlichen und zeitlichen Variabilität des atmosphärischen Ozongehalts auf die Berechnung der erythemwirksamen solaren ultravioletten Strahlung

Angestrebter akademischer Grad

Doktor der technischen Naturwissenschaften (Dr. nat. tech.)


| | |
|---|---|
| Verfasser: | Mag. rer. nat. Alois W. SCHMALWIESER |
| Matrikelnummer: | 8803006 |
| Dissertationsgebiet (lt. Studienblatt) | Landwirtschaft |
| Betreuer: | A.Univ.-Prof. Dr. Ph. Weihs |


Münchendorf, August 2008

Für

Susanne, Veronika, Matthias

und

Esther

# Inhaltsverzeichnis

# Zusammenfassung

Der UV-Index ist die international anerkannte dimensionslose Einheit für die Intensität der solaren erythemwirksamen (Sonnenbrand) Strahlung. In Österreich werden im Sommer Werte um 8 erreicht, in alpinen Regionen können sie auch 10 übersteigen. Die weltweit höchsten Werte werden in den südamerikanischen Anden und im Himalaya gemessen und liegen im Bereich von 16. Aus den UV-Index Werten können die erforderlichen Lichtschutzfaktoren für Sonnenschutzmittel und andere Sonnenschutzmaßnahem abgeleitet werden. Aktuelle und prognostizierte Werte des UV-Index sowie Empfehlungen für Schutzmaßnahmen findet man in Österreich im Teletext von ORF2, in einigen Zeitungen und im Internet. Die Genauigkeit der veröffentlichten Werte ist für den Anwender besonders wichtig, da speziell aus Unterschätzungen zu geringe Sonnenschutzmaßnahmen abgeleitet werden.

Der wichtigste Eingangsparameter zur Berechnung der erythemwirksamen Strahlung bei wolkenlosem Himmel ist der Gesamtozongehalt der Atmosphäre. Deshalb wurde in dieser Dissertation untersucht mit welcher Genauigkeit der UV-Index und der für einen ganztägigen Aufenthalt im Freien notwendige Lichtschutzfaktor aufgrund der Unsicherheiten des Gesamtozongehalts berechnet werden können. Unsicherheiten beim Gesamtozongehalt resultieren aus der Messunsicherheit, sowie aus der räumlichen und der zeitlichen Variabilität der Ozonschicht, da der Gesamtozongehalt nicht an jedem Ort für jeden beliebigen Zeitpunkt zu Verfügung steht.

Im Rahmen dieser Dissertation wurde gezeigt, dass aufgrund der Messunsicherheit der UV-Index auf ±1 genau berechnet werden kann und der erforderliche Lichtschutzfaktor für die empfindlichen Hauttypen 1 und 2 auf ±3 genau berechnet werden kann.

Die hohe räumliche Auflösung von Satellitendaten führt nur zu geringen Unsicherheiten. Mit der in dieser Dissertation vorgestellten Interpolationsmethode welche die Topographie mit einbezieht werden die Unsicherheiten vernachlässigbar klein.

Im Gegensatz dazu führt die zeitliche Variabilität des Gesamtozongehalts bereits innerhalb der ersten 24 Stunden zu Unsicherheiten, die im Bereich jener liegen, die von der Messunsicherheit verursacht werden.

Damit konnte gezeigt werden, dass der UV-Index unabhängig von der geographischen Position auf ±1 genau berechnet werden kann. Der empfohlene Lichtschutzfaktor, der sich aus diesem Ergebnis ableiten lässt, sollte in Hinblick auf den UV-Strahlenschutz, um einen Wert von +3 erhöht veröffentlicht werden.

# Summary

The UV Index is the internationally agreed dimensionless unit for the intensity of the erythema (sunburn) effective UV radiation. In Austria UV Index values may be around 8 during summer, whereas in the alpine regions values around 10 can be reached. The highest values in the world are measured in the South American Andes and in the Himalaya. There, UV Index values can be around 16.
From the UV Index a sun protection factor for sun screens and other sun protection tools can be derived.
In Austria recently measured and forecasted values of the UV Index as well as recommendations for sun protection can be found via videotext on ORF2, in some newspapers and on some web pages in the internet.
The accuracy of the published values is crucial because an underestimation of the UV intensity leads to too low sun protection factors. The most important input parameter for the calculations of the erythemally effective radiation under clear skies is the total ozone content of the atmosphere.
Therefore this thesis aims to estimate the uncertainty of the calculated UV Index values and sun protection factors for a whole day stay outdoor which results from uncertainties in the total ozone content.
Uncertainties in the total ozone content result from the intrinsic measurement uncertainty as well as the spatial and temporal variability of the ozone layer because total ozone values are not available for each location and each time.
In the frame of this thesis it is shown that because of the measurement uncertainty the UV Index can be calculated with an accuracy of ±1.
For the most sensitive skin types 1 and 2 this results in an uncertainty in the sun protection factor of ±3.
The high spatial resolution of satellite data causes only low uncertainties. Using the interpolation method as introduced in this thesis which takes into account the topography the uncertainties become negligible.
Contrary to this, the temporal variability of the total ozone content within the first 24 hours leads to uncertainties with are on the order of the measurement uncertainties.
To sum up, in this thesis it was shown that the UV Index can be calculated with an accuracy of ±1 independent of location. The recommended sun protection factor should be published by adding a value of +3.

# 1. Einführende Bemerkungen

## 1.1 Motivation

Im Laufe der letzten 3 Jahrzehnte hat das Interesse der Öffentlichkeit an der solaren ultravioletten (UV) Exposition und den damit verbundenen Gesundheitsrisiken stetig zugenommen. Die Publizität des Antarktischen Ozonlochs sowie Studien die den Anstieg an Hautkrebserkrankungen dokumentierten haben dazu entscheidend beigetragen. In den industrialisierten Ländern resultiert die UV Exposition der Bevölkerung vor allem aus Freizeitaktivitäten sowie aus Urlauben in südlichen Destinationen (z.B, Thieden et al. 2004). Letztere hat in den industrialisierten Ländern vor allem im Winter zugenommen, zu einer Jahreszeit also in der die Haut nur an geringe UV Expositionen adaptiert ist (z.B. Schauberger et al. 1992). Daneben gibt es eine Reihe von Berufsgruppen die der Sonnenstrahlung im täglichen Arbeitsprozeß ausgesetzt sind und nur beschränkte Möglichkeiten haben ihre Exposition einzuschränken.

Für die Prävention von UV-bedingten Haut- und Augenschäden ist es deshalb notwendig die Bevölkerung über die zu erwartende Intensität der solaren UV Strahlung zu informieren und Empfehlungen für einen adequaten Sonnenschutz auszugeben. Ende der 1980er entstanden bereits die ersten solcher Informationssysteme. In Neuseeland wurde zum Beispiel ab 1987 die Sonnenbrandzeit veröffentlicht. Anfang der 1990er waren in gut einem Dutzend Ländern die verschiedensten Einheiten und Indizes wie Bestrahlungsstärke, Minimale Erythemdosis pro Stunde, Mittagsdosis oder ähnliche in Verwendung. In den USA gab es gleichzeitig drei verschiedene Indizes (WMO 1994). Beim WMO/WHO Meeting in Les Diablerets (WMO 1994) wurde versucht eine einheitliche, für die Öffentlichkeit leicht verständliche Größe zu finden, welche die (im bezug auf den Menschen relevante) schädigende Intensität der UV Strahlung beschreibt. Aus dieser Größe sollten auch Sonnenschutzmaßnahmen abgeleitet werden können. Dabei einigte man sich auf den UV-Index, wie er zu dieser Zeit in Kanada verwendet wurde.

Der UV-Index ist eine dimensionslose Zahl die proportional zur erythemwirksamen solaren UV Strahlung ist. Die erythemwirksame UV Strahlung errechnet sich durch Gewichtung der spektralen UV Strahlung mit der Empfindlichkeitskurve der menschlichen Haut für das Erythem nach CIE (CIE 1987) und anschließender Summierung über den UV-Bereich. Per Definition entsprechen gewichtete 0,025W/m$^2$ einem UV-Index von 1. In Österreich erreicht der UV-Index im Sommer Werte um 8. In den hochalpinen Regionen können Werte von 10 erreicht werden. Die weltweit höchsten UV-Index Werte findet man in den südamerikanischen Anden sowie im Karakorum. Diese können einen Wert von 16 übersteigen (Ren et al. 1999). Mittlerweile haben mehrere internationale Organisationen (ICNIRP 1995, CIE 2003, EU 2006) den UV-Index als Standard übernommen. Außerdem werden Sonnenschutzmaßnahmen in Abhängigkeit des UV-Index angegeben (WHO 2002, Vanicek et al. 2000). Deshalb ist die Genauigkeit der veröffentlichten UV-Index Werte besonders wichtig, da es speziell bei einer Unterschätzung der tatsächlichen Werte zu Gesundheitsschädigungen kommen kann.

Die höchste Effektivität für die Erzeugung eines Erythems hat die solare Strahlung im Längenwellenbereich von 280 nm bis 320 nm. Dieser Wellenlängenbereich wird sehr stark vom Gesamtozongehalt der Atmosphäre beeinflußt. Je höher der Gesamtozongehalt ist, desto mehr UV-Strahlung wird absorbiert und desto geringer ist die UV Strahlung die an die Erdoberfläche gelangt.

UV-Index Werte stammen entweder aus Messungen oder aus Modellrechnungen bzw. Prognosen. Messungen werden in flächendeckenden Netzwerken vor allem mit Breitbandmessgeräten durchgeführt. Deren spektrale Empfindlichkeit entspricht nicht exakt der Empfindlichkeitskurve des Erythems. Daher müssen die Messwerte in Abhängigkeit der das Sonnenspektrum verändernden Parameter korrigiert werden (z.B. Bodhaine et al. 1998). Dies sind vor allem die Sonnenhöhe und der Gesamtozongehalt.
Bei den Modellen zur Berechnung der UV Strahlung auf ihrem Weg durch die Atmosphäre haben Weiterentwicklungen mittlerweile zu Modellen geführt deren Genauigkeit nur mehr von der Güte der Eingangsparameter beeinflußt werden (z.B. Weihs und Webb 1996, Schwander et al. 1997, Kylling et al. 1998). Der wichtigste atmosphärische Eingangsparameter bei der Berechnung der erythemwirksamen UV Strahlung, des UV-Index, bei wolkenlosem Himmel ist der Gesamtozongehalt.

Der Gesamtozongehalt variiert mit Zeit und Ort. Allgemein zeigt der Gesamtozongehalt einen Halbjahres- (Ozonphotochemie) und einen Jahresverlauf (atmosphärische Dynamik). Je nach geographischer Position ist einer der beiden stärker ausgebildet als der andere. Die Verläufe werden noch von höher frequenten synoptischen Variationen, der klassischen Ozon-Wetter-Beziehung (Dobson and Harrison 1926, Dobson et al. 1946, Meetham 1937 und Reed 1950) überlagert. Nieder frequente Variationen resultieren aus der Quasi-Biennalen Oszillation (Funk and Garnham 1962), El Nino/El Nina (Hasebe 1980), dem 11-jährigen Sonnenzyklus (z.B. Haigh 1996 oder Zerefos et al.1997) sowie aus Vulkanausbrüchen (Angell 1997). Je nach geographischer Position sind diese Variationen unterschiedlich stark ausgeprägt. Damit ist die gesamte zeitliche Verlaufsform des Gesamtozons und ihre Amplitude stark ortsabhängig genauso wie der Jahresmittelwert (z.B. Zerefos et al. 1992, Bojkov und Fioletov 1995). Die globale Verteilung der Jahresmittelwerte ist von einem ausgeprägten Gradienten in meridionaler Richtung gekennzeichnet. Am Äquator ist der Gesamtozongehalt vergleichsweise niedrig und nimmt mit der Entfernung vom Äquator zu. Am höchsten ist der Gesamtozongehalt in mittleren und hohen Breiten. Zu den Polen hin, nehmen die Werte wieder ab. In Längenrichtung zeigt der Gesamtozongehalt keinen kontinuierlichen Gradienten über größere Entfernungen.

Ozonmeßwerte stehen nur mit einer begrenzten zeitlichen und räumlichen Auflösung zur Verfügung. Durch die zeitliche und räumliche Variabilität des Ozongehalts müssen bei Anwendungen die eine höhere Auflösung benötigen, durch Datenlücken oder bei Persistenzannahme in die Zukunft Unsicherheiten in Kauf genommen werden. Weiters ist der Gesamtozongehalt mit einer gewissen Messunsicherheit behaftet. Die Messunsicherheit hängt nicht nur von der Messtechnik, dem Gerätetyp ab, sondern auch von der Jahreszeit, der Sonnenhöhe und verschiedenen atmosphärischen Parametern. Diese Unsicherheiten beeinflussen die Genauigkeit der Berechnung der erythemwirksamen Strahlung.

Ziel dieser Dissertation ist es den Einfluß der Meßgenauigkeit sowie der räumlichen und zeitlichen Variabilität des Gesamtozons auf die Bestimmung der erythemwirksamen ultravioletten Strahlung zu analysieren.
Umgekehrt sollen mit Hilfe dieser Arbeit die Anforderungen an die zeitliche und räumliche Auflösung abgeleitet werden können, die für eine gewählte Genauigkeit des UV-Index oder von Sonnenschutzmaßnahmen (z.B. Lichtschutzfaktor) erforderlich sind.

## 1.2 Publikationen

Die hier vorliegende Dissertation fasst 4 Publikationen zusammen.

Drei dieser Publikationen wurden als „Trilogie“ in der offiziellen Zeitschrift der American Society of Phtotobiology and Photochemistry „Photochemistry and Photobiology“ veröffentlicht.
Impact factor: 2,172
Rating: 39/69 in der Kategorie Biophysics
152/263 in der Kategorie Biochemistry and Molecular Biology

Die vierte Publikation wurde in der offiziellen Zeitschrift der American Geophysical Union dem „Journal of Geophysical Research“ publiziert.
Impact factor: 2,953
Rating: 12/137 in der Kategorie Geosciences, Multidisciplinary

Die 4 Publikationen sind:

1. Alois W. Schmalwieser, Günther Schauberger, Thilo Erbertseder, Michal Janouch, Gerrie J. R. Coetzee and Philipp Weihs (2007) Sensitivity of Erythemally Effective UV Irradiance and Daily Exposure to Uncertainties in Measured Total Ozone. Photochemistry and Photobiology 83: 433–443.

2. Alois W. Schmalwieser, Günther Schauberger, Philip Weihs, Rene Stubi, Michal Janouch, Gerrie J.R. Coetzee, and Stana Simic (2003) Preprocessing of total ozone content as an input parameter to UV Index forecast calculations. J. Geophys. Res. Vol. 108 No. D6, 4176- 4189.

3. Alois W. Schmalwieser, Thilo Erbertseder, Günther Schauberger and Philipp Weihs (2008) Sensitivity of UV Erythemally Effective Irradiance and Daily Dose to Spatial Variability in Total Ozone. Photochemistry and Photobiology 84: 1149–1163.

4. Alois W. Schmalwieser, Thilo Erbertseder, Günther Schauberger, Philipp Weihs (2008) Sensitivity of Erythemally Effective UV Irradiance and Daily Exposure to Temporal Variability in Total Ozone. Photochemistry and Photobiology, accepted for publication

## 1.3 Überblick über die Publikationen

In der ersten Publikation wurde der Einfluß der Messungenauigkeit des Gesamtozongehalts untersucht. Für diese Untersuchungen wurden sowohl Messungen von Satelliten als auch Bodenmessungen verwendet. Die Satellitendaten stammen von den drei zurzeit im Orbit befindlichen Ozonsatelliten: EPTOMS der NASA (McPeters et al. 1998), GOME der ESA (WDC-RSAT 2006) und TOVS der NOAA (Neuendorfer 1996). Die Bodenmessdaten wurden mit den am weitest verbreitetsten Spektralphotometern vom Typ Brewer (Brewer 1973, Komryn 1980) und Dobson (Dobson 1931) gewonnen. Die Messunsicherheit wurde an drei verschiedenen Orten, Hradec Kralove (50°N, CZ), Nairobi (0°N, KEN) und Springbok (30°S, RSA) bestimmt. Für alle drei Orte standen Daten von den drei Satelliten zur Verfügung. In Hradec Kralove wird parallel mit einem Dobsons Typ Beck und einem Brewer Typ MKII gemessen. An den beiden anderen Messstationen ist jeweils ein Dobson Typ Beck in Verwendung. Mit den Ozondaten jedes Instruments wurden der Mittagswert der erythemwirksamen UV-Strahlung (in Einheiten des UV-Index, (UVI)) sowie die Tagesdosis (in Einheiten von UV-Index-Stunden (UVIh)) berechnet. Für den Hauttyp 1 (nach Fitzpatrick et al. 1974, WHO 2002) beträgt die minimale erythemale Dosis (MED) ungefähr 2,5 UVIh, für den Hauttyp 2 ungefähr 3,5 UVIh, für den Hauttyp 3 ungefähr 4,5 UVIh und für den Hauttyp 4 etwa 5,5 UVIh.

Als Strahlungsmodell (wie in allen vier Publikationen) zur Berechnung der erythemwirksamen Strahlung diente das am Institut für Medizinische Physik operationell für eine weltweite UV-Index Prognose eingesetzte Modell. Dieses basiert auf einer Approximation von spektralen Messdaten (Bener 1972) nach Diffey (1977) mit einigen Verbesserungen (Schmalwieser und Schauberger 2000). Dieses Modell wurde sowohl im Vergleich zu anderen UV-Modellen (Koepke et al. 1998) als auch im Vergleich zu Messwerten der erythemwirksamen Strahlung zu mittag (Schmalwieser et al. 2002) und der Tagesdosis (Schmalwieser et al. 2005) auf 4 verschiedenen Kontinenten evaluiert. Das Modell zeig keinen systematischen Fehler.

Im Rahmen der ersten Publikation wurde die, durch Verwendung der mit unterschiedlichen Instrumenten gemessene Gesamtozongehalt, auftretenden Differenzen der erythemwirksamen Strahlung analysiert; ebenso die zugrunde liegenden Differenzen zwischen den Ozonmesswerten der verschiedenen Instrumente.
Für die Analyse und Beschreibung der Unsicherheiten beziehungsweise der Differenzen wurden der Median (50%-Perzentil), das 95%-Perzentil und der Höchstwert (100%-Perzentil) der Differenzen für jeden Kalendermonat als Deskriptoren verwendet. Der Median drückt jenen Fehler aus, der an der Hälfte der Tage überschritten wird. Das monatliche 95%-Perzentil beschreibt jenen Fehler der an einem Tag pro Monat überschritten wird. Würde die Häufigkeitsverteilung einer Normalverteilung folgen, dann entspräche das 95%-Perzentil der zweifachen Standardabweichung. Das 100%-Perzentil gibt den größten Fehler an, der für den entsprechenden Monat über den gesamten Beobachtungszeitraum von 5 Jahren erreicht wurde. Die nachfolgenden Zusammenfassungen beziehen sich auf das 95%-Perzentil.

Bei der Analyse des Einflusses der Messungenauigkeit zeigte sich, dass man in mittleren Breiten (50°N) zwischen April und September mit einem Fehler bei der maximalen Intensität

von ±0,7 UVI rechnen muss und von ±5,0 UVIh bei der Tagesdosis. Die Unsicherheit bei der Tagesdosis zwischen April und September entspricht daher ±2 MED für Hautyp 1, was wiederum eine Unsicherheit beim Lichtschutzfaktor (LSF) von ±2 bedeutet.
In den Subtropen (30S°) und den Tropen beträgt der Fehler ±1,0 UVI beim Tageshöchstwert und ±7,5 UVIh bei der Tagesdosis. Dies bedeutet eine Unsicherheit von ±3 MED beziehungsweise ±3 LSF für den Hauttyp 1.
Damit konnte gezeigt werden, dass UV-Index Werte unabhängig von der geographischen Position aufgrund der Messungenauigkeit des Gesamtozongehalts auf ±1 UVI genau berechnet werden können, der erforderliche Lichtschutzfaktor für den Hauttyp 1 auf ±3 genau.

In der zweiten Publikation wurde unter anderem die Änderung des Gesamtozongehalts mit der Seehöhe untersucht. In der Troposphäre befinden sich etwa 10% des Gesamtozongehalts. Damit nimmt der Gesamtozongehalt in der Troposphäre mit zunehmender Seehöhe ab. Der gemessene Gesamtozongehalt ist daher nur für die Seehöhe der Messstation gültig. Soll der Gesamtozongehalt an einen anderen Ort übertragen werden so ist eine etwaige Höhendifferenz zu berücksichtigen. Satellitendaten liefern einen mittleren Gesamtozongehalt über einer bestimmten Fläche (Pixel). Der Messwert gilt daher für die mittlere Seehöhe dieses Pixels. Befindet sich ein Ort innerhalb dieses Pixels auf einer anderen Seehöhe, so ist der tatsächliche Gesamtozongehalt an diesem Ort vom Messwert des Satelliten verschieden.
Um diesen Höheneffekt zu quantifizieren wurden Messungen von hochalpinen Messstationen herangezogen (Hoher Sonnblick, 3106 m, Österreich, Arosa, 1840 m, Schweiz) und mit den entsprechenden Messwerten des EPTOMS-Satelliten verglichen. Beide Messstationen weisen einen deutlichen Höhenunterschied zur mittleren Seehöhe des jeweiligen Satelliten-Pixels auf. Wie auch aus der ersten Publikation hervorgeht gibt es eine prinzipielle Differenz zwischen den Messungen der verschiedenen Instrumente. Zwischen EPTOMS und Dobson-Instrumenten beträgt der mittlere Unterschied 1,4%. Um Ozonmessungen vergleichbar zu machen muss dieser Unterschied korrigiert werden.
Aus dem Unterschied zwischen den am Sonnblick gemessenen Werten des Gesamtozongehalts, den entsprechenden Satellitenmesswerten und der Seehöhendifferenz von 2184 m zwischen Satellitenpixel und dem Sonnblick Observatorium wurde eine Abnahme des Gesamtozongehalts von 1,13% je 1000 Höhenmeter errechnet. Dieser Wert erklärt auch die Differenz der Messwerte von EPTOMS und jenen des Dobson Instruments in Arosa und steht in Übereinstimmung mit einer Reihe von Arbeiten (z.B. Bodecker et al. 2001, Kneiszys et al. 1988, Krzyscin 2000) die jedoch andere Methoden zur Herleitung verwendet haben. Die Höhenkorrektur verbessert auch die Übereinstimmung der Werte für Nairobi und Springbok. Hradec Kralove liegt etwa auf der mittleren Seehöhe des Satelliten-Pixels. Unter Berücksichtigung der prinzipiellen Differenz und der Höhenkorrektur liegt der mittlere Unterschied zwischen Satellitendaten und Bodenmessungen für alle 5 Stationen deutlich unter 1,0%.

Wie bereits erwähnt stehen Werte des Gesamtozongehalts nur mit einer bestimmten räumlichen Auflösung zur Verfügung. Bei den verwendeten Satellitendaten beträgt die Auflösung etwa 1° x 1°. Distanzen zwischen Bodenstationen sind im allgemeinen wesentlich größer. Soll die UV-Strahlung zwischen zwei Gitterpunkten oder zwischen zwei Messstationen berechnet werden oder fehlen Daten im Gitter, dann führt die räumliche Variabilität des Ozongehalts zu Unsicherheiten.

## *1. EINFÜHRENDE BEMERKUNGEN*

In der dritten Publikation wird dem Einfluss der räumlichen Variabilität des Ozongehalts auf die Berechnungsgenauigkeit der erythemwirksamen UV Strahlung nachgegangen.
Dazu wurden Satelliten Daten von EPTOMS über den drei Bodenstationen Hradec Kralove, Nairobi und Springbok verwendet. Ausgehend von einem Gitterpunkt wurde die UV Strahlung für diesen Punkt mit dem entsprechenden Gesamtozongehalt berechnet.
Danach wurde für diesen Gitterpunkt der Reihe nach die erythemwirksame UV Strahlung mit dem Gesamtozongehalt der umliegenden Gitterpunkte berechnet und die Differenzen ermittelt. Diese Prozedur wurde für den Gesamtozongehalt mit einem Abstand bis zu 1000 km durchgeführt wobei die Analyse der Differenzen richtungsabhängig getrennt in die Kardinalrichtungen erfolgte.

Auf den ersten Blick könnte man annehmen dass die Unsicherheiten in der erythemwirksamen Strahlung die aus der räumlichen Variabilität des Gesamtozongehalts resultieren dort am höchsten sind, wo auch die erythemwirksame Strahlung die höchsten Werte erreicht. Die Ergebnisse der vorliegenden Arbeit zeigen jedoch, dass die Unsicherheiten in den mittleren Breiten höher sind als in den Tropen. Dies resultiert aus dem Fakt, das in den mittleren Breiten die Variabilität des Gesamtozons um soviel höher ist als in den Tropen, dass sie den Unterschied in der erythemwirksamen Strahlung mehr als kompensiert.

In den mittleren Breiten (50°N) muss man mit einer Unsicherheit von ±0,5 UVI rechnen wenn man den Gesamtozongehalt über eine Distanz von 200 km verwendet. Die Unsicherheiten aus Persistenzannahmen von 1000 km erreichen ±1,0 UVI. Dabei gibt es keinen signifikanten Unterschied zwischen Nord-Süd und Ost-West Richtung.
In den Subtropen kann der Gesamtozongehalt über 300 km konstant angenommen werden, ohne einen Fehler von ±0,5 UVI hervorzurufen. In Abhängigkeit der Richtung führen Distanzen von 600 km (in Breite) und 1000 km (in Länge) zu einer Unsicherheit von ±1,0 UVI.
In den Tropen werden Unsicherheiten von ±0,5 UVI ebenso durch 300 km hervorgerufen. Im Gegensatz zu den beiden anderen Orten bleibt die Unsicherheit die durch Entfernungen von 1000 km verursacht werden unter ±1,0 UVI.
Für die Tagesdosis resultiert in den mittleren Breiten (50°N) ein Fehler von ±2,5 UVIh aus Entfernungen von 100 km, ±5,0 UVIh von 300 km und ±7,5 UVIh aus Entfernungen zwischen 700 bis 800 km.
In den Subtropen (30°N) sind die Unsicherheiten in meridionaler Richtung ähnlich jener der mittleren Breiten. Distanzen von 100 km ergeben eine Unsicherheit von ±2,5 UVIh, 400 km von ±5,0 UVIh und 1000 km von ±7,5 UVIh. In longitudinaler Richtung bleiben die Unsicherheiten unter ±7,5 UVIh auch wenn eine räumliche Persistenz über 1000 km angenommen wird.
Am Äquator nimmt der Einfluss von Datenlücken im Gesamtozongehalt mit der Entfernung nur wenig zu. Eine Unsicherheit von ±2,5 UVIh resultiert aus einer Datenlücke von 200 km und bleibt unter ±5 UVIh auch wenn Lücken 1000 km groß sind.
Zusammenfassend kann man daher sagen, dass eine räumliche Auflösung von 100 km Berechnungen des UV Index mit einer Unsicherheit von weniger als ±0,5 UVI und ±2,5 UVIh (1 MED für Hauttyp 1) zuläßt.
Um Unsicherheiten aus der räumlichen Auflösung zu verringern wurde in der zweiten Publikation eine Methode für die Interpolation beziehungsweise für das Auffüllen räumlicher Datenlücken vorgestellt. Diese Methode basiert auf dem Kriging-Verfahren (Krige 1981)

unter Berücksichtigung der Höhendifferenz zu der mittleren Höhe des Satelliten Pixels der umliegenden Gitterpunkte. Die Validierung der Methode an den fünf Observatorien zeigte, dass sich die Unsicherheiten der interpolierten Werte nicht mehr von den Messunsicherheiten unterscheiden lassen.

Ozonmesswerte stehen nur mit einer bestimmten Verspätung beziehungsweise einer bestimmten zeitlichen Auflösung zur Verfügung. Die Verspätung von Satellitendaten hängt von der Zeit ab, die der Satellit für einen gesamten Überflug benötigt. EPTOMS und TOVS benötigen einen Tag, GOME drei Tage. Bei Bodenmessungen hängt die Verspätung von der Mess- und Ausgabehäufigkeit ab. In der zweiten Publikation wird das, für die Verwendung von Satellitendaten typische Zeitintervall von zwei Tagen untersucht (Verwendung von Satellitendaten für den kommenden Tag). Diese Untersuchung zeigt, dass die Unsicherheiten die von einer Verspätung von 2 Tagen hervorgerufen werden im tropischen und subtropischen Raum im Bereich der Messunsicherheit liegen. Das bedeutet auch, dass Ozonprognosen die auf einer Persistenzannahme von zwei Tagen (wie in Publikation 2) basieren, nicht durch komplizierte Prognose verbessert werden können. Außerhalb dieses Bereichs sind Verbesserungen möglich.

In der vierten Publikation wird der Einfluss der zeitlichen Variabilität auf die Berechnung der erythemwirksamen UV Strahlung für einen Zeitraum bis zu von Tagen untersucht.
Auf den ersten Blick könnte man bezüglich der zeitlichen Variabilität annehmen, dass die Unsicherheiten mit der Länge des Zeitintervalls zunehmen. Das überraschendste Ergebnis dieser Analyse ist, dass der Einfluss mit der Zeit nur wenig zunimmt. An allen untersuchten geographischen Positionen ist die Unsicherheit durch die zeitliche Variabilität in den ersten 24 Stunden am höchsten. Für die folgenden Tage ist der Anstieg nur mehr sehr gering oder überhaupt nicht mehr evident. Die klassische Ozon-Wetter-Beziehung ist nämlich der dominierende Faktor für die zeitliche Variabilität bis zu 15 Tagen. Das bedeutet, dass die Veränderungen von Tag-zu-Tag Variationen ausschlaggebend sind.
In den mittleren Breiten (50°N) wird während sechs Monaten des Jahres nach 24 Stunden eine Unsicherheit von ±0,5 UVI und ±2,5 UVIh überschritten. Eine Datenlücke von 5 Tagen kann im Juni und Juli zu einer Unsicherheit von ±1,0 UVI führen, aber für Lücken bis zu 15 Tagen bleibt die Unsicherheit unter ±1,2 UVI. Bei der Tagesdosis bleiben die Unsicherheiten unter ±10,0 UVIh, jedoch erzeugt eine Datenlücke von 1 Tag bereits ±5,0 UVIh.
In den Subtropen (30°S) muss innerhalb der ersten 24 Stunden das ganze Jahr über bereits mit einer Unsicherheit von mehr als ±0,5 UVI und ±2,5 UVIh in Rechnung gestellt werden. Unsicherheiten größer als ±1,0 UVI werden erst von Lücken von mehr als 7 Tagen im August und Oktober hervorgerufen. Die größte Unsicherheit bei der Tagesdosis erreicht ±7,5 UVIh (Lücke von 8 Tagen). Am Äquator können Datenlücken in Unsicherheiten zwischen ±0,3 UVI und ±0,8 UVI resultieren. Eine Abhängigkeit von der Jahreszeit gibt es hier nicht. Der entsprechende Wert für die Tagesdosis liegt zwischen ±2,5 UVIh und ±5,0 UVIh.
Zusammenfassend kann man sagen, dass die zeitliche Variabilität des Ozons und deren Auswirkung am höchsten in den mittleren Breiten sind. Eine Lücke von einem Tag erzeugt an allen drei Orten eine Unsicherheit von mehr als ±0,5 UVI und ±2,5 UVIh. Deshalb sollte allgemein eine Unsicherheit von ±1,0 UVI und ±5,0 UVIh angenommen werden. Für eine zeitliche Distanz von bis zu 15 Tagen bleiben die Unsicherheiten unter ±1,5 UVI und ±10,0 UVIh.

Vergleicht man die Ergebnisse aus der dritten Publikation mit jenen aus der ersten Publikation, so stellt man fest dass die untere Grenze des Fehlers der aus der Messungenauigkeit resultiert etwa gleich groß ist wie jener aus räumlichen Datenlücken in der Größe von 100 km bis 200 km. Die obere Grenze des Fehlers aus der Messungenauigkeit unterscheidet sich deutlich in Abhängigkeit von der geographischen Position. In mittleren Breiten (50°N) sind sie vergleichbar mit Entfernungen von 400 km bis 500 km, in den Subtropen mit Entfernungen von 500 km bis 600 km und am Äquator sind sie größer als Unsicherheiten die aus Entfernungen von 1000 km resultieren. Die Jahresverläufe der Unsicherheiten aus räumlicher Entfernung und Messunsicherheit unterscheiden sich allerdings teilweise deutlich.

Vergleicht man die Ergebnisse aus der vierten Publikation mit jenen aus der ersten Publikation, so kann man schlußfolgern dass in den mittleren Breiten der Einfluss von einer Verspätung von einem Tag größer ist als jener der Messunsicherheiten. Das gleiche gilt in den Subtropen. Am Äquator kann der Einfluss der Messunsicherheit auch etwas größer sein als die Veränderung von Tag zu Tag. Bis zu einem gewissen Grad trägt die Messungenauigkeit natürlich zu den Unsicherheiten die durch eine Verspätung von 24 Stunden entstehen bei. Allerdings gibt es offensichtliche Unterschiede zwischen den Jahresgängen der Messunsicherheit und der zeitlichen Variabilität. In den mittleren Breiten ist der Unterschied in den ersten Monate des Jahres am deutlichsten. In diesen Monaten ist der Fehler aus der zeitlichen Variabilität doppelt so hoch wie im Sommer. Hingegen ist der Jahresverlauf der Messunsicherheiten relativ glatt. Ähnlich verhält es sich in den Subtropen. Am Äquator zeigen die beiden Unsicherheiten keine erkennbaren Jahresverläufe.

Vergleicht man nun die Ergebnisse aus der dritten Publikation mit jenen aus der vierten Publikation so findet man, dass in den mittleren Breiten die Unsicherheiten aus einer Verspätung von einem Tag vergleichbar mit den Unsicherheiten sind, die durch räumliche Distanzen von 400 km bis 500 km verursacht werden. In den Subtropen ist eine Verspätung von einem Tag vergleichbar mit räumlichen Distanzen von 300 km bis 400 km. Am Äquator ist eine Verspätung von 1 Tag vergleichbar mit 200 km bis 300 km.

Aus diesen Sensitivitätsstudien bezüglich räumlicher und zeitlicher Unsicherheit sowie der Messunsicherheit zeigt sich, dass sich die Messunsicherheit merkbar auf die Genauigkeit auswirkt. Die Verwendung von Ozondaten des Vortags führen zu zusätzlichen Unsicherheiten. Diese liegen im Bereich der Messunsicherheiten. Der Einfluss einer räumlichen Auflösung von 100 km (entspricht der derzeit üblichen Auflösung von Satellitendaten von 1°x 1°) ist deutlich kleiner als die der beiden anderen.

## 1.4 Schlussfolgerung und Ausblick

Der UV-Index wurde international als Standardeinheit eingeführt um die Bevölkerung auf leicht verständliche Weise über die maximale Intensität der erythemwirksamen Bestrahlungsstärke zu informieren. Zweck des UV-Index ist es, eine mögliche Gesundheitsschädigung durch solare UV-Strahlung mittels entsprechender UV-Strahlenschutzmaßnahmen zu vermeiden. Vom UV-Index ausgehend können Maßnahmen für den persönlichen Sonnenschutz abgeleitet werden (WHO 2002, Vanicek et al. 2000). Deshalb ist es besonders wichtig die Genauigkeit der zu veröffentlichenden Werte zu kennen. Fehler, besonders Unterschätzungen, können zu einem zu geringem Sonnenschutz und damit zu Gesundheitsschädigungen führen. Damit würde der Zweck des UV-Index klar verfehlt werden. Andererseits möchte man aber auch keinen übertriebenen Sonnenschutz propagieren, da sonst die Akzeptanz solcher Maßnahmen sinken würde.

Ist eine bestimmte Genauigkeit des UV-Index erforderlich, so ist es notwendig die Eingangsparameter für die Berechnung des UV-Index daraufhin zu prüfen ob sie eine solche Genauigkeit erlauben bzw. wie groß die Unsicherheit der Eingangsparameter sein darf um die vorgewählte Genauigkeit zu gewährleisten. Dabei ist der Ozongehalt der Atmosphäre der wichtigste Eingangsparameter zur Berechnung bei wolkenlosem Himmel.
Zu diesem Zweck wurde im Rahmen dieser Dissertation die Empfindlichkeit der erythemwirksamen UV Strahlung auf Unsicherheiten von Ozonmessungen und auf jene die aus der räumlich und zeitlich begrenzten Auflösung resultieren untersucht. Andererseits lassen sich aus dieser Untersuchung aber auch die Bedingungen an die zeitliche und räumliche Auflösung sowie die Messgenauigkeit der Gesamtozonmessungen ableiten, die für eine bestimmte vorgewählte Genauigkeit notwendig sind.

Im Rahmen dieser Dissertation konnte gezeigt werden, dass aufgrund der Messgenauigkeit des Gesamtozongehalts die UV-Index Werte weltweit, unabhängig von der geographischen Lage auf ± 1,0 UVI bzw. ±7,5 UVIh genau berechnet werden können. Dies entspricht einer Unsicherheit des Lichtschutzfaktors von ± 3 für die empfindlichen Hauttypen 1 und 2. Das legt die Empfehlung nahe, den berechneten Lichtschutzfaktor um +3 erhöht auszugeben.
Der Einfluss der räumlichen Auflösung in geographischer Breite ist etwas größer als in Länge. Ein Fehler von ±1,0 UVI wird bei einer Persistenzannahme über 600 km bis 700 km in Breite und über 900 km bis 1000 km in Länge verursacht. Auch hier spielt die geographische Position keine Rolle. Der Einfluss in vertikaler Richtung beträgt nur 1,1 % pro 1000m Höhendifferenz und kann außerdem sehr gut korrigiert werden (<0,1 UVI und <1,0 UVIh).
Aus der Zeitlichen Variabilitätsanalyse geht hervor dass mit einem Fehler von ±1,0 UVI gerechnet werden muss wenn der verwendete Gesamtozongehalt 2 bis 3 Tage alt ist.

Die Addition der Unsicherheiten wurde in dieser Dissertation nicht im Detail untersucht. Im allgemeinen kann die gesamte Unsicherheit gemäß der Fehlerfortpflanzung berechnet werden. Die gesamte Unsicherheit dürfte aber etwas geringer ausfallen, da die einzelnen Unsicherheiten nicht völlig unabhängig voneinander sind.

## 1.5 Literatur


Angell J.K. (1997) Estimated impacts of Agung, El Chichon, and Pinatubo volcanic eruptions on global and regional total ozone after adjustment for the QBO. *Geophys. Res. Lett.* **24**, 647-650.

Bener P. (1972) *Approximate values of intensity of natural radiation for different amounts of atmospheric ozone*. Eur. Res. Off., US Army, London, United Kingdom.

Bodecker G. E., J. C. Scot, K. Kreher and R. L. McKenzie (2001) Global ozone trends in potential vorticity coordinates using TOMS and GOME intercompared against the Dobson network: 1978– 1998. *J. Geophys. Res.* **106**, 23029– 23042.

Bodhaine B. A., E. G. Ellsworth, R. L. McKenzie and P. V. Johnston (1998) Calibrating broadband UV instruments: Ozone and solar zenith angle dependence. *J. Atmos. Oceanic Technol.* **15**, 916– 926.

Bojkov R. D. and V.E. Fioletov (1995) Estimating the global ozone characteristics during the last 30 years. *J. Geophys. Res.* **100**, 16537–16551.

Brewer A. W. (1973) A replacement for the Dobson spectrophotometer? *Pure Appl. Geophys.* **106–109**, 919.

CIE (Commission Internationale de l'Eclairage) (1987) A reference action spectrum for ultraviolet induced erythema in human skin. *CIE J.* **6**, 17–22.

CIE (Commission Internationale de l'Eclairage) (2003) *International Standard Global Solar UV Index*. CIE Standard S 013:2003. CIE, Vienna, Austria.

Diffey B.L. (1977) The calculation of the spectral distribution of natural ultraviolet radiation under clear day conditions. *Phys. Med. Biol.* **22**, 309-316.

DLR (Deutsches Zentrum für Luft- und Raumfahrt) (1996) *Product Specification Document of the GOME Data Processor*. ER-PS-DLR-GO-0016. Deutsches Fernerkundungszentrum, Oberpfaffenhofen, Germany.

Dobson G. M. B. and D.N. Harrison (1926) Measurements of the amount of ozone in the earth's atmosphere and its relation to other geophysical conditions. *Proc. Roy. Soc. Meteorol. London* **A 110**, 660–693.

Dobson G. M. B. (1931) A photoelectric spectrophotometer for measuring the amount of atmospheric ozone. *Proc. R. Soc.* **93**, 324.

Dobson G.M.B., A.W. Brewer and B.M. Cwilong (1946) Meteorology of the lower stratosphere. *Proc. Roy. Meteorol. Soc. London* **A185**, 144-175.

EU (European Union) (2006) *prEN 14255-3:2006, Measurements and assessment of personal exposure toincoherent optical radiation – Part 3: UV-Radiation emitted by the sun*. European Pre-Standard, Brussels, Belgium.

Fitzpatrick T.B., M.A. Pathak, L.C. Harber, M. Seiji and A. Kukita (1974) *Sunlight and man*. University of Tokyo Press, Tokyo, Japan.

Funk J.P. and G.L. Garnham (1962) Australian ozone observations and a suggested 24-month cycle. *Tellus* **14**, 378-382.

Hasebe F. (1980) A global analysis of the fluctuation of total ozone. II Non-stationary annual oscillation, quasi-biennial oscillation and long-term variations in total ozone. *J. Meteorol. Soc. Jpn.* **58**, 104-110.

Haigh J. (1996) The impact of solar variability on climate. *Science* **272**, 981–984.

ICNIRP (International Commission on Non-Ionizing Radiation Protection) (1995) *Global Solar UV-Index—WHO/WMO/ INCIRP recommendation*. INCIRP Publication No. 1/95. ICNIRP, Oberschleissheim, Germany.

Kneiszys F. X., G. P. Anderson, E. P. Sheetle, W. O. Gallery, L. W. Abreu, J. E. Selby, J. H. Chetwynd and S. A. Clough (1988) *User's Guide to LOWTRAN 7*. AFGL Tech. Rep., AFGL-TR-88-0177, Air Force Geophys. Lab., Bedford, Mass., USA.

Koepke P., A. Bais, D. Balis, M. Buchwitz, H. de Backer, X. de Cabo, P. Eckert, P. Eriksen, D. Gillotay, T. Koskela, B. Lapeta, Z. Litynska, J. Lorente, B. Mayer, A. Renaud, A. Ruggaber, G. Schauberger, G. Seckmeyer, P. Seifert, A. Schmalwieser, H. Schwander, K. Vanicek and M. Weber (1998) Comparison of models used for UV index calculations. *Photochem. Photobiol.* **67**, 657-662.

Komhyr W. D. (1980) *Operations Handbook—Ozone Observations with a Dobson Spectrophotometer*. WMO Global Ozone Research and Monitoring Project, Report 6. World Meteorological Organization, Geneva, Switzerland.

Krige D. G. (1981) Lognormal-de Wijsian Geostatistics for Ore Evaluation, *South African Institute of Mining and Metallurgy Monograph Series: Geostatistics*, **1**, pp. 51.

Krzyscin J. W. (2000), Impact of the ozone profile on the surface UV radiation: Analysis of the Umkehr and UV measurements at Belsk (52°N, 21°E), Poland. *J. Geophys. Res.* **105**, 5009–5015.

Kylling A., A. F. Bais, M. Blumthaler, J. Schreder, C. S. Zerefos and E. Kosmidis (1998) Effect of aerosols on solar UV irradiance during photochemical activity and solar ultraviolet radiation campaign. *J. Geophys. Res.* **103**, 26051–26060.

McPeters R. D., P. K. Bhartia, A. J. Krueger, J. R. Herman, C. G. Wellemeyer, C. J. Seftor, G. Jaross, O. Torres, L. Moy, G. Labow, W. Byerly, S. L. Taylor, T. Swissler and R. P. Cbula (1998) *Earth Probe Total Ozone Mapping Spectrometer (TOMS) Data Products User's Guide*. NASA Reference Publication, Greenbelt, MD.

Meetham A.R. (1937) The correlation of the amount of ozone with other characteristics of the atmosphere. *Quart. J. Roy. Meteorol. Soc.* **63**, 289-307.

Neuendorffer A. C. (1996) Ozone monitoring with TIROS-N operational vertical sounder. *J. Geophys. Res.* **101**, 18807–18827.

Reed R. J. (1950) The role of vertical motions in ozone-weather relationship. *J. Meteor.* **7**, 263–267.

Ren P. B. C., Y. Gjessing and F. Sigernes (1999) Measurements of solar ultra violet radiation on the Tibetan Plateau and comparisons with discrete ordinate method simulations. *J. Atmos. Sol. Terr. Phys.* **61**, 425–446.

Saxebøl G. (2000) UVH—A proposal for a practical unit for biological effective dose for ultraviolet radiation exposure. *Radiat. Prot. Dosimetry* **88**, 261.

Schauberger G., G. Keck and A. Cabaj (1992) Trend analysis of solar ultraviolet exposure of the Austrian population caused by holiday patterns since 1969. *Photodermatol. Photoimmunol. Photomed.* **9**, 72–77.

Schmalwieser A.W. and G. Schauberger (2000) Validation of the Austrian forecast model for solar, biologically-effective ultraviolet radiation - UV Index for Vienna, Austria. *J. Geophys. Res.* **105**, 26661-26668.

Schmalwieser A.W., G. Schauberger, M. Januch, M. Nunez, T. Koskela, D. Berger, G. Karamanian, P. Prosek and K. Laska (2002) Global validation of a forecast model for irradiance of the solar, erythemally effective UV radiation. *Optical Engineering* **40**, 3040-3050.

Schmalwieser A.W., G. Schauberger, M. Janouch, M. Nunez, T. Koskela, D. Berger and G. Karamanian (2005) Global Forecast Model to Predict the Daily Dose of the Solar Erythemally Effective UV Radiation. *Photochem. Photobiol.* **81**, 154-162.

Schwander H., P. Koepke and A. Ruggaber (1997) Uncertainties in modeled UV irradiances due to the limited accuracy and availability of input data. *J. Geophys. Res.* **102**, 9419–9429.

Thieden E., P.A. Philipsen, J. Sandby-Moller, J. Heydenreich and H.C. Wulf (2004) Proportion of Lifetime UV Dose Received by Children, Teenagers and Adults Based on Time-Stamped Personal Dosimetry. *The Journal of Investigative Dermatology* **123**, 1147-1150.

Vanicek K., Z. Lytinska, T. Frei and A. Schmalwieser (2000) *UV Index for the Public*. Publication of the European Communities, Brussels, Belgium.

WDC-RSAT (World Data Center for Remote Sensing of the Atmosphere) (2006) *The Global Ozone Monitoring Experiment, Data and Products*. Available at: htp://wdc.dlr.de/sensors/gome. Accessed on 16 February 2007.

Weihs P. and A. R. Webb (1996) Comparison of green and lowtran radiation schemes with a discrete ordinate method UV model. *Photochem. Photobiol.* **64**, 642–648.

WHO (World Health Organisation) (2002) *Global Solar UV Index: A Practical User Guide*. WHO, Geneva, Switzerland.

WMO (World Meteorological Organisation) (1994) *Report of the WMO Meeting of Experts on Standardization of UV Indices and their Dissemination to the Public*. WMO Rep. No. 95, Geneva, Switzerland.

Zerefos C.S., K. Tourpali, B.R. Bojkov, D.S. Balis, B. Rognerud and I.S.A. Isaksen (1997) Solar activity-total column ozone relationships: Observatons and model studies with heterogeneous chemistry. *J. Geophys. Res.* **102**, 1561-1569.

Zerefos C. S., A. Bais, I.C. Ziomas and B.R. Bojkov (1992) One the relative importance of Quasi-Biennial Oscillation and El Nino Southern Oscillation in the revised Dobson Total Ozone records. *J. Geophys. Res.* ***100***, 10135–10144.

# 2 Publikationen

## 2.1 Publikation 1:

### Sensitivity of Erythemally Effective UV Irradiance and Daily Exposure to Uncertainties in Measured Total Ozone

Alois W. Schmalwieser, Günther Schauberger, Thilo Erbertseder, Michal Janouch, Gerrie J. R. Coetzee and Philipp Weihs,

Photochemistry and Photobiology, 83: 433–443 (2007)

Photochemistry and Photobiology, 2007, 83: 433–443

# Sensitivity of Erythemally Effective UV Irradiance and Daily Exposure to Uncertainties in Measured Total Ozone

**Alois W. Schmalwieser*[1], Günther Schauberger[1], Thilo Erbertseder[2], Michal Janouch[3], Gerrie J. R. Coetzee[4] and Philipp Weihs[5]**

[1]Institute of Medical Physics and Biostatistics, University of Veterinary Medicine, Vienna, Austria
[2]Solar and Ozone Observatory Hradec Kralove, Czech Hydrometeorological Institute, Czech Republic
[3]Deutsches Fernerkundungsdatenzentrum, Deutsches Zentrum für Luft- und Raumfahrt, Oberpfaffenhofen, Germany
[4]South African Weather Service, Pretoria, South Africa
[5]Institute of Meteorology, University of Natural Resources and Applied Life Sciences, Vienna, Austria

**Received 16 June 2006; accepted 13 November 2006; published online 20 November 2006; DOI: 10.1562/2006-06-16-RA-931**

## ABSTRACT

**In this study the sensitivity of the erythemally effective radiation to uncertainties in operationally measured total ozone content of the atmosphere (TOC) was estimated. For this, daily operational TOC measurements from different instruments were applied covering the period from 1997 to 1999. Measurements were gained from space by Earth Probe Satellite, Earth Remote Sensing satellite/Global Ozone Monitoring Experiment and Operational Vertical Sounder and from the ground by Dobson and Brewer spectrophotometers for the locations of Hradec Kralove (Czech Republic, 50°N), Nairobi (Kenya, 1°S) and Springbok (Republic of South Africa, 30°S). The values were used as input parameter to model calculations of erythemally effective irradiance and daily radiant exposure. The differences due to the use of TOC from different sources were analyzed with respect to the Ultraviolet Index (UVI). The UVI was introduced as a tool for sun protection and health care. Therefore, it is of special importance to know the restriction of accuracy. As a tool of health care, the maximum uncertainties are of interest and are described in using the 95%-percentile and the maximum differences. This study shows that differences, *i.e.* uncertainties (95%-percentile) are in the order of 1 UVI. Independently on the location, however, extreme differences may overstep 3 UVI. For the daily dose the 95%-percentile is around 7.5 UVI hours (UVIh) but differences higher than 20 UVIh were also found.**

## INTRODUCTION

Stratospheric ozone shields the biosphere from a large part of the solar ultraviolet (UV) radiation by absorbing mainly at wavelengths below 320 nm. It is therefore an essential parameter whenever the photobiological effectiveness of solar UV radiation is studied. The photobiological effectiveness of UV radiation varies from effect to effect, depending strongly on the wavelength and described by the corresponding action spectrum. The higher the action spectrum in the UV-B, the higher is the sensitivity to the total ozone content of the atmosphere (TOC) and to its uncertainties.

The TOC values originate from measurements either from the ground or from space. Spectrophotometers of type Dobson (1,2), Brewer (3), M83/M124 (4,5), the SAOZ (Système d'Analyse par Observation Zénitale) (6), the UV–visible spectrometer (7), the handheld MicrotopsII (8), the UV Multifilter Rotating Shadow Band Radiometer (9,10) and others were designed for terrestrial observations.

For the period covered by the study, three different space-based instruments delivered daily data of TOC on a global scale: the Total Ozone Mapping Spectrometer (TOMS) aboard NASA's Earth Probe Satellite (EPTOMS) (11), the Global Ozone Monitoring Experiment (GOME) aboard European Space Agency's (ESA's) Earth Remote Sensing satellite (ERS-2) (12,13) and the Television Infrared and Observational Satellite (TIROS-N) Operational Vertical Sounder (TOVS) series of instruments (14).

During the past, several studies were undertaken to estimate the accuracy of TOC measurements. The best known, because extensively examined and intercompared, are the properties of measurements gained by the Brewer and the Dobson spectrophotometers (15). For all other instruments many studies are available too. Extensive work was carried out on data from TOMS by Fioletev *et al.* (16) validating data from Nimbus7 with respect to Dobson, Brewer and M83/M124 instruments. Measurements from all four TOMS instruments and GOME were compared by Bodecker *et al.* (17) to measurements from the Dobson Network. Lambert *et al.* (18) examined measurements from EPTOMS, the Advanced Earth Orbiting Satellite (ADEOS) and GOME using data from the Network for Detection of Stratospheric Change including SAOZ, Dobson, Brewer and UV–vis spectrometer. While up to 1997 TOMS and TOVS already had a long tradition starting from 1978, GOME was quite a new instrument. Concerning the ozone retrieval, a great deal of experience was gained in the meantime and the algorithm was significantly improved. In a recent study, Lambert and Balis (19) concluded that TOC of GOME version 4.0 reaches the accuracy of ground-based measurements of well-calibrated Dobson and Brewer instruments (13). Many other intercomparison examples can be found in the literature. Only for TOC from TOVS, intensive comparisons are still

*Corresponding author email: alois.schmalwieser@vu-wien.ac.at (Alois W. Schmalwieser)

missing. From all these studies it became evident that differences and uncertainties may depend on solar zenith angle, geographical position, altitude, cloud properties, cloud coverage, aerosol content and type and ozone vertical profiles as well as the intrinsic design of the instrument.

In general, the biologically effective UV radiation can be estimated either by weighting a measured solar spectrum, by converting measurements from broadband meter or by weighting a modeled spectrum. In many cases modeled values are necessary. Progress in UV model development has led to models, in which the main source of inaccuracy of model calculations (under clear sky) is no more the mathematical method used to solve the radiative transfer equations, but it is the inaccuracy of the input data, *i.e.* all the variables affecting UV such as ozone, single scattering albedo, aerosols and ground albedo. Uncertainties in model outputs in dependence on several variables were investigated in detail in the past by Schwander *et al.* (20), Weihs and Webb (21) and others. The TOC is the main input parameter for clear sky.

The UV Index (UVI) was jointly defined in 1995 by the International Commission on Nonionizing Radiation Protection (ICNIRP), the World Health Organization (WHO) and the World Meteorological Organization (WMO) (22) as a measure of the erythemally effective irradiance. The UVI is the internationally agreed (23,24) base for sun protection, risk assessment and health care and widely used in public information campaigns (25). Therefore, it is important to know the accuracy of promoted daily values.

In this paper, we focus on the sensitivity of the erythemally effective UV radiation, the UVI, to the uncertainties in measured TOC. It is not arbitrary which TOC measuring device is the golden standard. For this, measurements of TOC from the ground (Brewer and Dobson spectrophotometer) and from space borne instruments (EPTOMS, GOME, TOVS) for three different locations (50°N, 1°S and 30°S) are used to estimate the influence of measurement uncertainties to the erythemally effective UV radiation.

The sites were selected to examine the influence in dependence of latitude, especially solar height and the length of the day. Additionally, the ozone layer exhibits different behavior over each station. In the tropics, the ozone layer is mainly influenced by photochemistry. The annual mean value of TOC is rather low as well as the fluctuations within the year. In the subtropics, photochemical processes are still obvious but atmospheric dynamics get influenced. TOC values are higher and the annual course shows a higher amplitude. At higher latitudes the main influence is atmospheric dynamics. The TOC mean is the highest and TOC exhibits a strong annual course with high fluctuations.

The considered time series of TOC consist of data from the operational near-real-time data processing systems, which deliver the data within a few hours after the satellites overpass. This kind of data was gathered for the period January 1997 to December 1999. The data are not taken from reanalysis or improved algorithms.

The limitation in accuracy is estimated for the daily maximum irradiance (expressed in units of UVI) and the daily radiant exposure or daily dose. The latter is expressed in units of UVI hours (UVIh) following the suggestions of Saxebøl (26). As UVI is a tool of radiation protection, less attention has to be paid on a mean accuracy than on the highest inaccuracies. High errors in the UVI, especially an underestimation may lead to sun burn of applicants, *i.e.* an acute injury as well as a risk enhancement for developing skin cancer later on in life.

## MATERIALS AND METHODS

The different TOC data sets are applied separately as an input to model calculations. The resulting differences in calculated irradiance and daily dose are used as a proxy for the limitation in the accuracy in the erythemally effective UV radiation. To explain the resulting differences in irradiance and daily dose, the initial TOC values are intercompared too.

*Data of total ozone*. The first data set of TOC is derived from NASA's EPTOMS (11) which has provided data since July 1996. TOMS, on board the Earth Probe Satellite, measures incident solar radiation and backscattered UV sunlight at six near-UV wavelengths. Total ozone is retrieved from these measured spectra. The single retrievals of TOC are then gathered each day and gridded globally. In this study, we used these daily gridded data sets.

The second data set results from the GOME instrument, which has provided trace gas measurements since 1995 aboard the ESA's ERS-2 (12,27). The instrument has a broad spectral coverage (240–790 nm) which is coupled with a high spectral resolution (0.2–0.4 nm). TOC is retrieved from backscattered solar radiation by Differential Optical Absorption Spectroscopy (28). As global coverage is achieved after 3 days only, daily gridded TOC values are gained by using a spectral statistical interpolation method (29,30).

The third satellite-based data set of TOC is derived from TOVS. The TIROS-N TOVS series of instruments have flown aboard the National Oceanic and Atmospheric Administration's (NOAA) operational meteorological satellites since 1978 (14). They were primarily designed as a source of meteorological data (notably temperature and moisture). Information on the TOC is provided by exploiting the 9.7 μm channel which was originally included to remove ozone effects from the temperature sounding channels. TOVS measures mostly the lower stratospheric ozone and is quite insensitive to middle- and upper-stratospheric ozone. In contrast to TOMS and GOME, TOVS can provide data also during polar night.

The considered time series of TOC consist of data from the operational near-real-time data processing systems, which deliver the data within a few hours after the satellites overpass. Data of this kind were gathered for the period January 1997 to December 1999. The data were not taken from reanalysis or improved algorithms.

Measurements from the ground are performed at the Solar and Ozone Observatory in Hradec Kralove (50.183°N, 15.833°E, 285 m asl), Czech Republic. TOC measurements have a long tradition at this observatory dating back to the 1960s. The instruments are the Brewer Spectrometer MKIV No. 98 and the Dobson Spectrophotometer Beck No. 74 (15).

Springbok (Republic of South Africa, 29.7°S, 17.9°E, 1006 m asl) is the southernmost station of our sample. Data were collected by the South African Weather Service and originated from measurements of a Dobson spectrophotometer (Beck No. 123).

For Nairobi (Kenya, 1.3°S, 36.8°E, 1710 m asl) the measurements of a Dobson spectrophotometer (Beck No. 18), performed at the nearby observatory, are taken. This data set was provided by the World Ozone and Ultraviolet Data Centre (WOUDC). For analysis, only three complete years are taken (1997–1999). No newer data for Nairobi are delivered to the WOUDC and no other equatorial site with a similar longitude as Hradec Kralove and Springbok is on duty. To enable comparability, we have restricted all other data sets to this period.

All these ground-based TOC values are given as daily mean resulting from several measurements during a day. As we use the gridded data from the satellites, they are interpolated for the respective geographical location of the stations from the surrounding grid points.

*Limitations of accuracy in estimations of the erythemally effective UV radiation*. To quantify the influence of uncertainties in measured TOC to calculations of the erythemally effective radiation, model calculations were performed with a fast spectral UV radiation model. This model was developed at the Institute of Medical Physics and Biostatistics, University of Veterinary Medicine, Vienna, in 1995 (31) following a suggestion by Diffey (32) with several improvements. The

radiation model calculates the spectral irradiance at 17 discrete wavelengths between 297.5 and 400 nm with higher resolution in the UV-B than in the UV-A. The calculations based on the database from Bener (33) was gained from spectral measurements made over several years at Davos (46°48′N, 9°49′E, 1590 m asl). A detailed description of the model can be found in Schmalwieser *et al.* (34). The erythemally effective irradiance is gained by using the Commission Internationale de l'Eclairage (CIE) action spectrum of the erythema (35) for weighting followed by the integration over the whole spectral range. The erythemally effective irradiance is expressed in units of the UVI as defined by WHO, WMO, ICNIRP and CIE (22–24) and widely used in monitoring and forecasting (25). The UVI is gained numerically by multiplying the erythemally effective irradiance given in $W_{eff}$ $m^{-2}$ by 40; 1 UVI corresponds to 0.025 W $m^{-2}$. The erythemally effective daily dose is gained by integrating the daily course of the effective irradiance from sunrise to sunset. For the daily dose, a UVIh is used as a unit, following the suggestion of Saxebol (26) and as applied by Schmalwieser *et al.* (36). A received dose of 1 UVIh is equal to 90 J $m^{-2}$ or 0.9 SED (standard erythemal dose) (37).

The model was validated in the past by a comparison with other models (31,38,39) as well as by a comparison with measurements made at four continents for irradiance (34) and daily dose (36). These validations have shown that the model has no systemic bias corresponding to solar height and total ozone.

For this work, an aerosol free atmosphere and cloud free sky was assumed to point out the maximum influence as it is important for radiation protection. Therefore, the amount of input parameters is restricted to date, time, geographical position, altitude and TOC.

Using TOC data from each instrument separately as input parameter, the maximum daily irradiance (solar noon) and daily doses are calculated for each day. The statistical analysis of differences in the outcome provides the limitation of accuracy. Analysis of these differences is carried out using the mean bias, the median (50% percentile) of absolute amount of differences (p50), the 95% percentile of absolute differences (p95) and the maximum absolute differences (p100). On a monthly scale, p95 gives the uncertainty which is overstepped on one day per month.

We further compare the different data sets of TOC at each location. The comparison is made for the whole period of collected data in respect to annual, monthly and daily differences to characterize the TOC and uncertainties at the respective locations. The differences in TOC between the measurements of the different instruments are studied using the mean bias, p95 and p100.

## RESULTS

### Hradec Kralove (50°N)

*Total ozone measurements.* Total ozone content values of the atmosphere over Hradec Kralove show high seasonal variability (Fig. 1a) ranging from more than 500 DU down to below 200 DU. The highest values of TOC over Hradec Kralove are measured from January to May. Monthly mean values are the highest from February to June and the lowest between October and January. The variability of TOC shows a seasonal pattern as well, with high values from December to March. During this period TOC may vary within a month by more than 200 DU.

The extreme low TOC values are caused by ozone miniholes which appear periodically during the winter at middle and higher latitudes (40) and may raise biological effective radiation significantly (41). Two extremes examples of this event were found in the data sets. The first one showed its minimum value on 1 January 1998 where values from the Dobson, Brewer and EPTOMS lie between 194 DU and 208 DU. GOME and TOVS deliver, on the other hand, values of 234 DU and 245 DU for this date which were also the lowest values in 1998, but significantly higher. The second extreme ozone minihole within the data sets was found around 1

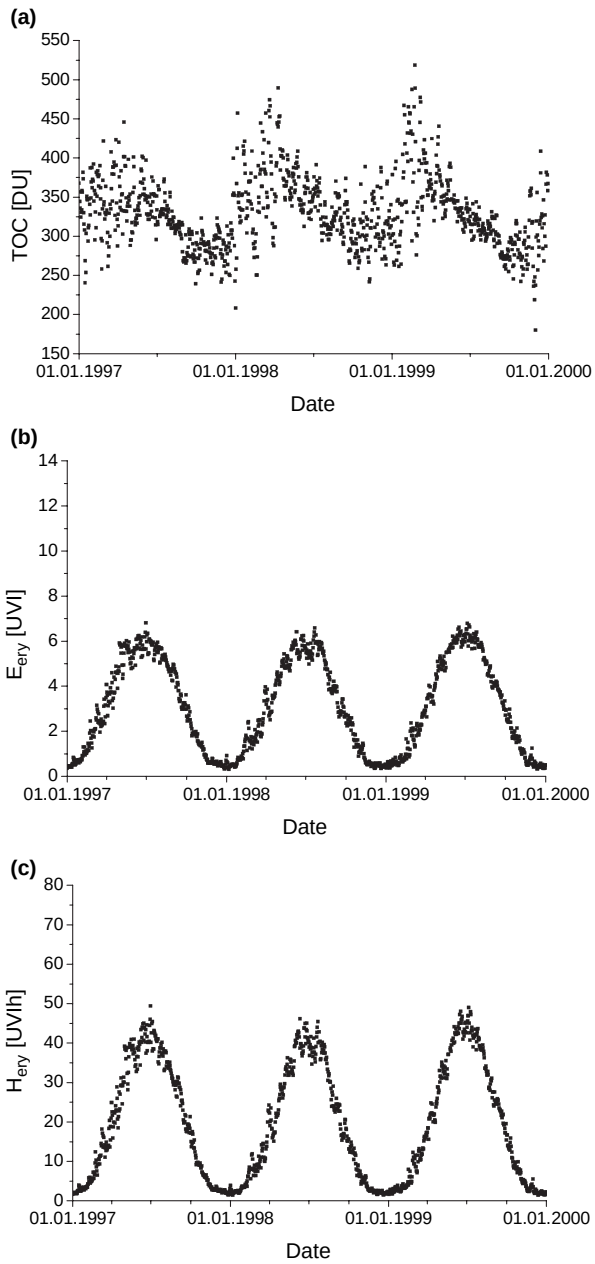


**Figure 1.** (a) Measurements of TOC taken with the Dobson spectrophotometer at Hradec Kralove (50.2°N, 15.8°E), (b) modeled erythemally effective daily maximum irradiance ($E_{ery}$) and (c) daily dose ($H_{ery}$) for clear skies.

December 1999. This event was recorded by Brewer (180 DU), EPTOMS (200 DU), GOME (201 DU) and Dobson (212 DU). Similar to the first event, TOVS delivered a value of 240 DU for this date.

The mean TOC values over the whole period (1997–1999), calculated for each instrument, are close to each other. Brewer, Dobson, EPTOMS and GOME agree within 1%, delivering 329, 328, 331 and 327 DU, respectively. For TOVS a value of 340 DU was obtained, which is 3% higher than the values calculated for the others.

These low differences do not hold when one considers shorter periods. The differences depend on the time of the year (Fig. 2a). The mean bias between TOVS and all other

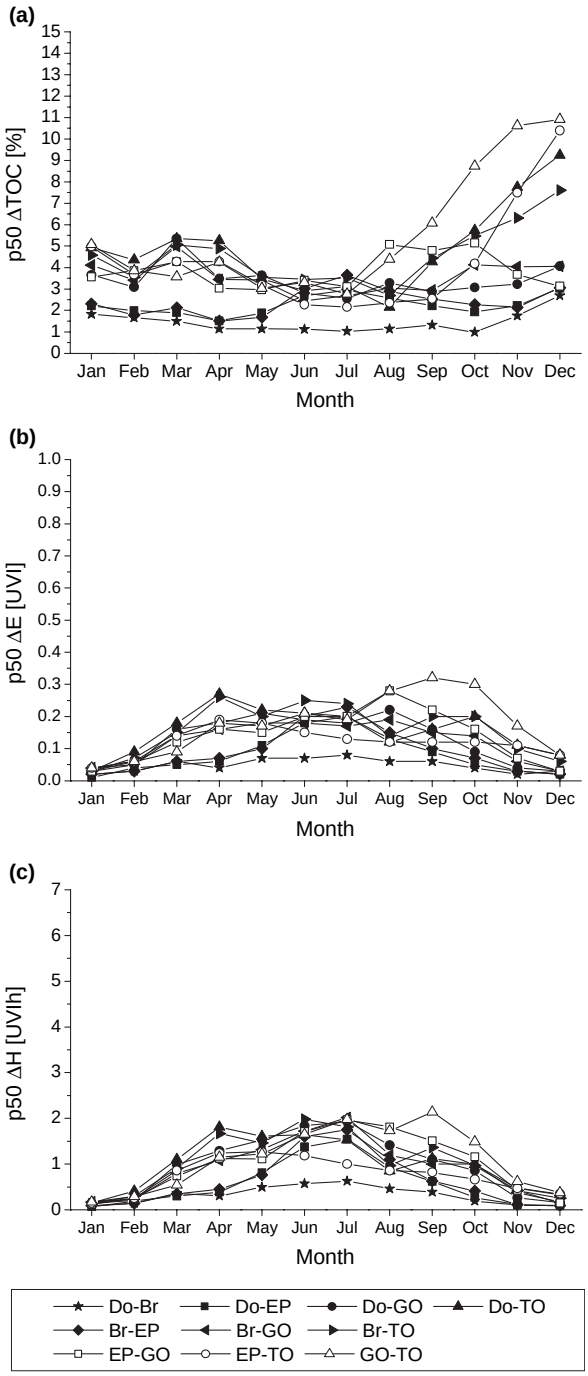


**Figure 2.** (a) 50%-percentile (p50) of absolute differences (ΔTOC) in TOC measurements between different instruments, (b) corresponding p50 of absolute differences in erythemally effective daily maximum irradiance (Δ*E*) and (c) daily dose (Δ*H*) for the location of Hradec Kralove (50.2°N, 15.8°E).

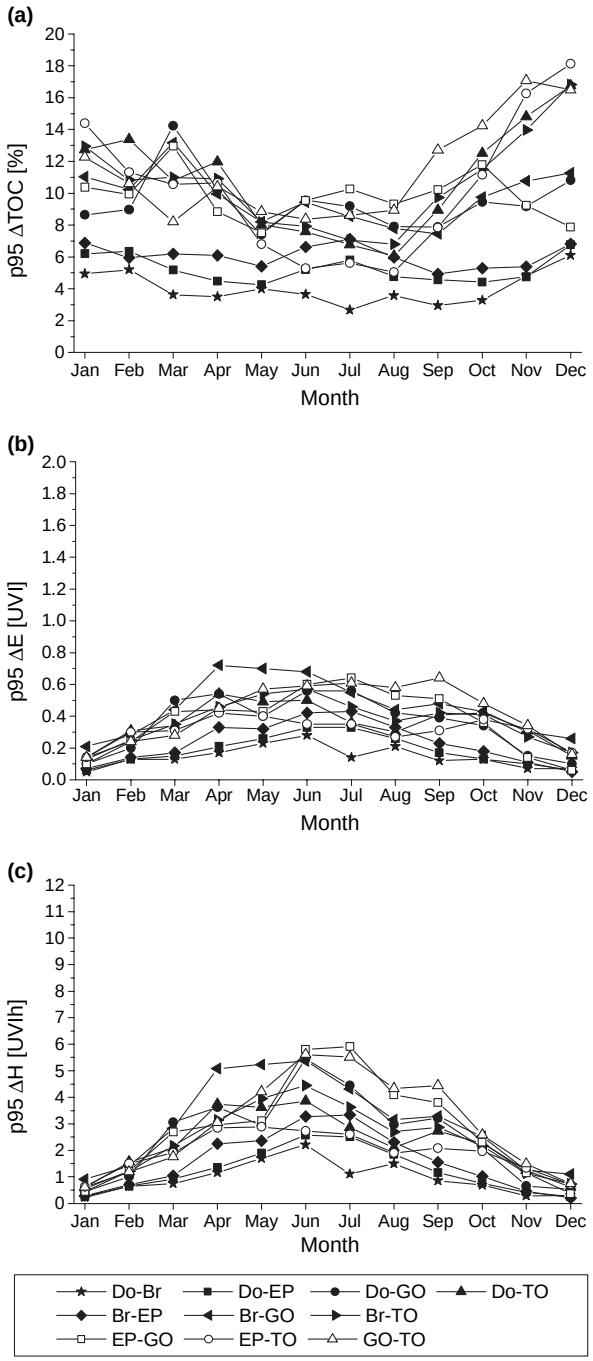


**Figure 3.** (a) 95%-percentile (p95) of absolute differences (ΔTOC) in TOC measurements between different instruments, (b) corresponding p95 of absolute differences in erythemally effective daily maximum irradiance (Δ*E*) and (c) daily dose (Δ*H*) for the location of Hradec Kralove (50.2°N, 15.8°E).

instruments shows the most obvious and asymmetric (around zero) seasonal course, with a tendency for high values between September and January which reach up to 11%. During spring and summer, the mean bias is quite close to 0%. The differences between GOME and all others show a similar behavior but being slightly smoother and in general symmetrically around zero, the mean bias is between ±4% with extremes around March (+4%) and around October (–4%). Comparisons including the Dobson deliver the smoothest courses, and the lowest amplitude of ±0.9% is found between Dobson and Brewer.

The p95 (Fig. 3a) of absolute differences shows a general trend toward higher values between October and March reaching up to 18.1% (EPTOMS-TOVS, December). The lowest p95 was found for Dobson–Brewer differences (2.7%, July). On certain days between November and February

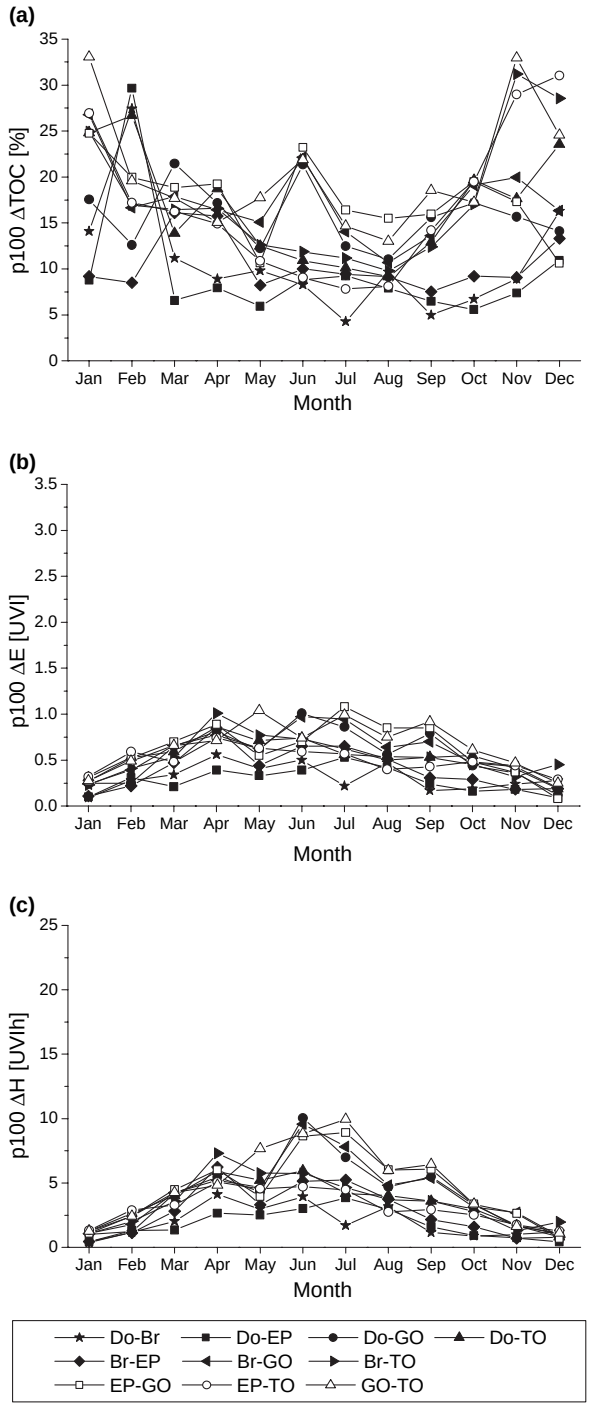


**Figure 4.** (a) 100%-percentile (p100) of absolute differences (ΔTOC) in TOC measurements between different instruments, (b) corresponding p100 of absolute differences in erythemally effective daily maximum irradiance ($\Delta E$) and (c) daily dose ($\Delta H$) for the location of Hradec Kralove (50.2°N, 15.8°E).

extreme differences (p100) are close to 30% or even above for most of the couples (Fig. 4a).

*Influence on the modeled erythemally effective UV radiation.* Using each TOC data set separately as input parameter, the erythemally effective UV radiation is calculated for clear sky over the whole period of collected data for solar noon and for the whole day. Irradiance and daily dose for the location of Hradec Kralove, modeled with TOC from the Dobson, are shown in Figs. 1b,c. It can be seen that values at solar noon range within a year from 0.5 (December) to 7.0 UVI (June) and the daily dose varies between 2 and 50 UVIh. The annual means are of 3.0 and 19.5 UVIh, respectively for solar noon irradiance and daily dose. The annual mean values of these parameters, derived from different instruments, agree within ±0.3 UVI and ±2.3 UVIh, respectively.

The monthly medians (p50) of absolute differences in irradiance (Fig. 2b) show a significant annual cycle. Differences between Brewer, Dobson and EPTOMS peak generally during June and July. Comparisons including GOME tend to peak in August and September, while comparisons including TOVS deliver the highest medians in April and May. The p50 ranges from 0.01 (Dobson-EPTOMS in January) to 0.32 UVI (EPTOMS-TOVS in September). For daily dose (Fig. 2c), the annual patterns of p50 peak mainly during June or July (beside GOME-TOVS [September] and DOBSON-TOVS [April]), which is associated clearly with the length of the day and are within 0.06 (Dobson-EPTOMS, January) and 2.2 UVIh (GOME-TOVS, September).

Similar to the annual patterns of the p50 are those of the p95 (Fig. 3b,c) which also peak between April and September in dependence on the instruments that are compared. They are below 0.21 (Dobson-EPTOMS, January) and 0.72 UVI (Brewer-GOME, April). The values of p95 in daily dose are below 0.91 (Brewer-GOME, January) and 6.0 UVIh (EPTOMS-GOME, July).

Values of p100 (Fig. 4b,c) are within 0.3 UVI (3.85 UVIh) (December and January) and 1.08 UVI (EPTOMS-GOME, July) for solar noon irradiance and between 3.85 (December and January) and 10.4 UVIh (Dobson-GOME, June) for daily dose. Similar values for irradiance can be found between April and August.

## Springbok (30°S)

*Total ozone measurements.* At Springbok the TOC exhibits a smoother seasonal course than at Hradec Kralove. Values range from 230 to 384 DU (Fig. 5a) and the highest daily TOC values as well as the highest monthly mean values are measured from August to December. The lowest values are found from February to July. From June to October, the TOC shows high variability with values changing by 100 DU within a month.

The mean TOC values over the whole period (1997–1999) do not agree so well as at Hradec Kralove: GOME 264 DU, Dobson 274 DU, EPTOMS 276 DU and TOVS 287 DU but are within ±5%. TOC values from GOME are generally lower than those measured by the others. The mean bias to Dobson and EPTOMS can be found at a level of −4% varying within the year between −3% and −6%. TOVS generally delivers the highest values which leads to an annual mean bias level of +4% compared with Dobson and EPTOMS. The comparison between GOME and TOVS delivers therefore the highest values of p50 (Fig. 6a), especially during winter (12%, June and July). During summer differences are in the order of 6%.

Dobson and EPTOMS agree quite well, with values for p50 lower than 2% with no seasonal dependence. Similarly, the p95 between Dobson and EPTOMS does not show a clear

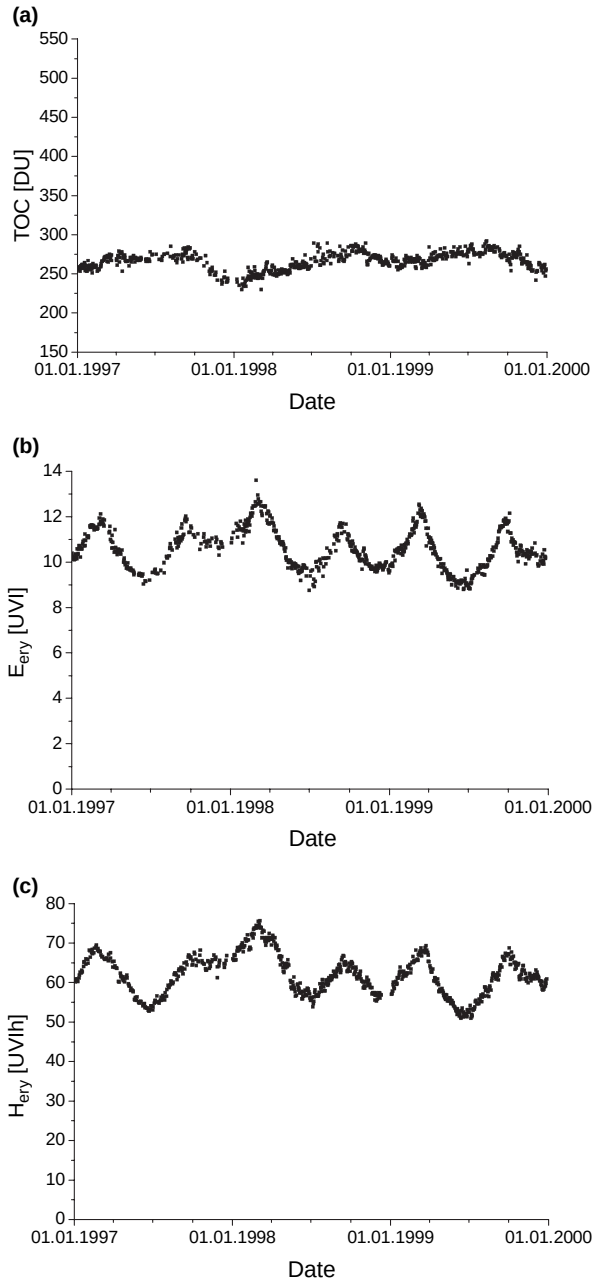


**Figure 5.** (a) Measurements of TOC taken with the Dobson spectrophotometer at Springbok (29.7°S, 17.9°E), (b) modeled erythemally effective daily maximum irradiance ($E_{ery}$) and (c) daily dose ($H_{ery}$) for clear skies.

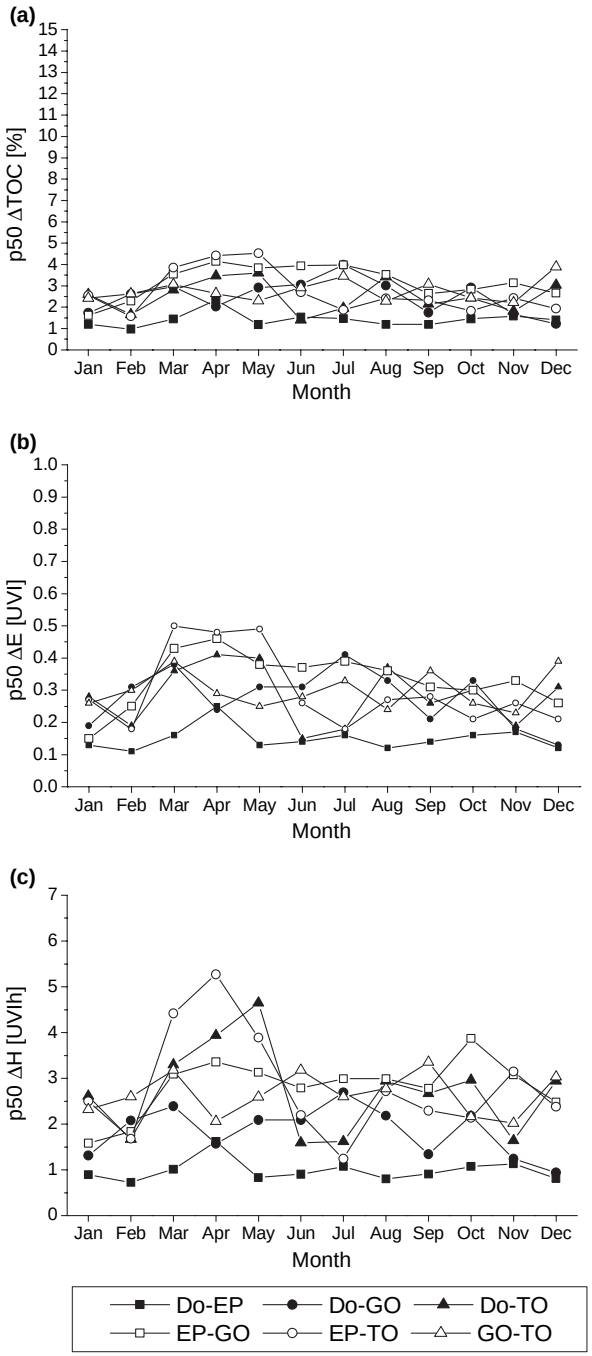


**Figure 6.** (a) 50%-percentile (p50) of absolute differences (ΔTOC) in TOC measurements between different instruments, (b) corresponding p50 of absolute differences in erythemally effective daily maximum irradiance (Δ*E*) and (c) daily dose (Δ*H*) for the location of Springbok (29.7°S, 17.9°E).

annual course (Fig. 7a) slightly varying around 3%. In contrast to this, the p95 for all other comparisons peaks between May and September reaching up to 19% (GOME-TOVS, June). The p100 values (Fig. 8a) may reach values of up to 24% (GOME-TOVS, May) with a slight tendency for being the lowest from February to March.

*Influence on the modeled erythemally effective UV radiation*. The erythemally effective UV irradiance and daily dose under clear sky range from 3 (July) to 11 UVI (December and January) and from 14 to 73 UVIh, respectively. The daily maximum irradiance and daily dose, modeled using TOC values from the Dobson are shown in Fig. 5b,c. The mean values of daily maximum irradiance and daily dose over the period of available data are calculated to be 6.8–7.2 UVI and 40.8–45.5 UVIh, respectively in dependence on the instrument.

The values of p50 do not show very significant annual cycles (Fig. 6b,c). The p50 ranges from 0.05 (Dobson-EPTOMS, June and July) to 0.67 UVI (GOME-TOVS, January and

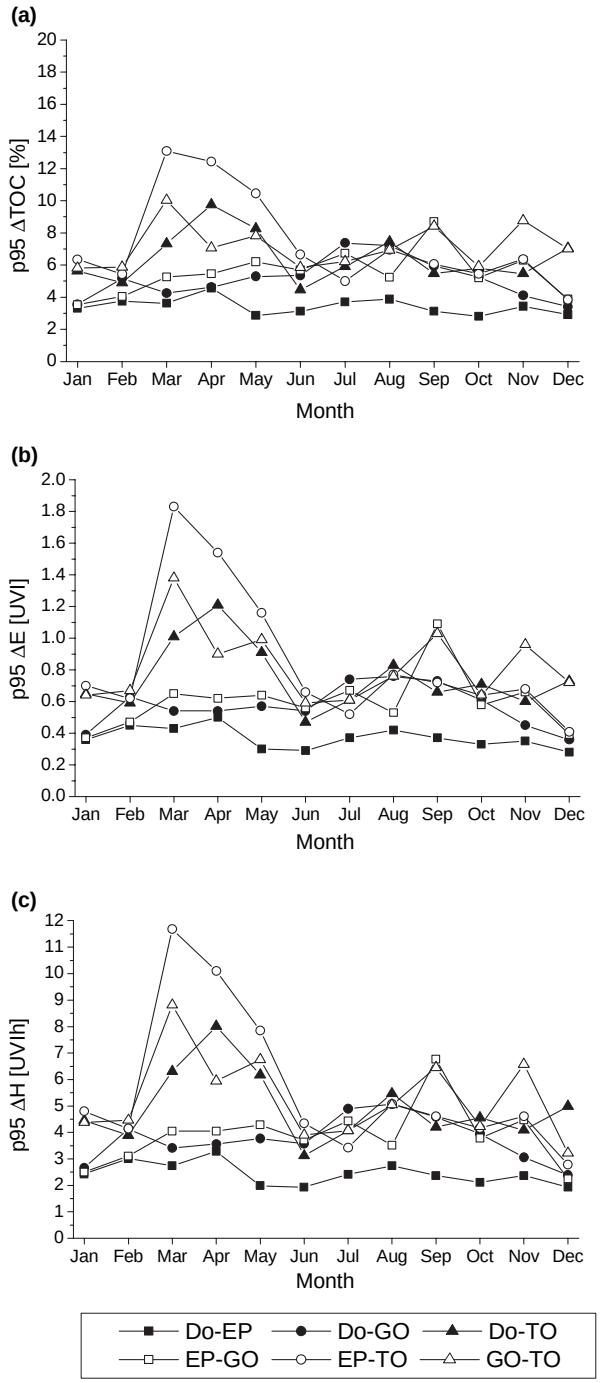


**Figure 7.** (a) 95%-percentile (p95) of absolute differences (ΔTOC) in TOC measurements between different instruments, (b) corresponding p95 of absolute differences in erythemally effective daily maximum irradiance (Δ*E*) and (c) daily dose (Δ*H*) for the location of Springbok (29.7°S, 17.9°E).

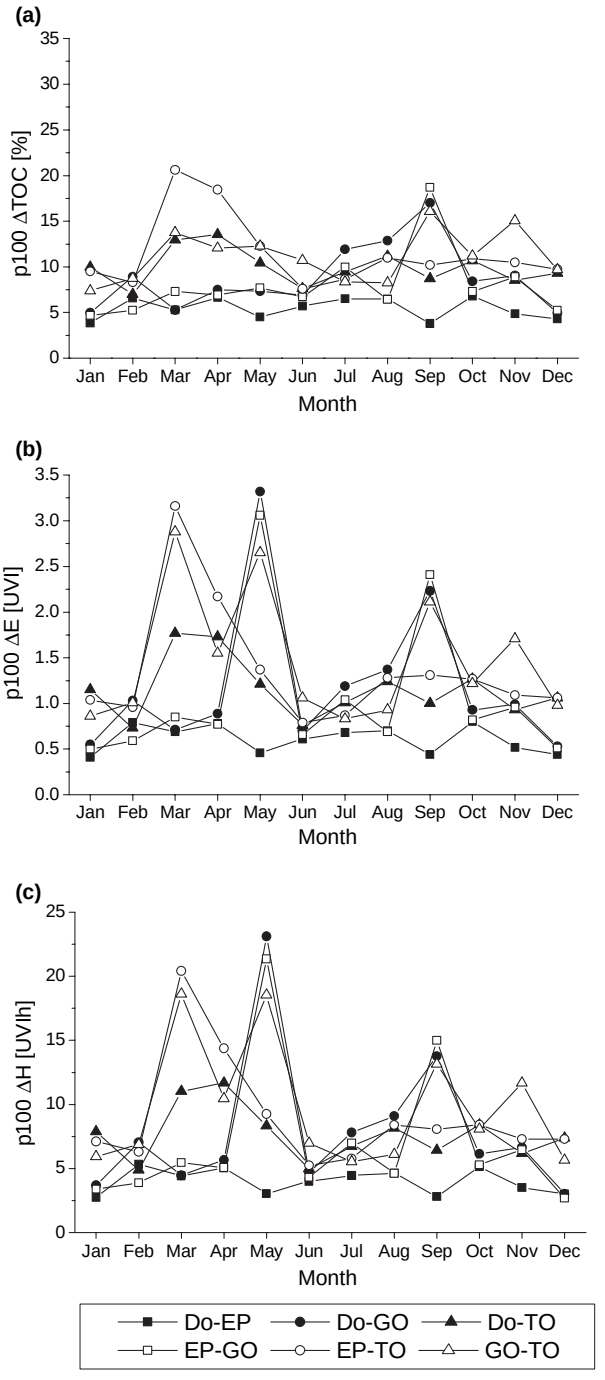


**Figure 8.** (a) 100%-percentile (p100) of absolute differences (ΔTOC) in TOC measurements between different instruments, (b) corresponding p100 of absolute differences in erythemally effective daily maximum irradiance (Δ*E*) and (c) daily dose (Δ*H*) for the location of Springbok (29.7°S, 17.9°E).

August). For daily dose the annual patterns of p50 values are slightly connected with the length of the day, however, EPTOMS-TOVS and Dobson-TOVS peak in August. They are within 0.3 (Dobson-EPTOMS, July) and 4.8 UVIh (GOME-TOVS, December).

The annual course of the p95 values does not show a significant pattern (Fig. 7b,c). The p95 values for daily maximum irradiance lie between 0.14 (Dobson-EPTOMS, June) and 1.16 UVI (GOME-TOVS, November). The p95 values for daily dose lie between 0.84 (Dobson-EPTOMS, June) and 8.2 UVIh (GOME-TOVS, November).

The p100 in irradiance reach up to 2.0 UVI and may occur all through the year (Fig. 8b). For daily dose p100 reach up to 14.3 UVIh and tend to occur between September and January (Fig. 8c).

**Nairobi (1°S)**

*Total ozone measurements*. At Nairobi measurements from the Dobson spectrophotometer are available until 1999 and from EPTOMS since mid of 1996, hence the period of comparability ranges from 1997 to 1999. The TOC over Nairobi (Fig. 9a) shows the lowest seasonal variability ranging from 220 (December and January) to 290 DU (August). The highest TOC values are found between July and November and the lowest TOC values occur between November and March. The variability is the highest from September to November, when TOC varies less than 50 DU within a month.

The mean TOC values of each instrument over the whole period agree within 9 DU: GOME 259, TOVS 263, Dobson 266 and EPTOMS 268, respectively ±3.5%. Only the mean biases between EPTOMS, Dobson and TOVS show clear seasonal patterns with higher values from March to May, reflected also in the p50 values of Fig. 10a.

The p95 values (Fig. 11a) range from 2.87% (DOBSON-EPTOMS, May) to 13.1% (EPTOMS-TOVS, March) and are generally in the order of 5%. Higher values are obvious from comparisons including TOVS, for which peaks occur from March to May. The p100 (Fig. 12a) may exceed 18% during

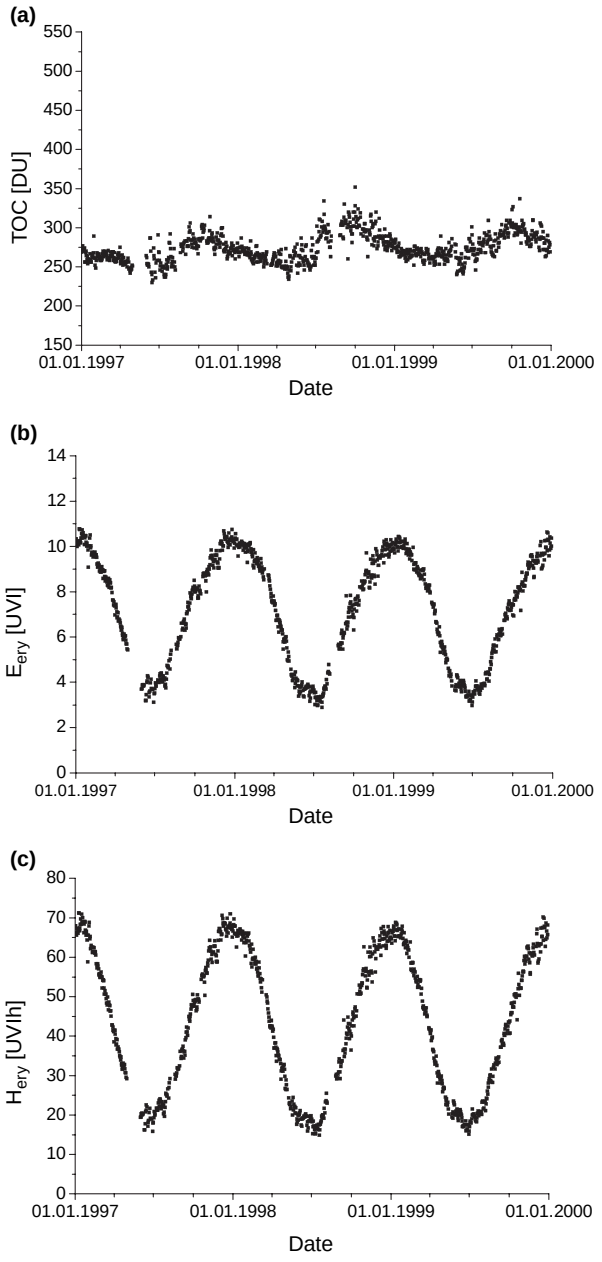


**Figure 9.** (a) Measurements of TOC taken with the Dobson spectrophotometer Nairobi (1.3°S, 36.8°E), (b) modeled erythemally effective daily maximum irradiance ($E_{ery}$) and (c) daily dose ($H_{ery}$) for clear skies.

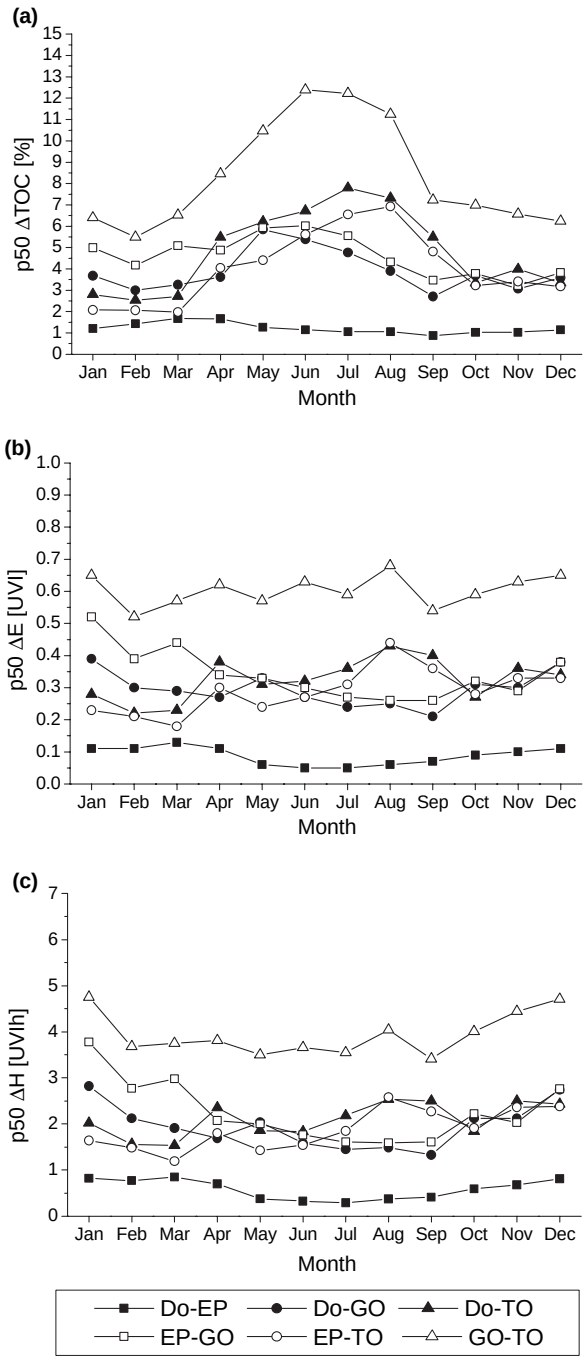


**Figure 10.** (a) 50%-percentile (p50) of absolute differences ($\Delta$TOC) in TOC measurements between different instruments, (b) corresponding p50 of absolute differences in erythemally effective daily maximum irradiance ($\Delta E$) and (c) daily dose ($\Delta H$) for the location of Nairobi (1.3°S, 36.8°E).

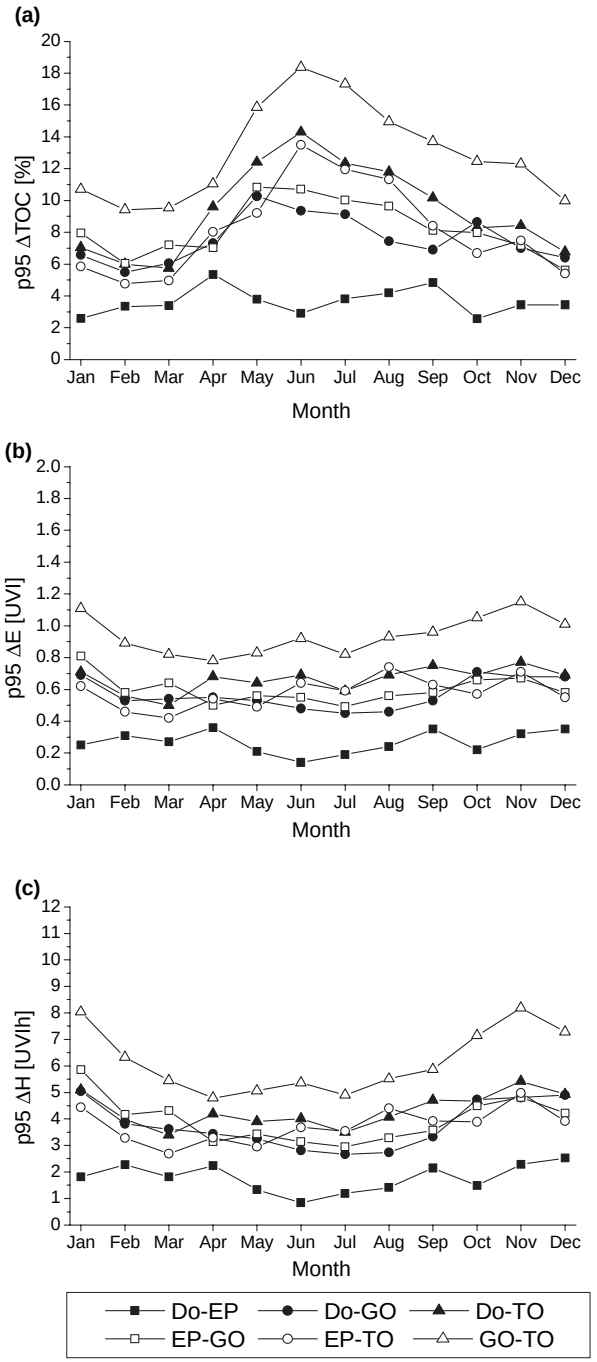


**Figure 11.** (a) 95%-percentile (p95) of absolute differences ($\Delta$TOC) in TOC measurements between different instruments, (b) corresponding p95 of absolute differences in erythemally effective daily maximum irradiance ($\Delta E$) and (c) daily dose ($\Delta H$) for the location of Nairobi (1.3°S, 36.8°E).

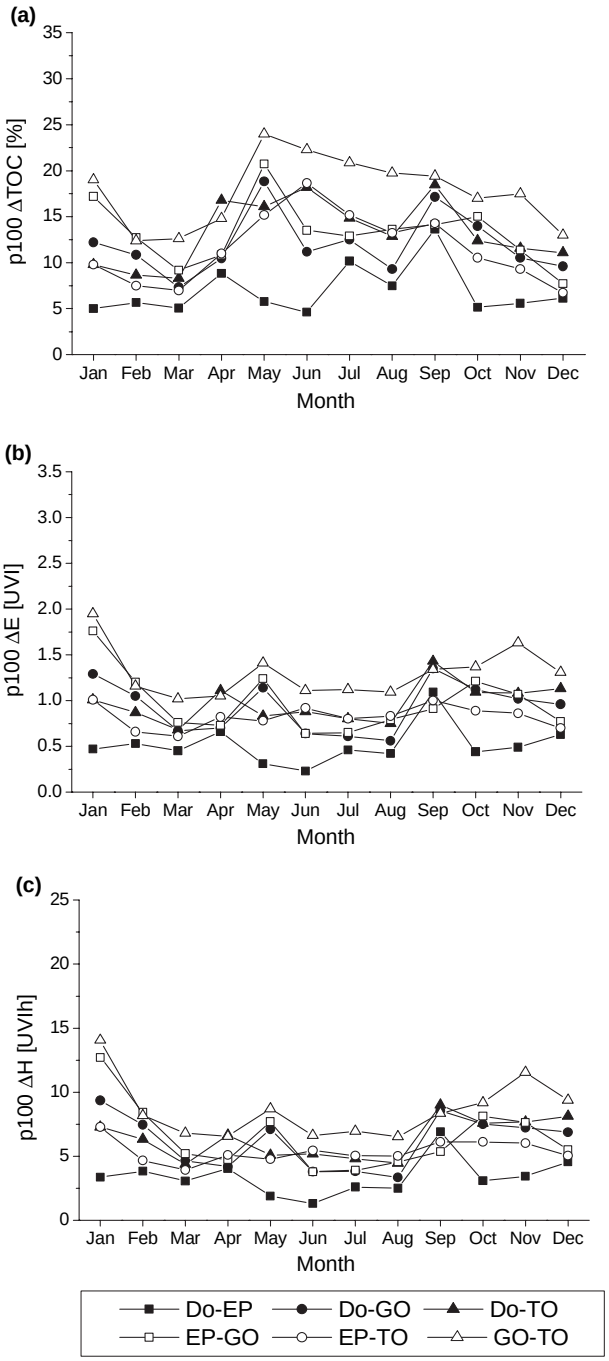


**Figure 12.** (a) 100%-percentile (p100) of absolute differences ($\Delta$TOC) in TOC measurements between different instruments, (b) corresponding p100 of absolute differences in erythemally effective daily maximum irradiance ($\Delta E$) and (c) daily dose ($\Delta H$) for the location of Nairobi (1.3°S, 36.8°E).

March and April (EPTOMS-TOVS) and in September (EPTOMS-GOME).

*Influence on the modeled erythemally effective UV radiation.* The erythemally effective UV radiation at solar noon varies between 9 and 13 UVI. In some extreme cases values up to 14 UVI were calculated. The daily dose values are within 50 and 80 UVIh. Their annual course has naturally two peaks, one in March and the other in September (Fig. 9b,c). As the TOC is close to its maximum in September, the erythemally effective UV radiation is somewhat higher in March. The calculated annual mean values are around 10.5 UVI (62.5 UVIh) and do not differ more than 0.3 UVI (1.8 UVIh).

The highest monthly p50 values of daily maximum irradiance (Fig. 10b), up to 0.50 UVI, were found for comparisons of EPTOMS and TOVS from March to May. In general, the lowest p50 values can be found for differences between Dobson and EPTOMS (0.10 UVI in February to 0.24 UVI in April).

The best agreement in daily dose at the p50 level (Fig. 10c) occurs between Dobson and EPTOMS (0.70–1.62 UVIh) while all other deliver values which are two to three times higher reaching 5.5 UVIh (GOME-TOVS, August).

Similar to the p50 values, the lowest p95 values are found for the couple of Dobson and EPTOMS (0.28–0.50 UVI [June, April] and 1.93–3.28 UVIh [June, April]) (Fig. 11b,c). The highest p95 is found for EPTOMS-TOVS (1.82 UVI and 11.84 UVIh in March). The highest value of p100 (Fig. 12b,c) results from DOBSON-GOME (3.3 UVI and 23.1 UVIh, May). Values of p100 that are higher than 3.0 UVI or 20 UVIh, are found also for EPTOMS-GOME (May) and EPTOMS-TOVS (March).

## DISCUSSION

The UVI was introduced as a standardized measure to express the erythemally effective irradiance as a unit less number. From the UVI recommendations for sun protection can be derived (23). Nowadays, current values of the UVI are published in many countries on a daily or even hourly basis as measured and/or modeled values (25). The aim of the UVI, *i.e.* sun protection, is to avoid health damage. Therefore, it is of special importance to know the accuracy of the promoted UVI values. Errors, especially underestimation, would lead to less sun protection and failure in its goal. In this paper, the limitation of accuracy (sensitivity) is estimated with respect to the uncertainties of measured TOC.

The usage of a certain source for TOC depends on several constraints and requirements like the availability at a certain site on the ground, required temporal or spatial resolution, or on the connection with other atmospheric and radiation parameters which can also be measured by an instrument. In many papers, the quality of TOC measurements was examined. From all these studies it became evident that differences and uncertainties may depend on solar zenith angle, geographical position, altitude, cloud properties, cloud coverage, aerosol content and type and ozone vertical profiles as well as the intrinsic design of the instrument. On the other hand, there is also a variety of studies which estimate the influence of TOC on model calculations of the UV radiation. This work bridges the gap between both fields by calculating the uncertainty in the UVI due to the uncertainty of TOC.

In agreement with earlier studies we find a high agreement in annual mean values of TOC. However, for the purpose of sun care daily values are necessary. Their agreement is much lower. The purpose of sun and health care needs a high degree of safety. It means that the highest errors are more meaningful than mean errors. Therefore, we have calculated the p95 for each month of the year as an indicator of accuracy. The p95 gives the error which may be reached on one day per month.

For this study we have assumed clear sky conditions as most relevant for sun protection. However, even on a cloudy day the duration when the sun is not occulted by clouds is long enough to cause sunburn. As some of us have recently shown for several locations around the world the UVI at solar noon measured under all sky conditions differs less than $\pm 0.5$ UVI in about 50% of all cases from clear sky values (34). For daily dose, a difference less than $\pm 2.5$ UVIh was for the range between 33% and 60% for all cases (36).

Comparing Figs. 3, 7 and 11 it becomes obvious that p95 in irradiance and daily dose are much less related to latitude than irradiance and daily dose are. At 50°N the annual course of the p95 in irradiance and dose is dominated by solar height and the length of the day. The high p95 values for TOC in winter raise the uncertainties in this season, but irradiance is by a factor 14 lower than in summer, and daily dose by a factor of 25, respectively. Therefore, solar height and the length of the day are dominators. At 30°S, similar to 50°N, the annual course of the p95 in TOC is the highest during winter and the lowest in summer. However, the relative annual course of irradiance and dose is not as strong. Therefore, the annual pattern of p95 in irradiance and dose shows only a smooth annual course. At the equator, the variation of irradiance at noon and daily dose during the year is rather low. Therefore, the annual pattern of p95 in TOC can be seen clearly in the annual courses of p95 in irradiance and daily dose.

This study shows that for the location at 50°N one has to take into account an error (p95) of 0.7 UVI between April and September, *i.e.* of 5–6 UVIh. The minimal erythemal dose (MED) for skin type 1 is approximately 2.5 and 3.5 UVIh for skin type 2, 4.5 UVIh for skin type 3 and 5.5 UVIh for skin type 4. Therefore, one can approximate the error in daily dose to be 2 MED (for skin type 1) which corresponds straightforward to an uncertainty in a sun protection factor (SPF) of 2. At 30°S the error is 1 UVI and 7.5 UVIh, respectively for daily maximum irradiance and daily dose. Like before, it results in an uncertainty of 3 MED and 3 SPF.

At the equator the values are quite similar to those at 30°S. Only in March and April, the p95 values of 1.8 UVI and 10 UVIh (4 MED, 4 SPF) could occur when using TOVS TOC. Otherwise the p95 values for daily maximum irradiance and daily dose are below 1.0 UVI and 7.5 UVIh respectively, denoting 3 MED and 3 SPF for skin type 1.

From these results we can summarize that on the global scale the UVI values can be given by $\pm 1$ UVI. For a promoted SPF for the most sensitive skin type 1, we recommend to add a value of 3 to the calculated value. Furthermore, the results of our study can be used to estimate the p95 errors for effects other than the erythema by using a radiation amplification factor (RAF). The RAF for a certain photobiological effect describes the change of the effective radiation due to a change or respectively a difference in the TOC. RAFs are frequently given in the literature.

## REFERENCES

1. Dobson, G. M. B. (1931) A photoelectric spectrophotometer for measuring the amount of atmospheric ozone. *Proc. R. Soc.* **93**, 324.
2. Komhyr, W. D. (1980) *Operations Handbook—Ozone Observations with a Dobson Spectrophotometer*. WMO Global Ozone Research and Monitoring Project, Report 6. World Meteorological Organization, Geneva, Switzerland.
3. Brewer, A. W. (1973) A replacement for the Dobson spectrophotometer? *Pure Appl. Geophys.* **106–109**, 919.
4. Gushchin, G. P. (1963) Universal ozonemeter. *Proc. Main Geophys. Obs. Leningrad* **141**, 83–98.
5. Gushchin, G. P. and S. A. Sokolenko (1984) Test model of the new instrument for total ozone measurements. *Proc. Main Geophys. Obs. Leningrad* **472**, 66–67.
6. Pommerau, J.-P. and G. Goutail (1988) $O_3$ and $NO_2$ ground based measurements by visible spectrometry during Arctic winter and spring 1988. *Geophys. Res. Lett.* **15**, 891–894.

7. Van Roozendael, M., P. Peeters, H. K. Roscoe, H. De Backer, A. E. Jones, L. Bartlett, G. Vaughan, F. Goutail, J.-P. Pommereau, E. Kyro, C. Wahlstrom, G. Braathen and P. C. Simon (1998) Validation of ground-based UV–visible measurements of total ozone by comparison with Dobson and Brewer spectrophotometers. *J. Atmos. Chem.* **29**, 55–83.
8. Morys, M., F. M. Mims III and S. E. Anderson (1996) *Design calibration and performance of MICROTOPS II hand-held ozonemeter*. 12th International Symposium on Photobiology, Solar Light Co., Vienna.
9. Slusser, J., J. Gibson, D. Bigelow, D. Kolinski, W. Mou, G. Koenig and A. Beaubien (1999) Comparison of column ozone retrievals by use of an UV multifilter rotating shadow-band radiometer with those from Brewer and Dobson spectrophotometers. *Appl. Opt.* **38**, 1543–1551.
10. Gao, W., J. Slusser, J. Gibson, G. Scott, D. Bigelow, J. Kerr and B. McArthur (2001) Direct-sun column ozone retrieval by the ultraviolet multifilter rotating shadow-band radiometer and comparison with those from Brewer and Dobson spectrophotometers. *Appl. Opt.* **40**, 3149–3155.
11. McPeters, R. D., P. K. Bhartia, A. J. Krueger, J. R. Herman, C. G. Wellemeyer, C. J. Seftor, G. Jaross, O. Torres, L. Moy, G. Labow, W. Byerly, S. L. Taylor, T. Swissler and R. P. Cebula (1998) *Earth Probe Total Ozone Mapping Spectrometer (TOMS) Data Products User's Guide*. NASA Reference Publication, Greenbelt, MD.
12. Deutsches Zentrum für Luft- und Raumfahrt (DLR) (1996) *Product Specification Document of the GOME Data Processor*. ER-PS-DLR-GO-0016. Deutsches Fernerkundungszentrum, Oberpfaffenhofen, Germany.
13. World Data Center for Remote Sensing of the Atmosphere (WDC-RSAT) (2006) *The Global Ozone Monitoring Experiment, Data and Products*. Available at: http://wdc.dlr.de/sensors/gome. Accessed on 16 February 2007.
14. Neuendorffer, A. C. (1996) Ozone monitoring with TIROS-N operational vertical sounder. *J. Geophys. Res.* **101**, 18807–18827.
15. Vanicek, K. (1998) Differences between Dobson and Brewer observations of total ozone at Hradec Kralove. In *Atmospheric Ozone. Proceedings of the XVII Quadrennial Ozone Symposium 12–21 September 1996, L'Aquila, Italy* (Edited by R. D. Bojkov and G. Visconti), pp. 81–84, Parco Scientifico e Tecnologica d'Abruzzo, L'Aquila, Italy.
16. Fioletov, V. E., J. B. Kerr, E. W. Hare, G. J. Labow and R. D. McPeters (1999) An assessment of the world ground-based total ozone network performance from the comparison of satellite. *J. Geophys. Res.* **104**, 1737–1747.
17. Bodecker, G. E., J. C. Scott, K. Kreher and R. L. McKenzie (2001) Global ozone trends in potential vorticity coordinates using TOMS and GOME intercompared against the Dobson network: 1978–1998. *J. Geophys. Res.* **106**, 23029–23042.
18. Lambert, J.-C., M. Van Roozendael, P. C. Simon, J.-P. Pommereau, F. Gotail, J. F. Gleason, S. B. Andersen, D. W. Arlander, N. A. Van Bui, H. Claude, J. de la Noë, M. De Mazirè, V. Dorokhov, P. Eriksen, A. Green, K. Karlsen Tørnkvist, B. A. Kåstad Høiskar, E. Kyrö, J. Leveau, M.-F. Merienne, G. Milinevsky, H. K. Roscoe, A. Sarkissian, J. D. Shanklin, J. Stähelin, C. Wahlstrøm Tellefsen and G. Vaughan (2000) Combined characterisation of GOME and TOMS total ozone measurements from space using ground-based observations from the NDSC. *Adv. Space Res.* **26**, 1931–1940.
19. Lambert, J.-C. and D. S. Balis (2004) *Delta validation report for ERS-2 GOME Data Processor upgrade to version 4.0*. ERSE-CLVL-EOPG-TN-04-0001. ESA/ESRIN, Frascati, Italy, Available at: http://wdc.dlr.de/sensors/gome/gdp4/validation.pdf. Accessed on 16 February 2007.
20. Schwander, H., P. Köpke and A. Ruggaber (1997) Uncertainties in modelled UV irradiances due to the limited accuracy and availability of input data. *J. Geophys. Res.* **102**, 9419–9429.
21. Weihs, P. and A. R. Webb (1997) Accuracy of spectral UV model calculations Part I: Consideration of the uncertainties in the input parameters. *J. Geophys. Res.* **102**, 1541–1550.
22. International Commission on Non-Ionizing Radiation Protection (ICNIRP) (1995) *Global Solar UV-Index—WHO/WMO/INCIRP recommendation*. INCIRP Publication No. 1/95. ICNIRP, Oberschleissheim, Germany.
23. World Health Organisation (WHO) (2002) *Global Solar UV Index: A Practical User Guide*. WHO, Geneva, Switzerland.
24. Commission Internationale de l'Eclairage (CIE) (2003) *International Standard Global Solar UV Index*. CIE Standard S 013:2003. CIE, Vienna, Austria.
25. Vanicek, K., Z. Lytinska, T. Frei and A. Schmalwieser (2000) *UV Index for the Public*. Publication of the European Communities, Brussels, Belgium.
26. Saxebøl, G. (2000) UVH—A proposal for a practical unit for biological effective dose for ultraviolet radiation exposure. *Radiat. Prot. Dosimetry* **88**, 261.
27. Burrows, J., M. Weber, M. Buchwitz, V. Rozanov, A. Ladstaetter-Weißenmayer, A. Richter, R. de Beek, R. Hoogen, K. Bramstedt, K.-U. Eichmann, M. Eisinger and D. Perner (1999) The Global Ozone Monitoring Experiment (GOME): Mission concept and first scientific results. *J. Atmos Sci.* **56**, 151–175.
28. Thomas, W., F. Baier, T. Erbertseder and M. Kaestner (2003) The Algeria severe weather event of November 1999 and its impact on ozone and $NO_2$ distributions. *Tellus B* **55**, 993–1006.
29. Bittner, M. and T. Erbertseder (2000) The STREAMER Project: An overview. In *Air Pollution VIII* (Edited by J. W. S. Longhurst, C. A. Brebbia and H. Power), pp. 473–482. WIT Press, Southampton, Boston.
30. Meisner, R., M. Bittner and S. Dech (1999) Computer animation of remote sensing based time series data sets. *IEEE Trans. Geosci. Remote Sens.* **37**, 1100–1106.
31. Schmalwieser, A. W. and G. Schauberger (2000) Validation of the Austrian forecast model for solar, biologically-effective ultraviolet radiation—UV Index for Vienna, Austria. *J. Geophys. Res.* **105**, 26661–26668.
32. Diffey, B. L. (1977) The calculation of the spectral distribution of natural ultraviolet radiation under clear day conditions. *Phys. Med. Biol.* **22**, 309–316.
33. Bener, P. (1972) *Approximate Values of Intensity of Natural Radiation for Different Amounts of Atmospheric Ozone*. Eur. Res. Off., US Army, London, UK.
34. Schmalwieser, A. W., G. Schauberger, M. Januch, M. Nunez, T. Koskela, D. Berger, G. Karamanian, P. Prosek and K. Laska (2002) Global validation of a forecast model for irradiance of the solar, erythemally effective UV radiation. *Opt. Eng.* **40**, 3040–3050.
35. Commission Internationale de l'Eclairage (CIE) (1987) A reference action spectrum for ultraviolet induced erythema in human skin. *CIE J.* **6**, 17–22.
36. Schmalwieser, A. W., G. Schauberger, M. Janouch, M. Nunez, T. Koskela, D. Berger and G. Karamanian (2005) Global forecast model to predict the daily dose of the solar erythemally effective UV radiation. *Photochem. Photobiol.* **81**, 154–162.
37. Commission Internationale de l'Eclairage (CIE) (1998) *Erythema Reference Action Spectrum and Standard Erythema Dose*. CIE S007E-1998. CIE, Vienna, Austria.
38. Köpke, P., A. Bais, D. Balis, M. Buchwitz, H. de Backer, X. de Cabo, P. Eckert, P. Eriksen, D. Gillotay, T. Koskela, B. Lapeta, Z. Litynska, J. Lorente, B. Mayer, A. Renaud, A. Ruggaber, G. Schauberger, G. Seckmeyer, P. Seifert, A. Schmalwieser, H. Schwander, K. Vanicek and M. Weber (1998) Comparison of models used for UV index calculations. *Photochem. Photobiol.* **67**, 657–662.
39. De Backer, H., P. Koepke, A. Bais, X. de Cabo, T. Frei, D. Gillotay, Ch. Haite, A. Heikkilä, A. Kazantzidis, T. Koskela, E. Kyrö, B. Lapeta, J. Lorente, K. Masson, B. Mayer, H. Plets, A. Redondas, A. Renaud, G. Schauberger, A. Schmalwiesser, H. Schwander and K. Vanicek (2001) Comparison of measured and modelled UV indices for the assessment of health risks. *Meteor. Appl.* **8**, 267–277.
40. James, P. M. (1998) A climatology of ozone mini-holes over the Northern hemisphere. *Int. J. Climatol.* **18**, 1287–1303.
41. Schmalwieser, A. W., G. Schauberger, M. Janouch and P. Skomorowski (2004) Mini-ozone-holes and extreme day-to-day changes of TOC over Central Europe and their influence to the biologically effective ultraviolet radiation. In *Proceedings of the XX Quandrennial Ozone Symposium, June 2004, Kos Greece* (Edited by C. S. Zerefos), pp. 1044–1045. Thessalonoki, Greece.

## 2.2 Publikation 2:

# Preprocessing of total ozone content as an input parameter to UV Index forecast calculations

Alois W. Schmalwieser, Günther Schauberger, Philip Weihs, Rene Stubi, Michal Janouch, Gerrie J.R. Coetzee, and Stana Simic

J. Geophys. Res. Vol. 108 No. D6, 4176- 4189 (2003)

# Preprocessing of total ozone content as an input parameter to UV Index forecast calculations

Alois W. Schmalwieser,[1] Günther Schauberger,[1] Philipp Weihs,[2] Rene Stubi,[3] Michal Janouch,[4] Gerrie J. R. Coetzee,[5] and Stana Simic[2]

Received 8 February 2002; revised 3 September 2002; accepted 6 September 2002; published 18 March 2003.

[1] In this paper we present a simple method to correct satellite based measurements of the total ozone content of the atmosphere (TOC) to be valid without any spatial restriction. The method delivers also a global data set of TOC, which can be used for the operational forecast of the erythemally effective ultraviolet (UV) irradiance, in the form of the UV Index. The method is based on TOC measurements made by NASA's Earth Probe TOMS. Corrections are applied to gain TOC values that are in good agreement with ground-based measurements. The algorithm of Kriging is applied for interpolation and for filling up gaps in grids. This method is validated by a comparison to measurements of TOC from the ground made at 5 observatories between 50°N and 30°S and between 285 m and 3106 m asl. From an auto-correlation analysis with different time lags it is shown that the assumption of TOC persistency of a 2-day period guarantees a quality that is convenient with the requirements of UV Index forecast procedures. For a wide zonal range covering 34% of the Earth's surface only a small improvement can be made by more sophisticated TOC forecast models, since uncertainties of our scheme are already on the order of the intrinsic uncertainties of the measuring devices. *INDEX TERMS:* 0305 Atmospheric Composition and Structure: Aerosols and particles (0345, 4801); 0360 Atmospheric Composition and Structure: Transmission and scattering of radiation; 0394 Atmospheric Composition and Structure: Instruments and techniques; 1640 Global Change: Remote sensing; *KEYWORDS:* UV Index, forecast, total ozone, EPTOMS, UV radiation

**Citation:** Schmalwieser, A. W., G. Schauberger, P. Weihs, R. Stubi, M. Janouch, G. J. R. Coetzee, and S. Simic, Preprocessing of total ozone content as an input parameter to UV Index forecast calculations, *J. Geophys. Res.*, *108*(D6), 4176, doi:10.1029/2002JD002186, 2003.

## 1. Introduction

[2] In several countries information on the surface ultraviolet (UV) intensity is given to the public to reduce the risks of health damage. This information is given in form of the UV Index like that pronounced by WHO, WMO, UNEP and ICNIRP [*ICNIRP*, 1995] and guided by COST (COST is an intergovernmental framework for European Co-operation in the field of Scientific and Technical Research) Action 713 "UV-B Forecasting" [*Vanicek et al.*, 2000]. This COST Action was founded to harmonize the UV Index forecast systems within Europe. The UV Index is a dimension-less value, proportional to the erythemally effective irradiance ($W/m^2$) of the solar UV radiation, using the erythema action spectrum [*CIE*, 1987]. The UV Index is expressed by multiplying the erythemal effective irradiance in $W/m^2$ by 40 [*ICNIRP*, 1995]. Therefore the highest values occurring on the globe can reach up to 16 [*Ren et al.*, 1999]. The information on the UV intensity can be given as forecasted or as measured value. UV-monitoring networks are often equipped with broadband meters [e.g., *Blumthaler and Silbernagl*, 1997; *Heimo et al.*, 1997]. Since their spectral sensitivity, in general, is not identical with that of a biological effect the measurements have to be corrected [e.g., *Bais et al.*, 2001]. Corrections have to be done corresponding to solar elevation and the total ozone content of the atmosphere (TOC) [*Bodhaine et al.*, 1998]. For most of the measuring sites no ground-based measurements of TOC are available. The gridded TOC measurements from satellites cannot be used directly because of their variability in longitude, latitude and altitude. In this paper we show a simple method how satellite based TOC measurements can be adapted to be valid without any spatial restriction. The UV irradiance can also be provided by operational forecast schemes. Several of these were established during the last years and their quality was evaluated [*Koepke et al.*, 1998; *De Backer et al.*, 2001]. Only few of them provide forecasted UV Index values for the whole globe, like the Austria UV Index forecast model [*Schmalwieser and Schauberger*, 2000; http://www-med-physik.vu-wien.ac.at/uv/uv_online.htm].

[1]Institute of Medical Physics and Biostatistics, University of Veterinary Medicine, Vienna, Austria.
[2]Institute of Physics and Meteorology, University of Agricultural Science, Wien, Austria.
[3]Aerological Station Payerne, MeteoSwiss, Payerne, Switzerland.
[4]Solar and Ozone Observatory, Czech Hydrometeorological Institute, Hvezdarna, Czech Republic.
[5]South African Weather Service, Pretoria, South Africa.


0148-0227/03/2002JD002186$09.00

[3] The amount of incoming irradiance depends in first order on cloudiness, TOC, aerosols and albedo. Cloudiness is the dominating factor. As shown by several authors in the past the influence depends strongly on the degree of coverage, cloud type, cloud height, optical depth as well as the Sun's position [e.g., *Kuchinke and Nunez*, 1999]. From cloudiness enhancements up to 1.2 may result and attenuation may reach 0.05. Recent studies [e.g., *Koepke et al.*, 2000; *Schmalwieser et al.*, 2001] have shown that the introduction of recent cloudiness forecasts to a UV Index forecast leads to errors, which fails the aim of radiation protection and health care. Reasons for this are the relatively low hit rate of the cloud cover forecast and the disability in providing the necessary UV relevant parameters on the global scale.

[4] Tropospheric aerosols, including mineral dust, seasalt particles, soil, organic aerosols, ammonium sulfate and diluted sulfuric acid droplets, can reduce surface UV irradiance to 50% [*Liu et al.*, 1991]. Stratospheric aerosols normally have a negligible effect on surface UV radiation expect in the case of significant enhancement, for example, volcanic eruptions [*Vogelmann et al.*, 1992]. The aerosol content, if introduced in a UV Index forecast, result either from climatological values like from the Lowtran 7 atmospheric model [*Kneiszys et al.*, 1988] or from statistical regression models as shown by *Kryscin et al.* [2001] for the location of Belsk, Poland.

[5] Reflection from the ground by water, vegetation, snow, or other surfaces may increase the UV radiation. Most surfaces have an albedo in the range from 0.02 to 0.09 with less seasonal variability. Detailed measurements can be found, for example, by *Blumthaler and Ambach* [1988], *Schauberger* [1990], or *Feister and Balzer* [1995]. Exceptions are snow and ice cover, which show high temporal and spatial variability and values from 0.2 to 1.0. In such a case the irradiance may be doubled on a vertical surface.

[6] On a global scale TOC, cloudiness, aerosols and surface reflectivity can be retrieved from satellite measurements. Such data are available, for example, from EPTOMS (http://jwocky.gsfc.nasa.gov/). The quality of the EPTOMS data products is well examined by considerable work on aerosols [e.g., *Torres et al.*, 1998; *Hsu et al.*, 1999; *Chiapello et al.*, 2000], cloudiness and surface reflectivity [e.g., *Herman et al.*, 1999].

[7] For calculating surface irradiance from EPTOMS data a method was developed which use measured values of extraterrestrial solar irradiance, ozone, aerosols, clouds and surface reflectivity, and radiative transfer calculations [*Krotkov et al.*, 1998, 2001]. This method delivers well estimations of weekly and monthly mean values [*Herman et al.*, 1999]. However, on a daily basis the accuracy is limited due to the satellites field of view, which delivers a mean value over the whole area. Additionally the field is observed once per day so that changes of clouds and aerosols during the day are not considered [*Kalliskota et al.*, 2000]. There were also other methods proposed for estimating surface UV radiation from satellite data products [*Eck et al.*, 1995; *Seckmeier et al.*, 1995; *Nunez et al.*, 1997; *Li et al.*, 2000; *Wang et al.*, 2000], which also deliver good data for weekly or monthly means.

[8] TOC values are the important base of accurate UV model calculations [e.g., *Schwander et al.*, 1997] since the inclusion of additionally parameters start with clear-sky irradiance values. To ensure high accuracy of UV Index forecasts appropriate TOC values have to be provided as well. For a worldwide UV Index forecast like in the case of the Austrian UV Index model global TOC data are needed for the time of forecast. A first approach is the use of climatological data based on satellites measurements (e.g., TOMS Version 7). Data are already analyzed and quality is well known [e.g., *Fioletev et al.*, 1999]. To increase accuracy, several short-time TOC forecast schemes were established. Most approaches to predict TOC are based on the existence of ozone-weather relationship. High-pressure systems are associated with a high tropopause and hence with a low total ozone amount. The TOC is known to be proportional to temperature in the lower stratosphere and inverse proportional with temperature in the troposphere [*Reed*, 1950]. Ozone also appears to be correlated with other meteorological variables, such as geopotential height, tropopause height, and vorticity. Most ozone forecasting models are based on this statistical kind of relations between ozone and meteorology [e.g., *Feister and Balzer*, 1991; *Allaart et al.*, 1993; *Poulin and Evans*, 1994; *Burrows et al.*, 1994; *Vogel et al.*, 1995; *Spänkuch and Schulz*, 1995; *Feister et al.*, 1996; *Vanicek*, 1998a; *Plets and Vynckier*, 2000; *Simic et al.*, 2000]. For each station a site-specific multilinear regression has to be performed. It is not possible to transfer the regression parameters from one station to another. Using this method, it is therefore also not possible to predict the total ozone content for the whole globe, since the regression coefficients are unique for each station. Nowadays only few institutes perform ozone forecasts for the whole world. It is quite customary to use the most recent ozone measurements at a given location as forecast assuming persistency over a few days. Some of them are based on data assimilation of satellite ozone measurements and ozone forecast using a chemistry-transport model.

[9] In this paper we will present a new approach, which is a simple method based on satellite measurements. As a first step, the measurements from the satellite are corrected to be comparable to measurements made by Dobson spectrophotometers. Second, the algorithm of Kriging is applied to fill up gaps in the gridded satellite data or to interpolate TOC values for certain sites. The last correction corresponds to the fact that certain sites do not posses the same altitude like the satellite pixel area that covers the sites. The difference in altitude is than connected to the height dependence of TOC. Global auto-correlation confirms an assumption of persistency for 2 days. This scheme ensures a quality that is comparable to the more sophisticated ozone forecast schemes.

[10] The quality of the calculated TOC values will be proved in this paper by a comparison to measurements made at 5 locations on the northern and southern hemisphere as well as close to the equator. Finally the influence of deviations and uncertainties in forecasted TOC to calculations of the erythemally effective solar UV radiation will be discussed.

## 2. Material and Method

[11] Starting from gridded data of satellite based measurements an equidistant and complete filled grid or values for

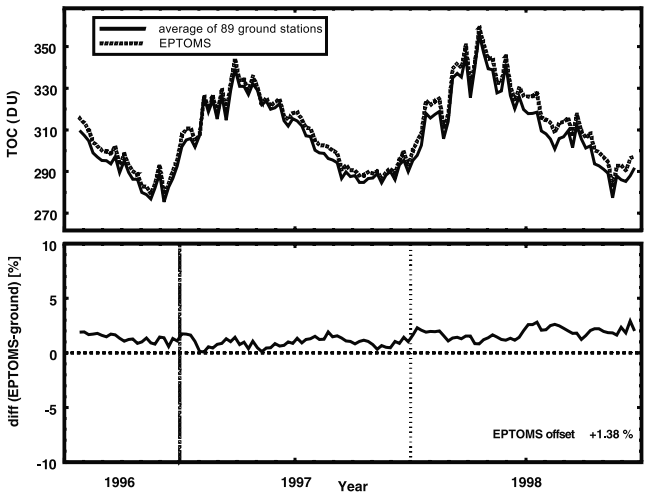


**Figure 1.** Comparison of measurements from EPTOMS and the averaged measurements of 89 ground stations (from R. D. McPeters, private communication, 2000).

special sites will be produced by a high-accuracy interpolation method. The resulting values have to be corrected corresponding to the properties of the measuring technique (offset) and in respect to the properties of TOC (altitude difference). These steps represent a method how to process TOC measurements from satellites in a way that they can be used under the assumption of persistency of 2 days as input data to UV model and forecast calculations or to recalculate measurements from broadband UV meters.

### 2.1. Data

[12] The goal of our simple forecast scheme is to provide TOC data for the whole globe. Therefore the base of our simple forecast scheme is TOC data measured by NASA's Earth Probe TOMS (EPTOMS). This Total Ozone Mapping Spectrometer (TOMS) on board the Earth Probe satellite measures incident solar radiation and backscattered UV radiation. TOC is derived from these measurements. The EPTOMS instrument is essentially the same as the first two TOMS, flown aboard Nimbus 7 and Meteor 3: a single, fixed monochromator, with exit slits at six near-UV wavelengths. A detailed description is given by *McPeters et al.* [1998]. Data are given on a 1° latitude by 1.25° longitude grid containing 180 × 288 grid points for the whole globe and as overpass data for 85 stations of the Dobson network. In this work we use the gridded data. These grids are not completely filled showing meridionaly crescent-like gaps as well as during polar night. Data are provided daily since July 1996 with a delay of 1 day. Ozone values from EPTOMS show in general a slight difference to ground-based measurements [*McPeters et al.*, 1998]. The difference between EPTOMS and the Dobson Network can be estimated to be 1.38% (R. McPeters, NASA, personal communication, 2000). A recent comparison is visualized in Figure 1. This comparison is mainly focused to the northern hemisphere due to the lower density of observatories on the southern hemisphere. For southern regions the difference becomes somewhat higher. Following the results of *Bodecker et al.* [2001] a latitudinal depending difference is introduced. Simplifying their derived function of 22 terms, a difference of 10.0% was assumed from 90°S to 70°S and a linear decrease between 70°S and 45°S to 1.38%.

[13] The altitude correction for the overhead column amount above a specific site were derived from ground-based TOC measurements made at Sonnblick High Mountain Observatory, cared by the Institute of Physics and Meteorology, University of Agricultural Sciences. The observatory is located at one of the highest peaks of the Austrian Alps (47.1°N, 12.9°E, 3106 m asl). TOC measurements were done there continuously since 1993 using the Brewer spectrophotometer MKIV No.093 [*Weihs et al.*, 1999].

[14] To validate the forecast scheme four additional data sets were used. One data set was provided by Meteo Swiss. These measurements were made at Arosa High Mountain Observatory (46.8°N, 9.9°E, 1840 m asl) by the Dobson spectrophotometer No. 101. These data enable us to prove the forecast scheme at another location of high altitude.

[15] With a data set, obtained from measurements at the Solar and Ozone observatory in Hradec Kralove (Czech Republic, 50.2°N, 15.8°E, 285 m asl), the forecast scheme can be examined for regions of low altitude. The measurements were done there with the Brewer spectrophotometer MKIV No.98 [*Vanicek*, 1998b].

[16] Since these observatories are located in the northern hemisphere, two additional data sets were involved to show the global validity of the scheme.

[17] From an observatory near Nairobi (Kenya, 1.3°S, 36.8°E, 1710 m asl) measurements of a Dobson spectrophotometer (Beck No. 18) were taken. These data were provided by the World Ozone and Ultraviolet Data Center (WOUDC).

[18] Springbok (Rep. South Africa, 29.7°S, 17.9°E, 1006 m asl) is the most southern station of our sample. Data were collected by the South African Weather Service and originate from measurements of the Dobson spectrophotometer (Beck No.123).

[19] All ground-based TOC values are given as daily mean resulting from several measurements during a day.

### 2.2. Topography and Altitude Dependence

[20] Since data of EPTOMS are retrieved for certain ground pixel area. They are valid for the mean altitude of this pixel. Locations that are situated significantly above or below this level need special considerations since overhead TOC depends on altitude. Within mountainous regions like the Alps such cases are omnipresent. The estimation of the mean altitude for a pixel and differences in altitude to a certain location within this pixel requires high resolved topographic data. For this purpose we used the topographic data set GTOPO30 [*Gesch and Larson*, 1996]. GTOPO30 is a global digital elevation model resulting from a collaborative effort led by the U.S. Geological Survey's EROS Data Center. Elevations in GTOPO30 are regularly spaced at 30-arc seconds, which corresponds to a resolution of approximately 1 km.

### 2.3. Kriging

[21] An important tool in TOC data handling is the application of an interpolation algorithm. For our scheme interpolation is needed for two purposes. One is to fill up the EPTOMS grid, the second is to deliver values for certain sites. For these approaches ordinary kriging [*Krige*, 1981]

was used. As shown by *Oliver and Webster* [1990], by the use of kriging the confidence in any interpolated value can be estimated in a better way than with other methods. Kriging possesses also the acronym B.L.U.E. (best linear unbiased estimator). The estimation of the unknown TOC at a certain position $\hat{O}(\rho_0)$ results from the weighted linear combination of all data:

$$\hat{O}(\rho_0) = \sum_{i=1}^{n} w_i \cdot O(\rho_i), \tag{1}$$

where as $O(\rho_i)$ are measurements made at locations $\rho_i$ and $w_i$ are the corresponding weights, with

$$\sum_{i=1}^{n} w_i = 1. \tag{2}$$

Since the expectation of the estimate $\varepsilon$ ($\hat{O}(\rho_0)$) should be equal to the expectation of the true values $\varepsilon$ ($O(\rho_0)$), Kriging is unbiased. The mean error is therefore zero:

$$\varepsilon\left(\hat{O}(\rho_0)\right) - \varepsilon(O(\rho_0)) = 0. \tag{3}$$

In difference to other linear estimation methods Kriging aims in minimizing the variance of errors.

$$\frac{\partial}{\partial w_i} s_\varepsilon^2 = 0, \tag{4}$$

where the error variance is given by

$$s_\varepsilon^2 = \frac{1}{k} \sum_{i=1}^{k} \left[\hat{O}(\rho_i) - O(\rho_i)\right]^2. \tag{5}$$

Following this, the acronym best holds.

[22] The derivations of these equations lead to a complete set of simultaneous equations. Details can be found by *Isaaks and Srivastava* [1989]. The equations can be expressed in matrix form, so that the weights are gained by simple matrix inversion. One may summarize that the weight $w_i$ of a measurement decreases with increasing distance to the location for which a value should be found. The weight of a measurement decreases also with increasing spatial density of measurements.

### 2.4. Temporal Auto-Correlation

[23] The developed scheme prepares TOC values for the use as input parameter to procedures which need a TOC forecast, like a UV Index forecast. For this an assumption of temporal persistency was made. The time lag is caused, on the one hand, by the fact that TOC from EPTOMS is provided with a certain delay and on the other hand by the fact that a UV Index forecast is made for a certain time in advance. TOC values over a certain location change with time. This temporal variability is rather low within a few days. The amount of the day-to-day changes depends on location as several studies have shown. While at northern latitudes temporal variation is lowest [e.g., *Chen and Nunez*, 1998] the variability increase at midlatitudes [e.g., *Casale et al.*, 2000]. In the subtropics [e.g., *Acosta and Evans*, 2000] variability becomes lower again. To describe the temporal behavior of TOC at any location over a certain period and to prove if an assumption of temporal persistency can be used, the auto-correlation was selected. The correlation coefficient can be calculated as follows:

$$C_{t,t-n}(\rho_i) = \frac{\sum_{t=1}^{T}\left[\left(O_t^{Meas}(\rho_i) - \overline{O^{Meas}(\rho_i)}\right)\cdot\left(O_{t-n}^{Meas}(\rho_i) - \overline{O^{Meas}(\rho_i)}\right)\right]}{\sqrt{\sum_{t=1}^{T}\left(O_t^{Meas}(\rho_i) - \overline{O^{Meas}(\rho_i)}\right)^2 \cdot \sum_{t=1}^{T}\left(O_{t-n}^{Meas}(\rho_i) - \overline{O^{Meas}(\rho_i)}\right)^2}}, \tag{6}$$

where $C_{t,t-n}$ ($\rho_i$) is the correlation coefficient for TOC at dates $t$ and $t-n$ at location $\rho_i$, $O_t^{Meas}$ ($\rho_i$) is the TOC at date $t$ and location $\rho_i$, $O_{t-n}^{Meas}$ is the TOC at date $t-n$ and location $\rho_i$, $n$ is the time lag in days, and $\overline{O^{Meas}(\rho_i)}$ is the mean TOC at location $\rho_i$, gained over the period T. $T$ denotes a certain period that should be equal to a multiple integer of the main period.

### 2.5. Model Validation

[24] Like every model and forecast, this scheme is affected by uncertainties that affect in our case the UV Index. The uncertainties result from assuming temporal persistency, interpolation and intrinsic uncertainties of measurements as well as from data processing. To assess the quality of our developed scheme the calculated values were compared to measurements.

[25] The first indicator for the quality of the scheme is the normalized mean bias error (MBE) expressed in percent:

$$MBE(\rho_i) = \frac{1}{N} \cdot \sum_{t=1}^{T} \frac{O_t^{FC}(\rho_i) - O_t^{Meas}(\rho_i)}{O_t^{Meas}(\rho_i)}, \tag{7}$$

where $O_t^{FC}$ ($\rho_i$) is the forecasted TOC for date $t$, at location $\rho_i$, $O_t^{Meas}$ ($\rho_i$) is the measured TOC at date $t$, at location $\rho_i$, $N$ is sample size, and $T$ is the temporal interval. The MBE is calculated for all observatories to show systematic deviations.

[26] The amount of uncertainties depends on TOC, which is varying with location. For this we take a look on the absolute amount of the differences between forecasted and measured TOC in relation to the measured TOC value, respectively on the global distribution of the annual means. This normalized mean absolute bias uncertainty (MABE) is defined as

$$MABE(\rho_i) = \frac{1}{N} \cdot \sum_{t=1}^{T} \frac{\left|O_t^{FC}(\rho_i) - O_t^{Meas}(\rho_i)\right|}{O_t^{Meas}(\rho_i)}, \tag{8}$$

where the denotations are the same as for the MBE.

[27] Beside these mean errors, the root mean square error (RMSE) is used to evaluate the quality. The annual courses of the RMSE were calculated for each observatory from the difference between ground-based measurements and TOC values gained by our scheme. The RMSE is given as

$$RMSE(\rho_i) = \sqrt{\frac{1}{N} \cdot \sum_{t=1}^{T}\left(O_t^{m1}(\rho_i) - O_t^{m2}(\rho_i)\right)^2}, \tag{9}$$

where $O_t^{m1}$ ($\rho_i$) is TOC values gained by method one for date $t$ at location $\rho_i$, $O_t^{m2}$ ($\rho_i$) is TOC values gained by method two for date $t$ at location $\rho_i$, $N$ is numbers of compared data, and T is the temporal interval.

[28] These RMSE were compared to RMSE caused by the use of climatological data to estimate the improvement to climatology. And finally the quality was also discussed by a comparison of RMSE of several forecast procedures. A comparison of various methods has already been published by *Vanicek* [1998a].

[29] Another step is to validate the intrinsic RMSE of the data processing techniques. The intrinsic uncertainties of measurements are difficult to estimate, since the used data are provided from operational runs and no absolute value is available. To estimate these uncertainties the RMSE were calculated from ground-based measurements and values calculated by the developed scheme but without assuming temporal persistency.

### 2.6. Influence of Uncertainties to UV Index Calculations

[30] Used as input parameter, TOC effects a UV model calculation or forecast in a certain way. Its influence depends on the sensitivity of the biologically action spectrum to TOC. Therefore the normalized indicators MBE, MABE and RMSE can be used to estimate roughly the effects of uncertainties.

[31] To quantify the influence of uncertainties in TOC to the UV Index in detail, model calculations were done for a period of three years using the Austrian UV model [*Schmalwieser et al.*, 2002]. UV Index was calculated for clear sky at noon. Input parameter were date, time, geographical position, altitude and TOC.

[32] For every station three runs were made using TOC from different sources as input parameter to the UV Index model. The first source was TOC measured from the ground, the second was EPTOMS TOC prepared by our scheme using TOC values for the specific day. And finally the third run was done with TOC values from our simple forecast scheme under the assumption of persistency. Differences between run one and run two reflect the influence of the intrinsic uncertainties of the measurement techniques and data processing. The third run shows the whole uncertainties when our developed scheme is used as forecast procedure and the differences between run two and three give the effect of assuming persistency. These differences are independent of the chosen model since intrinsic uncertainties of the model are cancelled.

## 3. Data Analysis

[33] Before developing the forecast scheme in detail, it is necessary to examine two essential assumptions. The first is the dependence of altitude; the second is the temporal variability.

### 3.1. Dependence of Altitude

[34] For locations that are located significantly above the mean altitude of the corresponding EPTOMS pixel a correction factor depending on the difference in altitude has to be found. An estimation of this altitude dependence of TOC can be made using observations from an observatory situated at an extraordinary level of altitude relative to the surrounding area. Therefore ground-based measurements made at 3106 meter asl were used. This data set was obtained at Sonnblick.

[35] Figure 2a shows measurements of TOC for the location of Sonnblick (47.1°N, 12.9°E, 3106 m asl). In the upper panel of this figure the Brewer measurements are shown. The middle panel shows the relative differences between these measurements and TOC values provided from EPTOMS and interpolated for the location of Sonnblick.

[36] Simple analysis makes evident that differences between EPTOMS and Brewer measurements of TOC are in the order of 3.84% and therefore 2.46% higher than that between EPTOMS and the Dobson Network. No significant trend for these differences can be recognized during the period of 3 years. Since Sonnblick Observatory is located 2184 m above the mean altitude of the corresponding EPTOMS pixel the altitude effect can be estimated to be 1.13% per 1000 m.

[37] This number is in good agreement with long-term measurements from the ground presented by *Krzyscin* [2000], who estimated 10% within the first 10 km over Belsk, Poland, from Umkehr measurements. Recent balloon soundings also deliver values around 1.15% per 1000 m (R. Stubi, personal communication, 2002; P. Skrivankova, personal communication, 2002). Similar values can also be found on the southern hemisphere [e.g., *Bodecker et al.*, 2001] or in atmospheric models like Lowtran 7 [*Kneiszys et al.*, 1988].

### 3.2. Temporal Auto-Correlation

[38] To proof the assumption of persistency we have analyzed the temporal variability of TOC within a few days. To examine the time-lag-dependence the temporal auto-correlation was used. For the location of Sonnblick correlation coefficients were calculated for a time lag up to 400 days to show them for a whole year. Analyzed data are TOC from EPTOMS prepared by our scheme covering the period from 1.1.1996 to 31.12.1999. Figure 3 shows the time course. The correlation decreases rapidly within the first 10 days down to a level of +1/e. During the next 3 months correlation is within +1/e and zero. The decrease continues over 3 months reaching the minimum of $-1/e$. After this the correlation starts to increase, reaching zero around 3 months later and reaching +1/e after another 3 months. This behavior reflects the typical annual cycle of TOC.

[39] Since measurements of EPTOMS are available with a delay of 1 day and the UV Index forecast is done one day in advance, the temporal interval of interest is 2 days. At the location of Sonnblick the annual mean of the auto-correlation coefficient for a time-lag of 2 days $C_{t,t-2}$ is 0.65.

[40] For this delay the global distribution of correlation is calculated from all data between 1997 and 1999. The resulting visualization (Figure 4) demonstrates the global distribution of the temporal variability of TOC by showing annual means of the correlation coefficient for a time lag of 2 days $C_{t,t-2}$.

[41] Isopleths are oriented zonally, with maximum values occurring around the equator (10°S to 15°N). Temporal

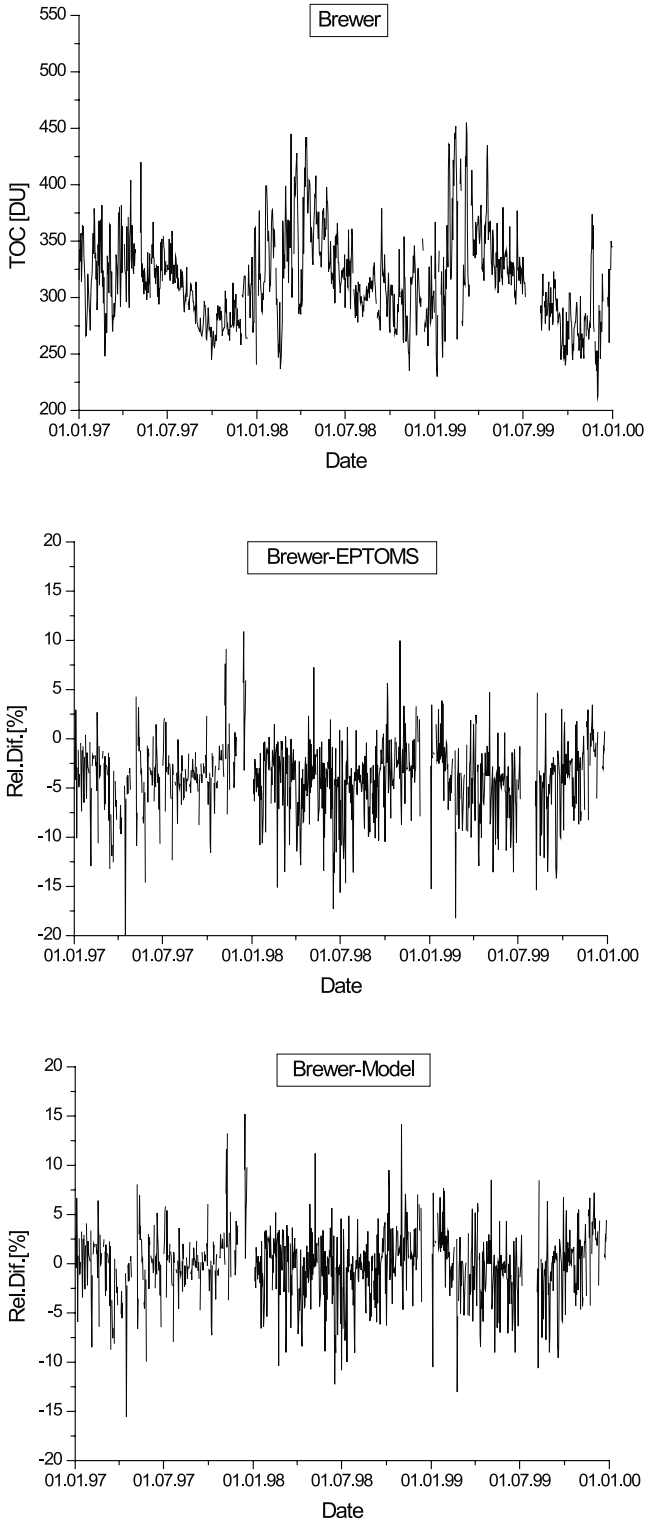


**Figure 2a.** TOC measurements for the location of Sonnblick high mountain observatory (47.1°N, 12.9°E), Austria. The upper panel shows ground-based TOC measurements gained during January 1997 to December 1999. The measurements are made at Sonnblick at an altitude of 3106 m asl using Brewer MKIV (No. 93). The middle panel shows relative differences between ground-based and EPTOMS data, and the lower panel shows the relative differences between ground-based measurements and EPTOMS data prepared by the developed scheme.

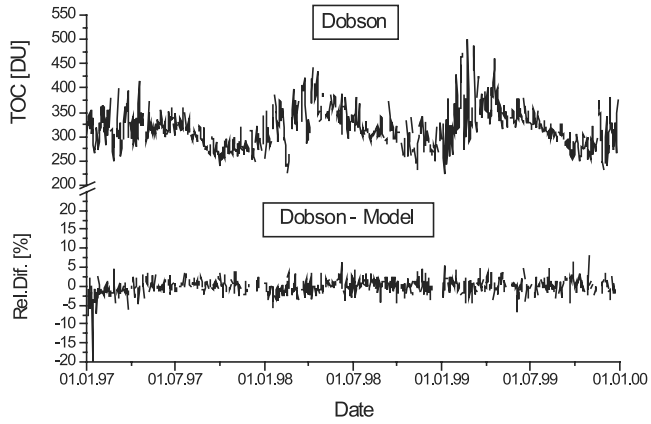


**Figure 2b.** TOC measurements for the location of Arosa (46.8°N, 9.9°E), Switzerland. The upper panel shows ground-based TOC measurements gained during January 1997 to December 1999. The measurements are made at an altitude of 1840 m asl using a Dobson (No. 101). The lower panel shows the relative differences between ground-based measurements and EPTOMS data prepared by the developed scheme.

TOC variability increase rapidly within subtropical regions down to values of $C_{t,t-2}$ of 0.75. On the northern hemisphere correlation increase at 45°N, reaching 0.9 at 60°. Different to that, at the southern hemisphere correlation decrease further, establishing a zonal band of values below 0.6 at 45°S. At 70°S TOC becomes more stable again.

[42] Since areas poleward of the polar circle cannot be observed by EPTOMS during polar nights isolines are therefore shaded in gray, to mark the decrease of available data. From this correlation analysis it can be seen, that at the extreme location of Sonnblick variability of TOC is rather high, but fits quite well within the global distribution of

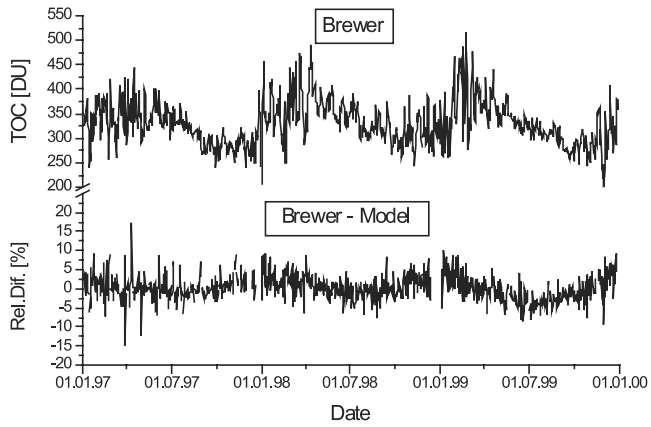


**Figure 2c.** TOC measurements for the location of Hradec Kralove (50.2°N, 15.8°E), Czech Republic. The upper panel shows ground-based TOC measurements gained during January 1997 to December 1999. The measurements are made at Hradec Kralove at an altitude of 285 m asl using Brewer MKIV (No. 98). The lower panel shows the relative differences between ground-based measurements and EPTOMS data prepared by the developed scheme.

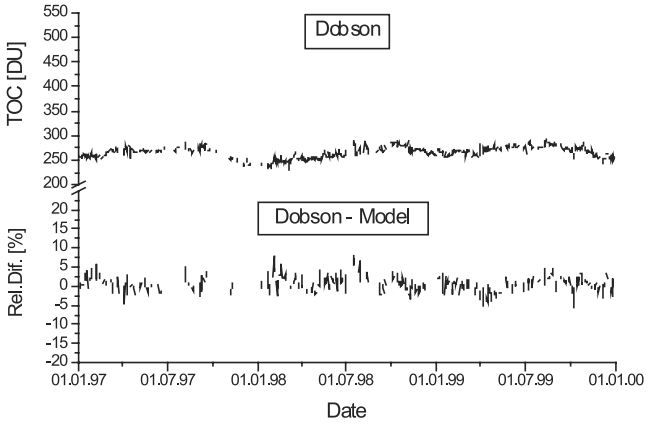


**Figure 2d.** TOC measurements for the location of Nairobi (1.3°S, 36.8°E), Kenya. The upper panel shows ground-based TOC measurements gained during January 1997 to December 1999. The measurements are made at an altitude of 1710 m asl using Dobson (No. 18). The lower panel shows the relative differences between ground-based measurements and EPTOMS data prepared by the developed scheme.

$C_{t,t-2}$ and is therefore typical for a broad range in latitude (15°N to 50°N) on the northern hemisphere.

## 4. Results

[43] The intrinsic properties of the used data sets and the analysis of temporal and spatial variability have provided the necessary information on how to process the measurements of TOC to get a global data set which can be used instead of an sophisticated TOC forecast.

### 4.1. Simple Model to Calculate TOC

[44] The basic ozone values are given from satellite based observations. These values from EPTOMS $O^{EPTOMS}(x, y, \bar{z})$

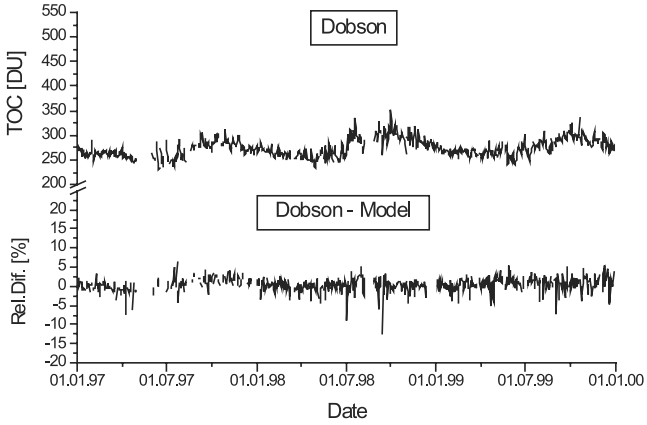


**Figure 2e.** TOC measurements for the location of Springbok (29.7°S, 17.9°E), South Africa. The upper panel shows ground-based TOC measurements gained during January 1997 to December 1999. The measurements are made at an altitude of 1006 m asl using Dobson (No. 123). The lower panel shows the relative differences between ground-based measurements and EPTOMS data prepared by the developed scheme.

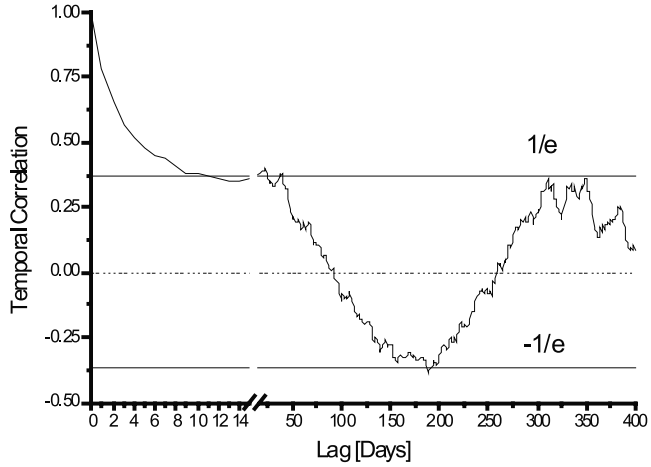


**Figure 3.** Temporal auto-correlation of TOC. Correlation coefficients were calculated for the location of Sonnblick for a lag up to 400 days using EPTOMS data. On the left side the detailed behavior of coefficients is shown for temporal lags up to 14 days. The straight horizontal lines indicate the level of de-correlation defined as ±1/e. For these calculations the available data during the period of January 1996 to 31 December 1999 were considered.

are available as equidistant but not completely filled grid. They are valid for a certain pixel which center is determined by $x$ and $y$ and the mean altitude of the pixel by $\bar{z}$. First of all the mean relative difference $c_{DN}$ of EPTOMS measurements to measurements made by the ground-based Dobson Network has to be taken into account. Due to this the EPTOMS values become comparable to ground-based measured TOC $O^{GB}(x, y, \bar{z})$:

$$O^{GB}(x, y, \bar{z}) = O^{EPTOMS}(x, y, \bar{z}) \cdot (1 + c_{DN}), \tag{10}$$

where $c_{DN}$ can be supposed to be constant at 1.38% between 90°N and 45°S, to be increasing linear to 10% at 70°S and to be constant up to 90°S.

[45] From these values a complete grid $O(\lambda, \varphi, \bar{h})$ can be calculated as well as values for a certain site $O(\lambda, \varphi, \bar{h})$ using Kriging:

$$O^{GB}(x, y, \bar{z}) \xrightarrow{Kriging} O(\lambda, \varphi, \bar{h}). \tag{11}$$

Since the EPTOMS values are valid for a certain pixel $(x, y)$ for which a mean altitude $\bar{z}$ is assumed, a new level of altitude $\bar{h}$ will result for every interpolated site $(\lambda, \varphi)$. This level can also be calculated explicitly by the same use of kriging, only changing TOC against altitude:

$$\bar{z}(x, y) \xrightarrow{Kriging} \bar{h}(\lambda, \varphi). \tag{12}$$

The next step is to involve the effect, which is related to topography: the higher the altitude, the less TOC is. The interpolated TOC $O(\lambda, \varphi, \bar{h})$ is valid for the level of altitude $\bar{h}$, which results from interpolating. The altitude difference $\Delta h$ between this level $\bar{h}$, and the real altitude of the certain site $h$ has to be taken into account. The altitude $h$ may either be given (e.g., for a certain location) or taken from

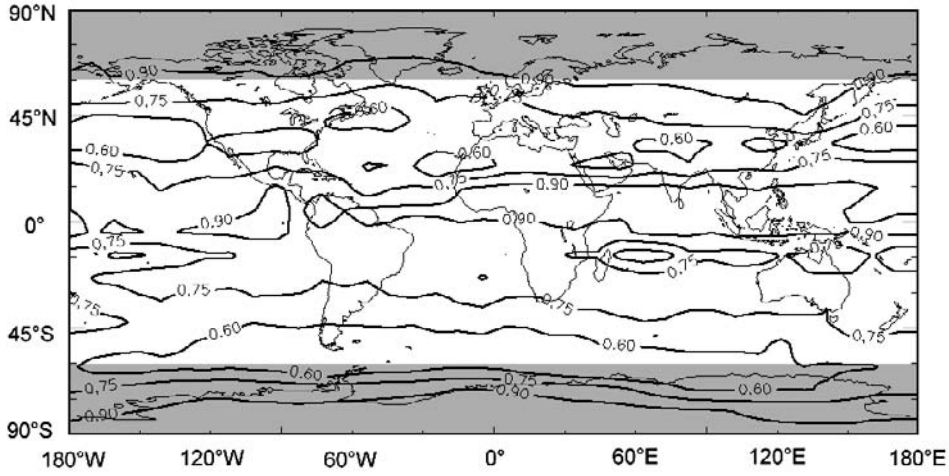


**Figure 4.** Global distribution of correlation coefficients $C_{t,t-2}$ according equation (6) for a temporal delay of 2 days calculated for each grid point (288 × 181) of EPTOMS data. Regions showing polar nights are marked gray since data of TOC are only available if solar radiation is reflected.

GTOPO30. The altitude corrected TOC $O(\lambda, \varphi, h)$ can be calculated as follows:

$$O(\lambda, \varphi, h) = O\left(\lambda, \varphi, \bar{h}\right) \cdot (1 + c_{alt} \cdot \Delta h). \quad (13)$$

As mentioned above, from comparison of EPTOMS, the Dobson Network and measurements taken at Sonnblick observatory, the correction factor $c_{alt}$ is estimated by 1.13% per 1000 m. Following the auto-correlation analysis, these TOC values can be used under the assumption of persistency of 2 days as TOC forecast since correlation for a temporal-lag of two days is greater than 0.5 all over the globe.

### 4.2. Validation

[46] As a first step the MBE was calculated for all stations. This was done from ground observations and forecast values over the whole period of available data. The MBE are listed in Table 1. Since the scheme was developed for Sonnblick it is not surprisingly that the MBE is 0.00%. For Hradec Kralove $\Delta h$ is vanishing and the MBE is 0.26%. For Arosa, which is located significantly above the EPTOMS pixel height ($\Delta h$ = 949 m), the MBE is 0.02%. This indicates that the effect of altitude was well derived. Also for Nairobi and Springbok the MBE is below 1%.

[47] For taking a look on the deviations between forecasted and measured TOC as well as on the consequences to a further use, the global distribution of MABE is used. Figure 5 shows isopleths of the MABE of the forecast TOC values. A broad zonal band of differences less than 2.5% covers equatorial regions, reaching further south than north (15°N to 25°S). The following isoline of 5% is very close and as close as the next one of 7.5%. The areas where polar nights occur are over plotted by gray to denote decreasing amount of available data. MABE were also calculated for all stations (Table 1). For the European stations MABE are in the order of 7%, while for the stations located in Africa the MABE is significantly lower (Nairobi: 1.8%, Springbok: 3.4%).

[48] A further step in validating is to examine the annual behavior of the deviations between predicted and measured TOC. For all stations the RMSE was calculated. The monthly means of RMSE of the developed scheme are shown in Table 2. It can be seen that the highest RMSE occur during winter and early spring when the variability of TOC is highest (Figures 2a–2e). During late spring RMSE values decrease, reaching minimum during August in the northern hemisphere and during February in the southern hemisphere. Alternatively one has to have a look to the intrinsic uncertainties that result from the use of a certain data processing technique. For an operational run this is difficult to handle since no absolute measure is available. By a comparison of TOC measurements gained by two different techniques for the same location the intrinsic

**Table 1.** Statistical Description of Measured TOC and Validation of the Developed Method Used as TOC Forecast for Each Observatory[a]

| | Characteristics of TOC and Bias Errors | | | | | | | | | |
|---|---|---|---|---|---|---|---|---|---|---|
| Observatory | Longitude, deg. | Latitude, deg. | Altitude, m, asl | $D_h$, m | Device | $O_3$ Minimum, DU | $O_3$ Mean, DU | $O_3$ Max, DU | MBE (FC), % | MABE (FC), % |
| Sonnblick, AUT | 12.9 | 47.1 | 3106 | +2184 | Brewer MK IV No. 93 | 225 | 317 | 461 | 0.00 | 6.79 |
| Arosa, CH | 9.9 | 46.8 | 1840 | +949 | Dobson Beck 101 | 198 | 314 | 485 | 0.02 | 7.02 |
| Hradec Kralove, CZE | 15.8 | 50.2 | 285 | +92 | Brewer MK IV No. 98 | 180 | 329 | 519 | 0.26 | 7.21 |
| Nairobi, KEN | −1.3 | 36.8 | 1710 | +290 | Dobson Beck 18 | 230 | 266 | 292 | 0.70 | 1.78 |
| Springbok, ZAF | −29.7 | 17.9 | 1006 | +334 | Dobson Beck 132 | 230 | 274 | 352 | 0.28 | 3.42 |

[a]Columns denoted as US and DWD2 give the RMSE of the American and the German TOC forecast schemes [from *Vanicek*, 1998a], while the last column represents the RMSE if climatological values are used as forecast at the location of Sonnblick. The last two columns give the mean bias error (MBE) and the mean absolute bias uncertainty (MABE) of the developed scheme used as TOC forecast (FC).

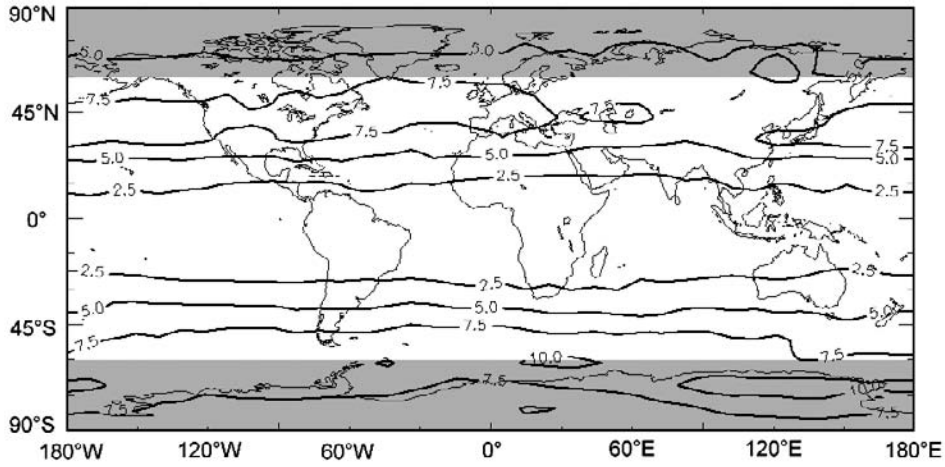


**Figure 5.** Global distribution of the yearly Mean Absolute Bias Uncertainty (MABE) in percent, which result from assuming persistency in TOC of 2 days. Regions showing polar nights are marked gray since data of TOC from EPTOMS are only available if solar radiation is reflected.

uncertainties can be estimated. The comparison is done for all stations using ground-based measurements and TOC from EPTOMS prepared by our scheme without assuming persistency. Monthly means of the RMSE for the period of 1.1.1997 to 31.12.1999 were calculated (columns signed with "MOD" in Table 2). These monthly means show a slight annual course, with a maximum near the winter solstice and a minimum after the summer solstice.

### 4.3. Influence of Uncertainties to UV Index Calculations

[49] Since TOC can be used as input parameter to a UV Index forecast the direct consequences of the intrinsic uncertainties in data processing have to be examined as well as the direct consequences from uncertainties by assuming persistency. Therefore three UV Index calculations for noon under clear sky were done for all stations over the period from 1.1.1997 to 31.12.1999 using the Austrian UV Index Model. For the first run ground-based TOC was used (black squares in Figure 6); for the second EPTOMS prepared by our scheme was used. The third run was done using data prepared by our scheme under the assumption of persistency for 2 days.

[50] From the first two runs the differences were calculated. The gray circles in Figure 6 denote the absolute amount of these differences. Figure 7 shows the frequency distribution of these differences classified in units of UV Index. Deviations less than 0.5 UV Index occur between 99.7% (Arosa) and 95.7% (Nairobi). The following class (0.5 to 1.0 UV Index) posses 0.3% to 4.3% and fill up therefore 100% for all stations. This denotes that differences due to the use of different data processing methods are in the range of ±1 UV Index. The third run was done using data prepared by our scheme under the assumption of persistency for 2 days. The result is added to Figure 7 (gray bars).

**Table 2.** RMSE of Our Developed Scheme (MOD) and Used as Forecast (FC) for All Observatories for Each Month of the Year[a]

| Root Mean Square Error | | | | | | | | | | | | | |
|---|---|---|---|---|---|---|---|---|---|---|---|---|---|
| Model | AUT | | | | | | | | | | US | DWD2 | CLIMA |
| Location | Sonnblick | | Arosa | | Hrad. Kralove | | Nairobi | | Springbok | | USA | Germany | Sonnblick |
| Month | MOD | FC | MOD | FC | MOD | FC | MOD | FC | MOD | FC | FC | FC | FC |
| January | 3.40 | 8.44 | 3.31 | 8.92 | 3.46 | 9.47 | 2.55 | 2.79 | 2.13 | 5.49 | 7 | 7 | 17 |
| February | 3.30 | 11.24 | 1.73 | 10.42 | 3.19 | 10.24 | 2.11 | 2.53 | 2.07 | 5.64 | 6 | 6 | 19 |
| March | 3.40 | 11.65 | 1.77 | 10.67 | 3.21 | 9.05 | 1.69 | 1.71 | 2.65 | 5.83 | 6 | 6 | 14 |
| April | 3.76 | 9.33 | 1.78 | 8.48 | 3.29 | 6.86 | 1.67 | 1.97 | 1.44 | 4.56 | 4 | 4 | 13 |
| May | 3.67 | 6.15 | 1.34 | 4.24 | 2.24 | 4.45 | 1.32 | 1.70 | 1.69 | 5.11 | 3 | 3 | 12 |
| June | 3.62 | 5.48 | 2.09 | 4.09 | 2.97 | 4.11 | 1.49 | 1.61 | 2.12 | 3.97 | 4 | 3 | 8 |
| July | 3.68 | 4.59 | 1.34 | 3.95 | 2.82 | 4.12 | 1.77 | 2.08 | 1.06 | 2.96 | 4 | 3 | 8 |
| August | 2.84 | 2.99 | 1.39 | 3.43 | 2.42 | 3.69 | 2.01 | 2.19 | 1.32 | 2.64 | 3 | 3 | 6 |
| September | 3.10 | 4.29 | 1.62 | 5.42 | 2.08 | 4.35 | 1.69 | 2.10 | 1.38 | 2.77 | 4 | 4 | 8 |
| October | 2.95 | 6.47 | 1.57 | 7.09 | 2.52 | 5.86 | 1.78 | 2.45 | 1.85 | 4.00 | 5 | 4 | 8 |
| November | 3.60 | 6.23 | 1.92 | 7.40 | 2.54 | 6.82 | 1.61 | 2.06 | 1.85 | 4.86 | 7 | 6 | 12 |
| December | 3.96 | 9.06 | 2.07 | 8.90 | 3.56 | 9.43 | 1.91 | 2.03 | 1.23 | 5.52 | 6 | 5 | 14 |
| Mean | 3.44 | 7.33 | 1.83 | 7.08 | 2.86 | 6.54 | 1.80 | 2.10 | 1.73 | 4.45 | 4.92 | 4.50 | 11.58 |

[a]Numbers for the month are related to the summer solstice. Therefore, 5 denotes January for the Northern Hemisphere and July for the Southern Hemisphere. The values of 0 correspond to June on the Northern Hemisphere and December on the Southern Hemisphere. The next 2 columns give the RMSE of the American and the German TOC forecast schemes [from *Vanicek*, 1998a, 1999b], while the last column represents the RMSE if climatological values are used as forecast at the location of Sonnblick.

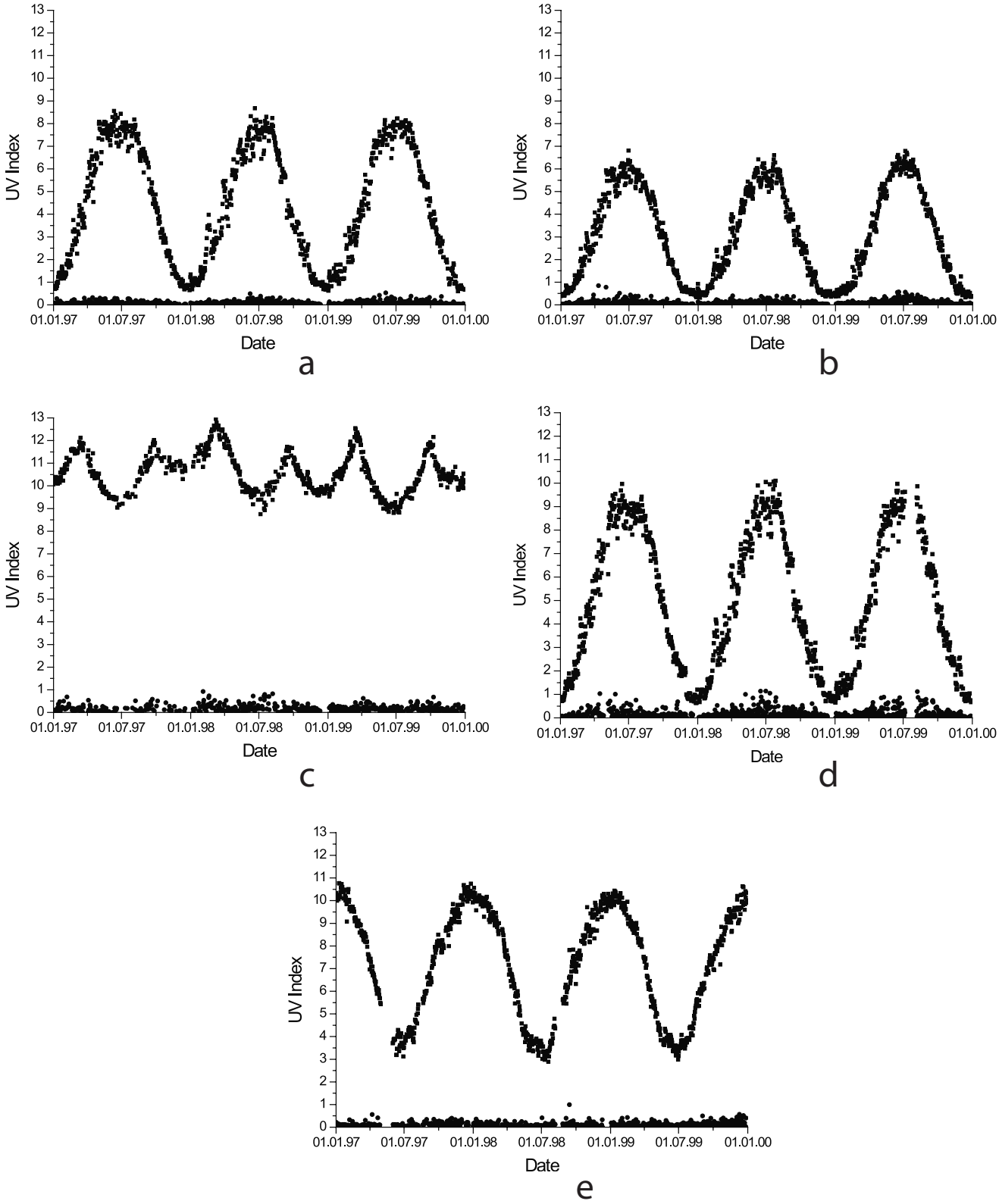


**Figure 6.** UV Index calculated for all observatories using TOC measurements from the ground (squares) and absolute amount of differences in UV Index (circles), which result from intrinsic uncertainties of TOC measurements. Data cover the period from January 1997 to December 1999. (a) Arosa. (b) Hradec Kralove. (c) Nairobi. (d) Sonnblick. (e) Springbok.

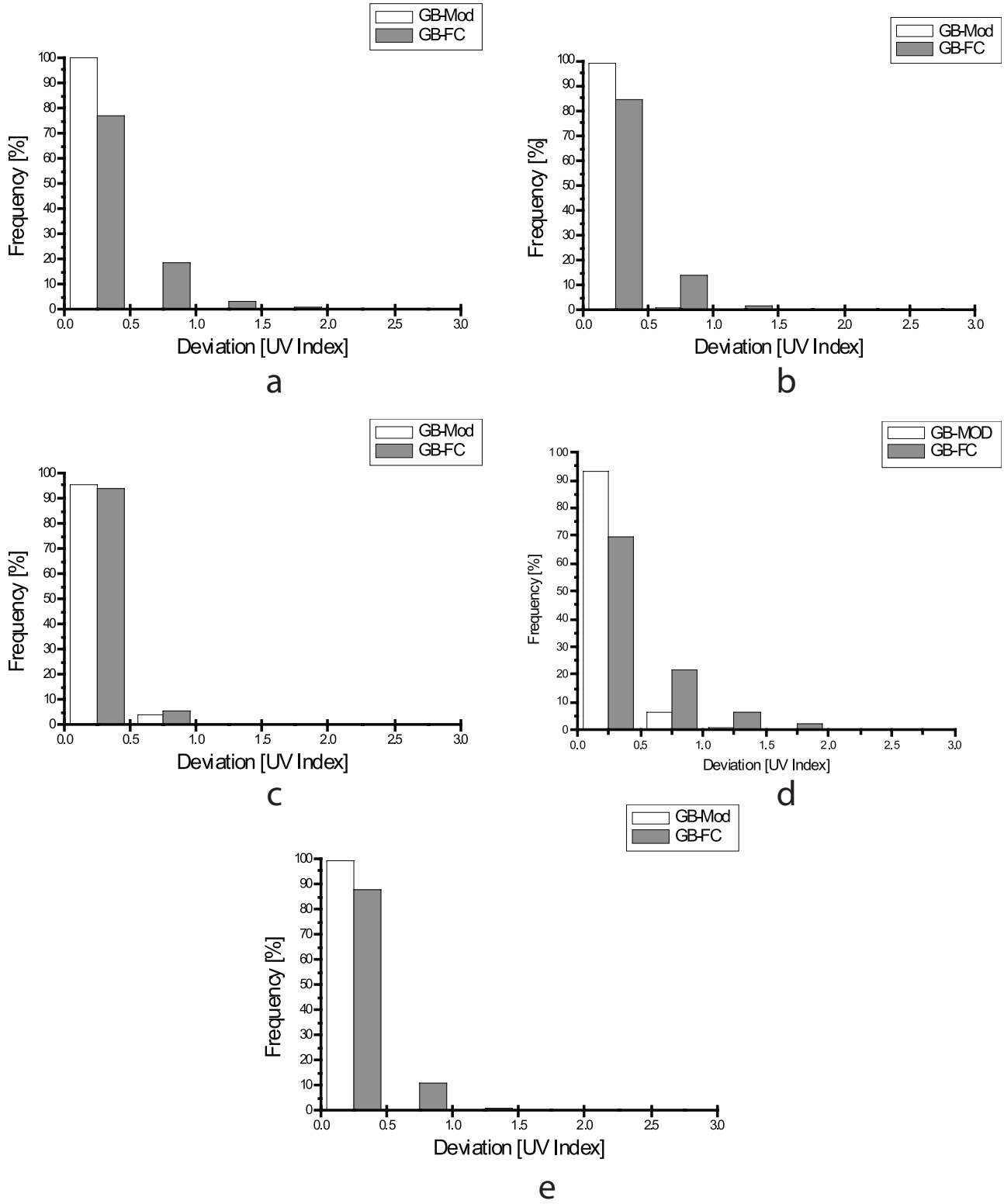


**Figure 7.** Frequency distribution of deviations classified in units of UV Index for all observatories. Empty bars show deviations, which occur because of the use of different data processing techniques (ground-based Brewer measurements versus EPTOMS prepared by the presented scheme). Gray, filled bars show deviations that result from the developed forecast scheme. (a) Arosa. (b) Hradec Kralove. (c) Nairobi. (d) Sonnblick. (e) Springbok.

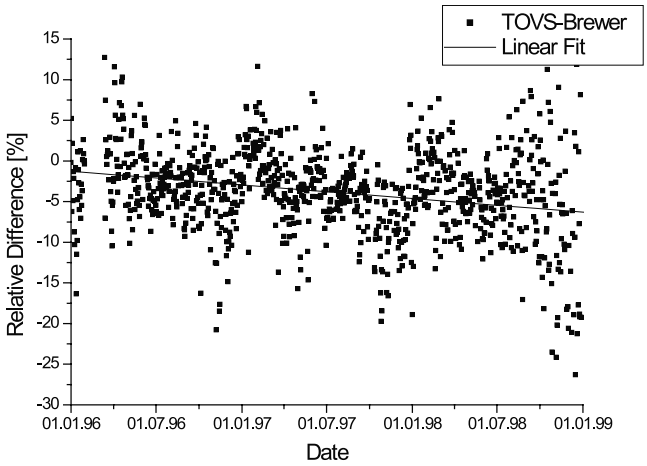


**Figure 8.** Relative differences of TOVS to ground-based Brewer TOC measurements for the period of January 1996 to January 1999. The relative differences of TOVS to the observations made at Sonnblick high mountain observatory are shown.

[51] The frequencies of deviations less than 0.5 UV Index decrease, lying between 76.7% and 93.9%. 18.8% to 4.0% can be found in the second class covering 0.5 UV Index to 1.0 UV Index. For Hradec Kralove and Nairobi the third class (1.0 to 1.5 UV Index) fills up 100% while for Springbok and Arosa differences can be found reaching 2 UV Index. The frequency of them comes to 1.5%.

## 5. Discussion

[52] We have developed a method that can be seen as a simple TOC forecast scheme. It delivers global information of TOC based on measurements from satellites and has no spatial restriction since the database is global. Corrections have been applied to account for differences in altitude and for the bias between EPTOMS and ground-based data. As shown, for example, by *Chen and Nunez* [1998] the temporal variation of TOC over a certain location is rather low within in a few days. For Sweden they estimated an average in the day-to-day changes of 7.9%. Following this, we showed that under an assumption of persistency the gained values can be used as global TOC forecast without any spatial restrictions. The scheme was developed for Sonnblick High Mountain Observatory (3106 m asl), located in the highest part of the Austrian Alps. The quality was proved by a comparison with another High Mountain Observatory, and observatories at low altitude, near the equator and in the southern hemisphere. Since the forecasted values can be used as input to a UV forecast procedure, the influence of its uncertainties to UV forecast were examined as well.

[53] To ensure high accuracy when interpolation is needed a method developed by *Krige* [1981] was used. The application of Kriging is a powerful tool in interpolating actual meteorological data like in the case of monitoring spatial measurements, as done for the Austrian UVB-Network [*Schmalwieser and Schauberger*, 2001] or in constructing climatological data bases like the spatial distribution of global solar radiation [*Venäläinen and Heikinheimo*, 1997]. *Simpson* [1998] has even shown that Kriging, used as an alternative statistical based approximation method, can substitute traditional response surface approaches for constructing polynomial approximation models.

[54] At the time two satellites deliver almost daily global information on TOC. One is EPTOMS, mentioned above. Another data set of TOC can be derived from TOVS (TIROS Operational Vertical Sounder). TOVS measurements were made onboard the NOAA satellite series. TOC values are calculated from measurement at 9.6 μm. Therefore values are also available during polar nights. TOVS data set is provided daily by NOAA with a temporal delay of 2 days. TOVS measurements have a spatial resolution of 1° in latitude and longitude. Therefore a grid of 180 × 360 points is available for the whole globe. Opposite to EPTOMS the differences between the Dobson network and the satellite values are not constant. The differences increase with time and show an additional seasonal behavior. In Figure 8 the differences are shown for Sonnblick calculated for the period from January 1996 to July 1999. At the beginning of this period differences were in the order of 2%, showing a continuous drift reaching a level of 10% in July 1999.

[55] Another possibility to get global information of TOC is to use climatological data sets. Since they are calculated as mean values for certain day of the year over several years, they show a long-term trend due to ozone depletion. Even if the trend is corrected there are still high uncertainties in the daily mean values. Climatological data are calculated from measurements over the period 1 July 1996 to 1 January 2000. Table 2 gives the annual course of the RMSE for the use of climatological data as TOC forecast for Sonnblick. This comparison shows that the presented forecast scheme delivers a good improvement compared to the use of climatological data. The RMSE is reduced from 11.6% to 7.3%. To improve the accuracy of UV Index calculations is a necessary step. High accuracy in clear sky UV Index will provide a proper base for the inclusion of other atmospheric parameters like clouds and aerosols, which will introduce additional uncertainties.

[56] *Vanicek* [1998a] investigated the RMSE of two other forecast schemes shown in Table 2. The first was developed and validated for the United States [*Long et al.*, 1996], the other for Germany [*Spänkuch and Schulz*, 1995]. Both forecast schemes are using statistical models with the following input parameter: actual ozone, temperatures of the atmosphere at 50, 100, 200, 500 and 700 hPa levels and the changes in geopotential height within the last days at 100 and 500 hPa.

[57] For the European stations RMSE of our forecast are slightly higher during winter and spring, but during summer and autumn the differences almost vanish. From this it can be seen that "more expenses than invested" in our method will lead only to a slight decrease of deviations, which are less remarkable because of the low UV values during these seasons. During summer, when the highest UV Index values occur all methods deliver the same high quality, a RMSE less than 4.6%. These RMSE are already in the order of the intrinsic uncertainties of different measuring techniques. As reported by *Basher* [1982] uncertainties for Dobson spectrophotometers are in the order of 3% as well as for the

ground-based Brewer spectrophotometers [*Kerr and McElroy*, 1995] and EPTOMS [*McPeters et al.*, 1998].

[58] For Nairobi the difference between the RMSE from the forecast and that from the intrinsic uncertainties is vanishing. This station is representative (MABE < 2.5%) for a broad zonal range (15°N to 25°S) covering 34% of the Earth's surface (Figure 5). For this band no improvement can be made since the assumption of persistency causes an increase of the RMSE between 0.42% and 0.02%.

[59] In Table 2 also the monthly mean RMSE are listed which results from the differences due to the use of measured TOC and due to the use of TOC from our scheme without assuming persistency (MOD). These RMSE are almost constant during the year and do not exceed a level of 3%. This level is surprisingly low, since it results from data, gained by operational runs also at extreme locations and spatial interpolation is involved.

[60] The radiation amplification factor (RAF) defines the effectiveness of changes in TOC to a certain biological effect (e.g., erythema, skin cancer, etc.) expressed by the biologically effective radiation. For the erythemally effective UV radiation and therefore for the UV Index the RAF is in the order of 1.2 [*McKinlay and Diffey*, 1987]: A change (increase/decrease) of 1% in TOC effects a inverse change (decrease/increase) of 1.2% in UV Index. A modeled course of the UV Index for all stations under clear sky is shown as squares in Figure 6. These courses were calculated by the Austrian UV Index Model [*Schmalwieser et al.*, 2002] using ground-based measurements. The dots in these figures denote deviations that are caused by the use of TOC gained by the different techniques. As mentioned above (section 2) these deviations are independent of the used model. They visualize that the resulting differences for the UV Index are lower than ±0.5 in more than 95% of all cases and that highest values reach up to ±1.0. This can be seen as the limit of accuracy for UV Index model calculations, because of the uncertainties in measured TOC values.

[61] For a broad zonal band (15°N to 15°S) the uncertainties in forecasted UV Index resulting from an assumption of persistency of 2 days is also ±1.0 UV Index. Outside this band more than 95% of all forecasts are also below this value.

[62] **Acknowledgments.** The measurements of TOC at Sonnblick High Mountain Observatory were supported by the Austrian Ministry of Environment, Family and Youth Affairs. The measurements of TOC at Nairobi were made available by the World Ozone and UV Data Center (WOUDC).

## References

Acosta, L. R., and W. F. J. Evans, Design of the Mexico city UV monitoring network: UV-B measurements at ground level in the urban environment, *J. Geophys. Res.*, *105*, 5017–5026, 2000.

Allaart, M. A. F., H. Kelder, and L. C. Heijboer, On the relation between ozone and potential vorticity, *Geophys. Res. Lett.*, *20*, 811–814, 1993.

Bais, A., C. Topaloglou, S. Kazadtzis, M. Blumthaler, J. Schreder, A. Schmalwieser, D. Henriques, and M. Janouch, The LAP/COST/WMO Intercomparison of Erythemal Radiometers, *WMO Report 141*, Geneva, Switzerland, 2001.

Basher, R. E., Review of the Dobson spectrophotometer and its accuracy, *WMO Global Ozone Research and Monitoring Project, Rep. No. 13*, Geneva, Switzerland, 1982.

Blumthaler, M., and W. Ambach, Solar UVB-albedo of various surfaces, *Photochem. Photobiol.*, *48*, 85–88, 1988.

Blumthaler, M., and R. Silbernagl, The Austrian UVB monitoring network—Calibration and quality control of broadband detectors, in *Report of the WMO-WHO Meeting of Experts on Standardization of UV Indices and their Dissemination to the Public*, *WMO Rep. No. 127*, pp. 29–32, Geneva, Switzerland, 1997.

Bodecker, G. E., J. C. Scot, K. Kreher, and R. L. McKenzie, Global ozone trends in potential vorticity coordinates using TOMS and GOME intercompared against the Dobson network: 1978–1998, *J. Geophys. Res.*, *106*, 23,029–23,042, 2001.

Bodhaine, B. A., E. G. Ellsworth, R. L. McKenzie, and P. V. Johnston, Calibrating broadband UV instruments: Ozone and solar zenith angle dependence, *J. Atmos. Oceanic Technol.*, *15*, 916–926, 1998.

Burrows, W. R., M. Vallée, D. I. Wardle, J. B. Kerr, L. J. Wilson, and D. W. Tarasick, The Canadian operational procedure for forecasting total ozone and UV radiation, *Meteorol. Appl.*, *1*, 247–265, 1994.

Casale, G. R., D. Meloni, S. Miano, S. Palmieri, A. M. Siani, and F. Cappellani, Solar UV-B irradiance and total ozone in Italy: Fluctuations and trends, *J. Geophys. Res.*, *105*, 4895–4902, 2000.

Chen, D., and M. Nunez, Temporal and spatial variability of total ozone in southwest Schweden revealed by ground-based instruments, *Int. J. Clim.*, *18*, 1237–1246, 1998.

Chiapello, I., P. Goloub, D. Tanre, A. Marchand, J. Herman, and O. Torres, Aerosol detection by TOMS and POLDER over oceanic regions, *J. Geophys. Res.*, *105*, 7133–7142, 2000.

CIE, A reference action spectrum for ultraviolet induced erythema in human skin, CIE Research Note, *CIE Journal*, *6*, 17–22, 1987.

De Backer, H., et al., Comparison of Measured and Modelled UV Indices, *J. Meteorol. Apps.*, *8*, 267–277, 2001.

Eck, T. F., P. K. Bhartia, and J. B. Kerr, Satellite estimation of spectral UVB irradiance using TOMS derived total ozone and UV reflectivity, *Geophys. Res. Lett.*, *22*, 611–614, 1995.

Feister, U., and K. Balzer, Surface ozone and meteorological predictors on a subregional scale, *Atmos. Environ., Ser. A*, *25*(9), 1781–1790, 1991.

Feister, U., and R. Grewe, Spectral albedo measurements in the UV and visible region over Different Types of Surfaces, *Photochem. Photobiol.*, *62*, 736–744, 1995.

Feister, U., A. Nötlich, and R. Grewe, Short-term forecast of biologically effective UV radiation: Comparison between modelled and measured irradiation, *Meteorol. Appl.*, *3*, 75–89, 1996.

Gesch, D. B., and K. S. Larson, Techniques for development of global 1-kilometre digital elevation models, in *Pecora Thirteen, Human Interactions with the Environment—Perspectives from Space*, EOS Data Center, Sioux Falls, S.D., 1996.

Heimo, A., R. Philipona, and C. Fröhlich, The Swiss UV Radiation Monitoring Network, in *Report of the WMO-WHO Meeting of Experts on Standardization of UV Indices and their Dissemination to the Public*, *WMO Rep. No. 127*, pp. 55–58, Geneva, Switzerland, 1997.

Herman, J. R., N. Krotkov, E. Celarier, D. Larko, and G. Labow, Distribution of UV radiation at the Earth's surface from TOMS-measured UV-backscattered radiances, *J. Geophys. Res.*, *104*, 12,059–12,076, 1999.

Hsu, N. C., J. R. Herman, O. Torres, B. N. Holben, D. Tanre, T. F. Eck, A. Smirnov, B. Chatenet, and F. Lavenu, Comparisons of the TOMS aerosol index with Sun-photometer aerosol optical thickness: Results and applications, *J. Geophys. Res.*, *104*, 6269–6280, 1999.

ICNIRP, *Global Solar UV Index*, WHO, WMO, UNEP, ICNIRP- 1/95 Oberschleißheim, 1995.

Isaaks, E. H., and R. M. Srivastava, *An Introduction to Applied Geostatistics*, Oxford Univ. Press, New York, 1989.

Kalliskota, S., J. Kaurola, P. Taalas, J. R. Herman, E. Celarier, and N. A. Krotkov, Comparison of daily UV doses estimated from Nimbus 7/TOMS measurements and ground-based spectroradiometric data, *J. Geophys. Res.*, *105*, 5059–5068, 2000.

Kerr, J. B., and C. T. McElroy, Total ozone measurements made with the Brewer ozone spectrophotometer during STOIC 1989, *J. Geophys. Res.*, *100*, 9225–9230, 1995.

Kneiszys, F. X., G. P. Anderson, E. P. Sheetle, W. O. Gallery, L. W. Abreu, J. E. Selby, J. H. Chetwynd, and S. A. Clough, *User's Guide to LOWTRAN 7*, AFGL Tech. Rep., AFGL-TR-88-0177, Air Force Geophys. Lab., Bedford, Mass., 1988.

Koepke, P., et al., Comparison of models used for UV Index calculations, *Photochem. Photobiol.*, *67*, 657–662, 1998.

Koepke, P., et al., An overview of the results from the comparison of UV-Index forecasted and measured at all atmospheric conditions including clouds, in *IRS 2000: Current Problems in Atmospheric Radiation*, edited by W. L. Smith and Y. M. Timofeyev, A. Deepak Publishing, Hampton, Va., 1181–1185, 2001.

Krige, D. G., Lognormal-de Wijsian Geostatistics for Ore Evaluation, *South African Institute of Mining and Metallurgy Monograph Series: Geostatistics*, *1*, pp. 51, 1981.

Krotkov, N. A., P. K. Bhartia, J. R. Herman, V. Fioletov, and J. Kerr, Satellite estimation of spectral surface UV irradiance in the presence of

tropospheric aerosols, 1, Cloud-free case, *J. Geophys. Res.*, *103*, 8779–8794, 1998.

Krotkov, N. A., J. R. Herman, P. K. Bhartia, V. Fioletov, and Z. Ahmad, Satellite estimation of spectral surface UV irradiance, 2, Effects of homogeneous clouds and snow, *J. Geophys. Res.*, *106*, 11,743–11,760, 2001.

Krzyscin, J. W., Impact of the ozone profile on the surface UV radiation: Analysis of the Umkehr and UV measurements at Belsk (52°N, 21°E), Poland, *J. Geophys. Res.*, *105*, 5009–5015, 2000.

Kryscin, J. W., J. Jaroslawski, and P. Sobolewski, On an improvement of UV index forecast: UV index diagnosis and forecast for Belsk, Poland in Spring/Summer 1999, *J. Atmos. Sol. Terr. Phys.*, *63*, 1593–1600, 2001.

Kuchinke, C., and M. Nunez, Cloud Transmission Estimates of UV-B Erythemal Irradiance, *Theor. Appl. Climatol.*, *63*, 149–161, 1999.

Li, Z., P. Wang, and J. Cihlar, A simple and efficient method for retrieving surface UV radiation dose rate from satellite, *J. Geophys. Res.*, *105*, 5027–5036, 2000.

Liu, S., S. A. McKeen, and S. Madronich, Effects of athropogenic aerosols on biologically active ultraviolet radiation, *Geophys. Res. Lett.*, *18*, 2265–2268, 1991.

Long, C. S., A. J. Miller, H. Lee, J. D. Wild, R. C. Pryzwarty, and D. Hufford, Ultraviolet Index forecasts issued by the National Weather Service, *Bull. Am. Meteorol. Soc.*, *77*, 729–748, 1996.

McClatchey, R. A., R. W. Fenn, J. E. A. Selby, F. E. Volz, and J. S. Garing, *Optical Properties of the Atmosphere*, *Rep. AFCRL-72-0497*, Air Force Cambridge Res. Lab., Cambridge, Mass., 1972.

McKinlay, A. F., and B. L. Diffey, A reference action spectrum for ultraviolet induced erythema in human skin, in *Human Exposure to Ultraviolet Radiation: Risks and Regulations*, edited by W. R. Paschier and B. F. M. Bosnjakovic, Excerpta Medica, Elsevier Sci., New York, 1987.

McPeters, R. D., et al., *Earth Probe Total Ozone Mapping Spectrometer* (*TOMS*) *Data Products User's Guide*, NASA Ref. Publ., Greenbelt, Md., 1998.

Nunez, M., K. Michael, D. Turner, M. Wall, and C. Nilsson, A satellite-based climatology of UV-B irradiance for Antartic coastal regions, *Int. J. Climatol.*, *17*, 1029–1054, 1997.

Oliver, M. A., and R. Webster, Kriging: A method of interpolation for geographical information system, *Int. J. Geograph. Inf. Syst.*, *4*, 313–332, 1990.

Plets, H., and C. Vynckier, A comparative study of statistical total column ozone forecasting models, *J. Geophys. Res.*, *105*, 26,503–26,517, 2000.

Poulin, L., and W. J. F. Evans, METOZ: Total ozone from meteorological parameters, *Atmos. Ocean*, *32*, 285–297, 1994.

Reed, R. J., The role of vertical motions in ozone weather relationships, *J. Meteorol.*, *7*, 263–267, 1950.

Ren, P. B. C., Y. Gjessing, and F. Sigernes, Measurements of solar ultra violet radiation on the Tibetan Plateau and comparisons with discrete ordinate method simulations, *J. Atmos. Sol. Terr. Phys.*, *61*, 425–446, 1999.

Schauberger, G., Model for the global irradiance of the solar biologically-effective ultraviolet-radiation on inclined surfaces, *Photochem. Photobiol.*, *52*, 1029–1032, 1990.

Schmalwieser, A. W., and G. Schauberger, Validation of the Austrian forecast model for solar, biologically-effective ultraviolet radiation—UV Index for Vienna, Austria, *J. Geophys. Res.*, *105*, 26,661–26,668, 2000.

Schmalwieser, A. W., and G. Schauberger, Monitoring network for erythemally-effective solar ultraviolet radiation in Austria: Determination of the measuring sites and visualisation of the data, *Theor. Appl. Climatol.*, *69*, 221–229, 2001.

Schmalwieser, A. W., G. Schauberger, and H. Dobesch, Die Bewölkungsprognose als Eingangsparameter für die UV Index Prognose, *Österreichische Beiträge zu Meteorologie und Geodynamik*, *399*(7A), 1–4, 2001.

Schmalwieser, A. W., G. Schauberger, M. Janouch, M. Nunez, T. Koskela, D. Berger, G. Karamanian, P. Prosek, and K. Laska, Global validation of a forecast model for irradiance of the solar, erythemally effective UV radiation, *J. Opt. Eng.*, *41*(12), 3040–3050, 2002.

Schwander, H., P. Koepke, and A. Ruggaber, Uncertainties in modeled UV irradiances due to the limited accuracy and availability of input data, *J. Geophys. Res.*, *102*, 9419–9429, 1997.

Seckmeyer, G., et al., Geographical differences in the UV measured by intercompared spectroradiometers, *Geophys. Res. Lett.*, *22*(14), 1889–1892, 1995.

Simic, S., P. Weihs, G. Rengarajan, F. Eywo, and H. Kromp-Kolb, *Messungen der direkten spektralen Sonnenstrahlung und Prognose des Gesamtozons über Österreich*, Report to the Ministry of Agriculture, Forestry and Environment, Vienna, Austria, 2000.

Simpson, T. W., *Comparison of Response Surface and Kriging Models in the Multidisciplinary Design of an Aerospike Nozzle*, ICASE Rep. No. 98-16, NASA/CR-1998-206935, 1998.

Spänkuch, D., and E. Schulz, Diagnosting and forecasting total ozone column ozone by statistical relations, *J. Geophys. Res.*, *100*, 18,873–18,895, 1995.

Torres, O., P. K. Bhartia, J. R. Herman, Z. Ahmad, and J. Gleason, Derivation of aerosol properties from a satellite measurements of backscattered ultraviolet radiation: Theoretical basis, *J. Geophys. Res.*, *103*, 17,099–17,110, 1998.

Vanicek, K., Predpovedi UV-Index v ceskem hydrometeorologickem ustavu, *Meteorol. Bull.*, *51*, 129–135, 1998a.

Vanicek, K., Differences between dobson and brewer simultaneous observations of total ozone at Hradec Kralove, in *Atmospheric Ozone: Proceedings of the XVIII Quadrennial Ozone Symposium, 12–21 September 1996, L'Aquila, Italy*, edited by R. D. Bojkov and G. Visconti, pp. 81–84, Parco Scientifico e Tecnologico d'Abruzzo, L'Aquila, Italy, 1998b.

Vanicek, K., Z. Lytinska, T. Frei, and A. Schmalwieser, *UV Index for the Public*, Publ. of the Eur. Commun., Brussels, Belgium, 2000.

Venäläinen, A., and M. Heikinheimo, The Spatial variation of long-term mean global radiation in Finland, *Int. J. Climatol.*, *17*, 1–12, 1997.

Vogel, G., D. Spänkuch, E. Schulz, U. Feister, and W. Döhler, Regional short-term forecast of total column ozone, *Atmos. Environ.*, *29*, 1155–1163, 1995.

Vogelmann, A. M., T. P. Ackermann, and R. P. Turco, Enhancements in biologically effective ultraviolet radiation following volcanic eruptions, *Nature*, *359*, 47–49, 1992.

Wang, P., Z. Li, J. Cihlar, D. I. Wardle, and J. Kerr, Validation of an UV inverserion algorithm using satellite and surface measurements, *J. Geophys. Res.*, *105*, 5037–5048, 2000.

Weihs, P., S. Simic, W. Laube, W. Mikielewicz, G. Rengarajan, and M. Mandl, Albedo influence on surface UV irradiance at the High Mountain Observatory (3106 m altitude), *J. Appl. Meteorol.*, *38*, 1599–1610, 1999.

---

G. J. R. Coetzee, South African Weather Service, Forum Building, Private Bag X097, 159 Struben Street, Pretoria, 0001, South Africa. (coetzee@weathersa.co.za)

M. Janouch, Solar and Ozone Observatory, Czech Hydrometeorological Institute, Hvezdarna 456, 500 08 Hradec Kralove 8, Czech Republic. (janouch@chmi.cz)

G. Schauberger and A. W. Schmalwieser, Institute of Medical Physics and Biostatistics, University of Veterinary Medicine, Veterinaerplatz 1, A-1210 Vienna, Austria. (gunther.schauberger@vu-wien.ac.at; alois.schmalwieser@vu-wien.ac.at)

S. Simic and P. Weihs, Institute of Physics and Meteorology, University of Agricultural Science, Tuerkenschanzstrasse 18, A-1180 Wien, Austria. (simic@edv1.boku.ac.at; h515t3@tornado.boku.ac.at)

R. Stubi, Aerological Station Payerne, MeteoSwiss, Box 316, CH-1530 Payerne, Switzerland. (rene.stubi@meteoswiss.ch)

## 2.3 Publikation 3:

# Sensitivity of UV Erythemally Effective Irradiance and Daily Dose to Spatial Variability in Total Ozone

Alois W. Schmalwieser, Thilo Erbertseder, Günther Schauberger and Philipp Weihs

Photochemistry and Photobiology 84: 1149–1163, 2008

Photochemistry and Photobiology, 2008, 84: 1149–1163

# Sensitivity of UV Erythemally Effective Irradiance and Daily Dose to Spatial Variability in Total Ozone

**Alois W. Schmalwieser*[1], Thilo Erbertseder[2], Günther Schauberger[1] and Philipp Weihs[3]**

[1]Institute of Medical Physics and Biostatistics, University of Veterinary Medicine, Vienna, Austria
[2]Deutsches Fernerkundungsdatenzentrum, Deutsches Zentrum für Luft- und Raumfahrt, Oberpfaffenhofen, Germany
[3]Institute of Meteorology, University of Natural Resources and Applied Life Sciences, Vienna, Austria

**Received 30 April 2007, accepted 1 December 2007, DOI: 10.1111/j.1751-1097.2007.00285.x**

## ABSTRACT

**The total ozone column (TOC) is the most significant quantity for estimating the erythemally effective UV radiation under clear sky conditions. Uncertainties in TOC measurements and a limited spatial and temporal resolution therefore influence the quality of calculated erythemally effective radiation. The UV Index, the internationally accepted measure of the erythemally effective radiation, is used in public and the media to inform about current levels of UV radiation and builds the base for sun protection. Thus, the accuracy of the promoted values is essential. While in a preceding study we estimated the influence of measurement uncertainties, in this study we analyze the influence of spatial gaps and variability of TOC to the erythemally effective irradiance at noon and to the daily dose. The results allow defining the necessary spatial resolution of TOC values when a certain accuracy for the UV Index or for the purpose of sun protection is required. In case of the erythemally effective irradiance this study reveals that spatial gaps in TOC or the assumption of spatial invariability causes similar uncertainties independent of the geographic location. At higher latitudes the higher spatial variability of TOC counteracts the lower level of irradiance. For the daily dose gaps in TOC have an even higher impact at higher latitudes.**

## INTRODUCTION

During the past two decades public interest in exposure to sunlight has risen continuously. The publicity of the ozone hole and studies that documented the increase of skin cancer have contributed to the rise in interest. In many countries most of the UV exposure results from spare time activities and from holidays in southern destinations (1). The latter has increased in industrial countries strongly in the winter season when the skin is photoadopted to low levels of solar radiation (2). Information on the expected intensity level and recommendations for sun protection is therefore a helpful tool in health care.

More than 10 years ago the UV Index was introduced as a dimensionless number to indicate the intensity levels of solar UV radiation. Nowadays several international organizations and standards agree on the UV Index (International Commission on Nonionizing Radiation Protection, World Health Organization, World Meteorological Organization or European Commission [3–6]) and it is proposed to be used in public information. The UV Index is also a base for sun protection recommendations, risk assessment and health care (*e.g.* 4,7). Hence, the accuracy of promoted UV Index values is crucial. The promoted UV Index values are gained by measurements or by models sometimes including forecast calculations.

An ongoing process in model development and improvement has led to a variety of models where the main source of inaccuracy is no longer the radiative transfer calculation itself. In fact, the quality of the model output depends on the availability and accuracy of the input parameters. The most important parameters under cloudless sky conditions are the total ozone column (TOC) (*e.g.* 8,9) as well as the aerosol content (*e.g.* 10).

During the past years some studies were published which deal with the accuracy of calculated UV Index values. For example Koepke *et al.* (11) inter-compared different models with respect to the erythemally effective UV radiation and De Backer *et al.* (12) compared model results to ground-based measurements. Furthermore, several studies on the promotion and accuracy of the UV Index were carried out, like validations of worldwide forecasts of the erythemally effective irradiance (*e.g.* 13,14) as well as the daily dose (15). Recently, the uncertainty of the erythemally effective irradiance and daily dose resulting from uncertainties in TOC measurements was investigated (16).

Measurements of TOC are taken at a certain (discrete) location. When such a measured value is used to represent the surrounding region, one has to take into account an error which results from the assumption of spatial invariability of TOC. Consequently, spatial variability can be defined as a function of spatial distance and can be divided into a longitude, latitude and altitude component. Changes in TOC with topographic altitude are rather low (*e.g.* 17–19) and can be corrected in a satisfactory way (*e.g.* 20).

*Corresponding author email: alois.schmalwieser@vu-wien.ac.at (Alois W. Schmalwieser)

The latitudinal and longitudinal variability of TOC is caused by a variety of phenomena of different temporal and spatial scales (21). In general, the total ozone distribution is determined by photochemical production, transport and destruction (22). While in the tropics ozone variability can mainly be attributed to photochemical processes, at higher latitudes variability is mainly governed by atmospheric dynamics, *i.e.* planetary wave activity. Planetary waves are the dominating source mechanism for transport processes in the stratosphere. In polar regions they are responsible for the erosion and breakdown of the polar vortices, where effective ozone depletion is caused by complex chemical processes (23). In the mid-latitudes planetary waves are responsible for advection of tropical (ozone poor) or polar (ozone rich) air masses leading to steep gradients in TOC. There, the classical ozone–weather relationship (*e.g.* 24–26) dominates the spatial variability on the synoptic scale, as studied in this paper. As a result of these processes steep gradients with more than 100 DU per 1000 km in both latitudinal and longitudinal directions can occur in the TOC distribution at the polar vortex edge, at ozone mini-holes and whenever polar air masses are advected into mid- and subtropical latitudes and *vice versa* associated with planetary wave activity. In the tropics ($<30°$N, $<30°$S) there is hardly any gradient in longitude, *i.e.* zonal direction.

The global mean distribution of total ozone is characterized by a continuous latitudinal gradient (*e.g.* 27) increasing from the tropics to mid- and high latitudes. The latitudinal gradient strongly depends on the season. It is small in summer and autumn, but steep in winter and spring. This gradient varies with season and is on the order of 0.05–0.4% per 100 km.

In this paper we focus on quantifying the sensitivity of the erythemally effective UV radiation under clear sky conditions to spatial TOC variability. Hence we examine the effects caused by spatial gaps in TOC data or by assuming spatial invariability, *i.e.* neglecting spatial variability. We aim at quantifying the latitudinal and longitudinal contribution to the uncertainty.

The analysis is performed for calculated values of both irradiance at solar noon and daily dose as the length of the day varies significantly with latitude and therefore the ratio between irradiance and dose changes as well. The results of this study allow us further to stipulate requirements for the spatial resolution of TOC data when a certain accuracy in the UV Index or sun protection is demanded.

## MATERIALS AND METHODS

The uncertainty of the erythemally effective UV radiation resulting from spatial gaps in TOC measurements or the assumption of spatial invariability is quantified by using satellite-borne observations from the Total Ozone Mapping Spectrometer (TOMS). These data are available in gridded form at a certain spatial discretization.

Starting with a fixed geolocation, we calculate the erythemally effective UV radiation using the according TOC measured at this site. Afterwards the erythemally effective UV radiation for this site is calculated by consecutively inputting TOC from distant grid points. The differences between the UV value derived for the geographically correct TOC and the UV values gained when using TOC from distant grid points allow us to estimate the uncertainty as a function of distance. The differences are calculated separately in latitudinal and longitudinal direction.

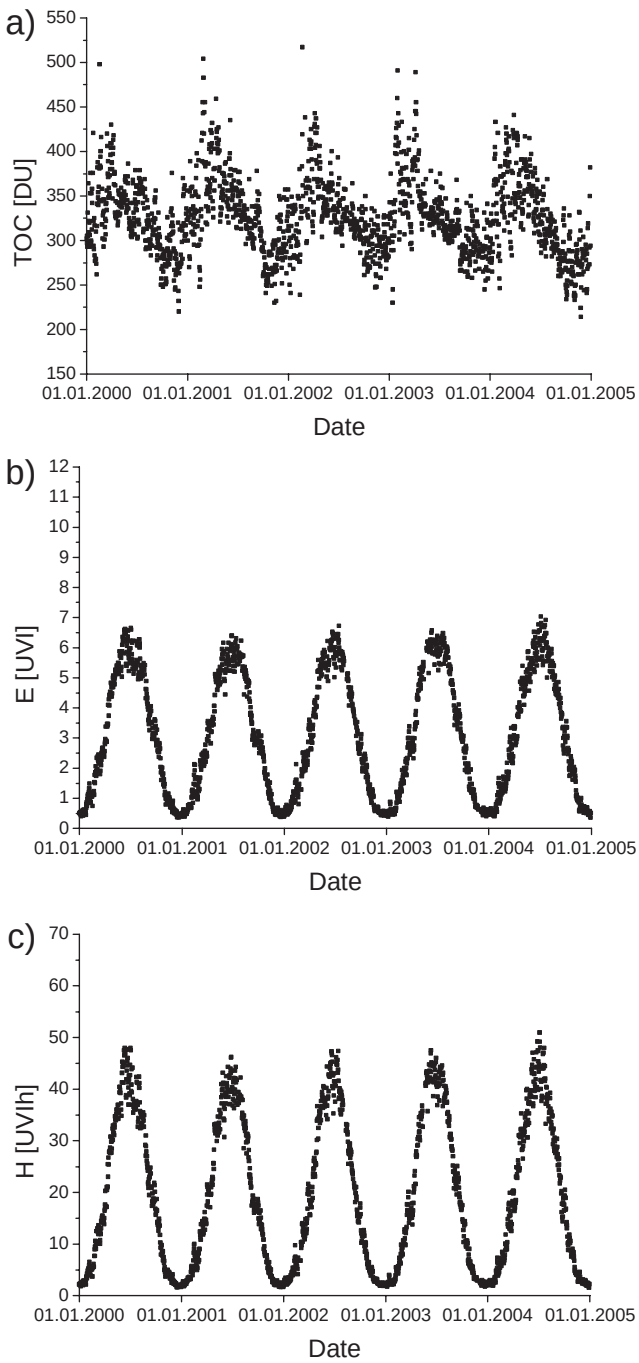


**Figure 1.** (a) Total ozone content of the atmosphere (TOC), (b) modeled erythemally effective irradiance at solar noon ($E$) and (c) daily dose ($H$) for the location of 50.0°N, 15.6°E (near Hradec Kralove, Czech Republic) under clear skies.

In connection to an earlier paper (16), where we estimated the influence of uncertainties in measured TOC, we selected the same three geolocations at 50°N, 1°S and 30°S representing the mid-latitudes, tropics and subtropics. The chosen geolocations have a similar longitude. This selection enables to estimate the influence of latitude regarding solar elevation, length of the day and TOC and exhibits the different statistical behavior over each site.

*TOC data.* The TOC data are taken from the TOMS on board NASA's Earth Probe satellite, hereafter called EPTOMS (28). The EPTOMS instrument is essentially similar to its three TOMS predecessors, flown aboard Nimbus 7 (from October 1978 to May 1993),

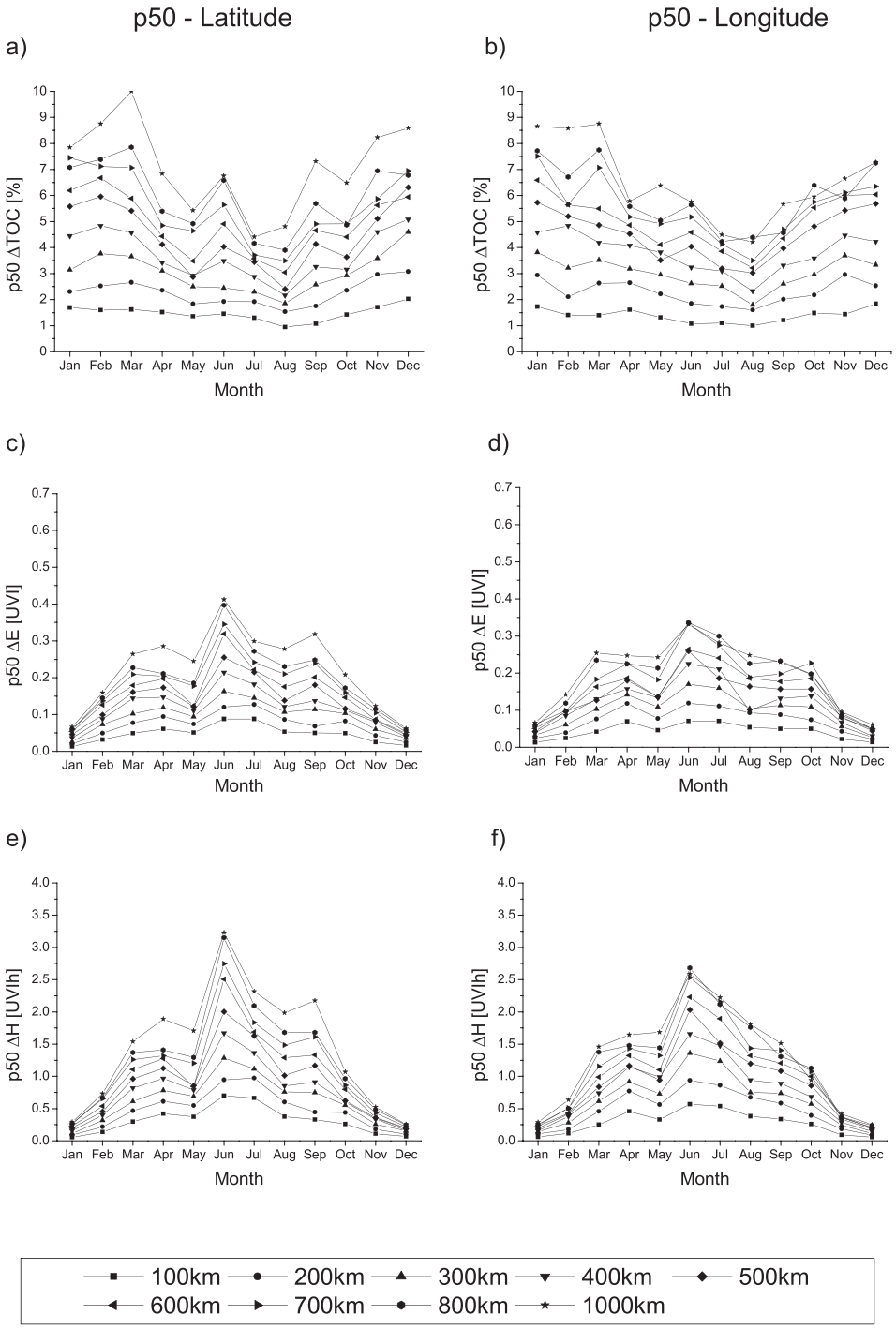


**Figure 2.** Fiftieth percentiles for absolute amount of differences in total ozone p50ΔTOC (a, b), irradiance at solar noon p50Δ*E* (c, d) and daily dose p50Δ*H* (e, f) for the region from 50°N to 60°N and 16°E to 26°E for certain spatial distances in latitude (left panels) and in longitude (right panels).

aboard Meteor 3 (August 1991 to December 1994) and on Adeos (September 1996 to June 1997)—a single, fixed monochromator, with exit slits at six near-UV wavelengths, which measures the incident solar radiation and backscattered UV sunlight. TOCs are retrieved from these measurements at a horizontal resolution of typically 50 × 50 km at nadir. Measurements are taken close to solar noon. For this study we use gridded Level 3 near real-time data, which are delivered on a 1° latitude by 1.25° longitude grid and are disseminated a few hours after overpassing (29). For reason of consistency with a preceding paper (16), we apply near real-time data from 2000 to 2004, which was processed at the time of acquisition by TOMS Version 7.

The data domains are also chosen in correspondence to the abovementioned paper (16). There we estimated the uncertainties of TOC measurements and the limitation of accuracy in UV index calculations resulting from these uncertainties. The region on the northern hemisphere covers the latitudinal range from 50°N to 60°N and in longitude from 16°E to 28°E and includes the location of the Solar and Ozone Observatory of Hradec Kralove (50.183°N, 15.833°E,

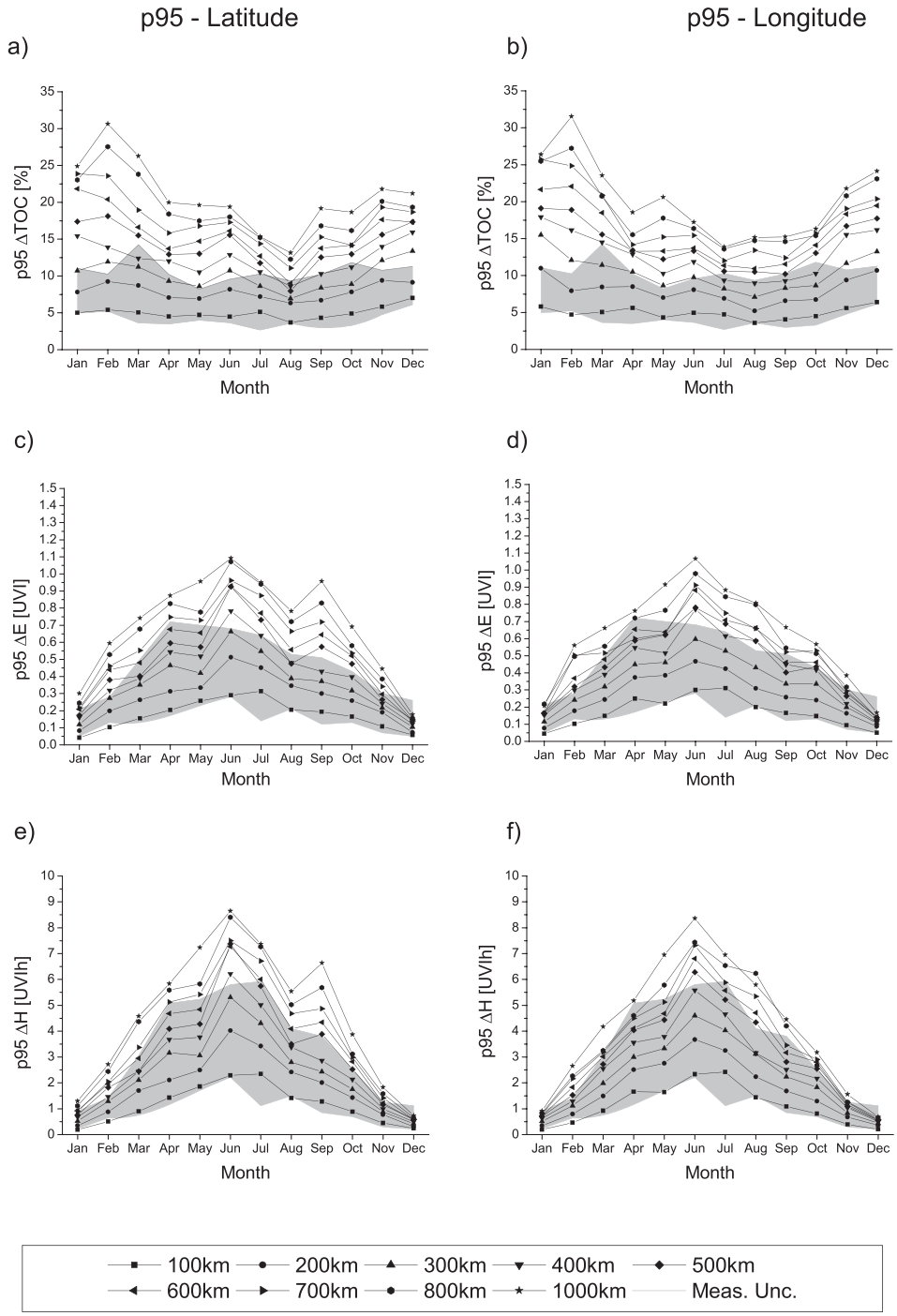


**Figure 3.** Ninety-fifth percentiles for absolute amount of differences in total ozone p95ΔTOC (a, b), irradiance at solar noon p95Δ*E* (c, d) and daily dose p95Δ*H* (e, f) for the region from 50°N to 60°N and 16°E to 26°E for certain spatial distances in latitude (left panels) and in longitude (right panels).The gray areas indicate the p95 of uncertainties of TOC measurements and the corresponding p95 for irradiance and daily dose, as given in Schmalwieser *et al.* (16).

Czech Republic). The region at the equator ranges from 5°S to 5°N and from 26°E to 38°E and includes the ozone observatory near Nairobi, Kenya (1.3°S, 36.8°E). The southern region around Springbok (29.7°S, 17.9°E), Republic of South Africa is between 30°S and 19°S and between 16°E and 28°E.

For our analysis we included all available EPTOMS data between 1 January 2000 and 31 December 2004. Since 2002 there has been an ongoing problem in calibration of EPTOMS data especially for the mid-latitudes (30). However, statistical descriptors (see below) estimated for 1 January 2000 to 31 December 2001 do not show a systematic difference to those when estimated for 1 January 2002 to 31 December 2004. With the end of the year 2004 EPTOMS data delivery was terminated and replaced by data from the new Ozone Mapping Instrument onboard NASA's Aura satellite launched in July 2004 (31).

*Uncertainty from spatial gaps and variability*. In order to quantify the error introduced in the erythemally effective radiation by assuming spatial invariability or spatial gaps in TOC data, model calculations were performed with a fast spectral UV radiation model. This model was developed by some of us in 1995 in order to forecast the erythemally effective radiation on a global scale. The development

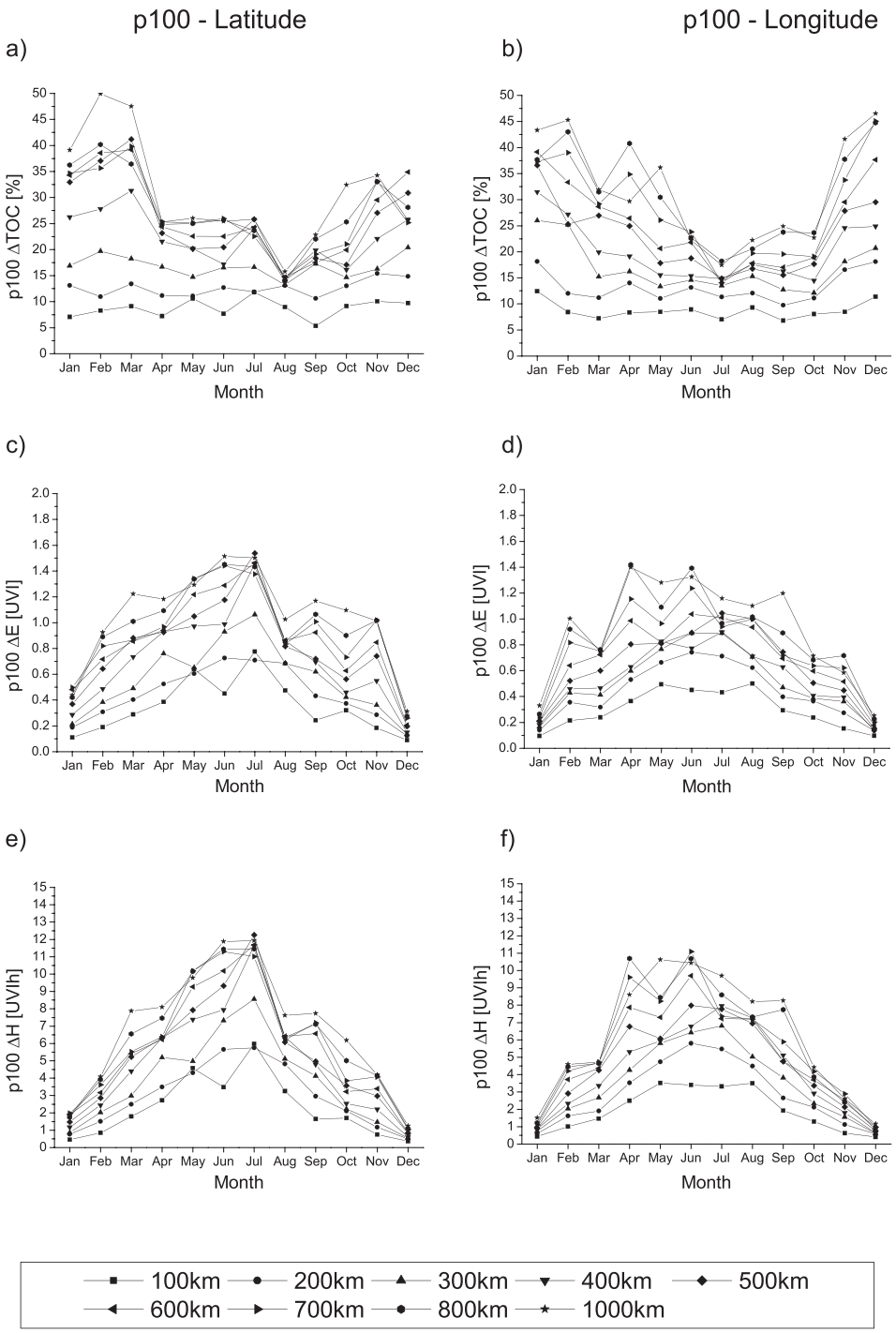


**Figure 4.** Hundredth percentiles for absolute amount of differences in total ozone p100ΔTOC (a, b), irradiance at solar noon p100Δ*E* (c, d) and daily dose p100Δ*H* (e, f) for the region from 50°N to 60°N and 16°E to 26°E for certain spatial distances in latitude (left panels) and in longitude (right panels).

followed a suggestion of Diffey (32) incorporating several improvements. The radiation model calculates the spectral irradiance at 17 discrete wavelengths between 297 and 400 nm with a higher resolution in the UVB than in the UVA range. The database from Bener (33), which was obtained from spectral measurements made over several years at Davos (46°48′N, 9°49′E, 1590 m a.s.l.), was used for parameterization. A detailed description of the model can be found in Schmalwieser *et al.* (13). The model was validated considering the erythemally effective UV radiation in the past by a comparison with other models (11,12,34) as well as by a comparison with measurements made on four continents for irradiance (13) and daily dose (15).

The erythemally effective irradiance is derived using the Commission Internationale de l'Eclairage (CIE) action spectrum of the erythema (35) for weighting, followed by the integration over the whole spectral range. The erythemally effective irradiance is expressed in units of the UV Index, gained by multiplying the effective irradiance given in $W_{\mathrm{eff}}\,\mathrm{m}^{-2}$ by 40. The erythemally effective daily dose is expressed in units of UV Index hours (UVIh) following a suggestion of Saxebøl (36). The daily dose is gained by integrating the daily course of the effective irradiance from sunrise to sunset. A received dose of 1 UVIh is equal to 90 J $\mathrm{m}^{-2}$ or 0.9 standard erythemal dose (37).

For this work an aerosol-free atmosphere and cloud-free sky are assumed to point out the influence of the TOC only. Therefore, the input parameters comprise date, time, geographic position, altitude and TOC.

The influence of spatial variability and data gaps in TOC is estimated by using TOC data from different grid points to calculate the erythemally effective radiation for a selected fixed geolocation. The erythemally effective radiation is calculated for the selected initial point and a certain day. Step by step TOC from distant grid points is applied to calculate the erythemally effective radiation at the initial point for the same date. Due to the spatial variability of TOC the calculated erythemally effective radiation differs. Consequently, the absolute differences between the outcome when using the geographically correct TOC and the outcome when using TOC from a distant geolocation are calculated. These differences build the base for the statistical analysis. It is expected that the differences become larger with increasing distance. The influence of spatial gaps or assumed spatial invariability in TOC is estimated up to distances of 1000 km for longitude and latitude.

Analysis of the differences was performed using the 50th percentile (p50), the 95th percentile (p95) and the 100th percentile (p100) of absolute differences for each month of the year. p50 denotes that every second day the difference is larger. p95 denotes that on one day in a month the difference is larger than this one. p100 denotes simply the highest difference which was found for this month within the 5 year period.

The percentiles of differences in longitude and latitude were interpolated to distances to multiples of 100 km for comparability in latitude and longitude at all locations. At Hradec Kralove 1° in longitude corresponds to 65 km, at Springbok 88 km and at Nairobi 101 km whereas the longitudinal resolution of gridded EPTOMS total ozone data is 1.25°.

## RESULTS

### Influence of spatial total ozone variability at 50°N

At 50°N the TOC exhibits high variability not only during the year but also within a few days. The latter mainly coupled to the planetary wave activity and the associated advection of tropical (ozone poor) or polar (ozone rich) air masses in the stratosphere into mid-latitudes TOC values can be found between 200 DU and 500 DU (Fig. 1a) and may change by more than 100 DU within a month. The erythemally effective irradiance at solar noon modeled for clear sky (Fig. 1b) changes from 0.5 UVI in winter to 7 UVI in summer. The length of the day undergoes large changes of more than 8 hours. The modeled daily dose (Fig. 1c) may be below 2 UVIh in winter and can reach 50 UVIh near the summer solstice.

The error in TOC arising from assuming a spatially homogeneous ozone distribution is presented in Figs. 2a,b, 3a,b and 4a,b. At the p50, p95 and p100 level the differences in TOC show an annual cycle which develops with increasing distance. For a distance of 100 km differences are only somewhat higher between November and March than between April and October. Through a distance of 1000 km the values are two times higher in winter than in summer. This means that the atmospheric structures responsible for spatial variability are stronger in winter. Differences are similar in latitudinal and longitudinal directions, which denotes that the atmospheric structures which are responsible for spatial variability are of circlet extension. Higher values in the annual course occur when the temporal variability of TOC is also high as it can be estimated from the annual course of TOC measurements (Fig. 1a).

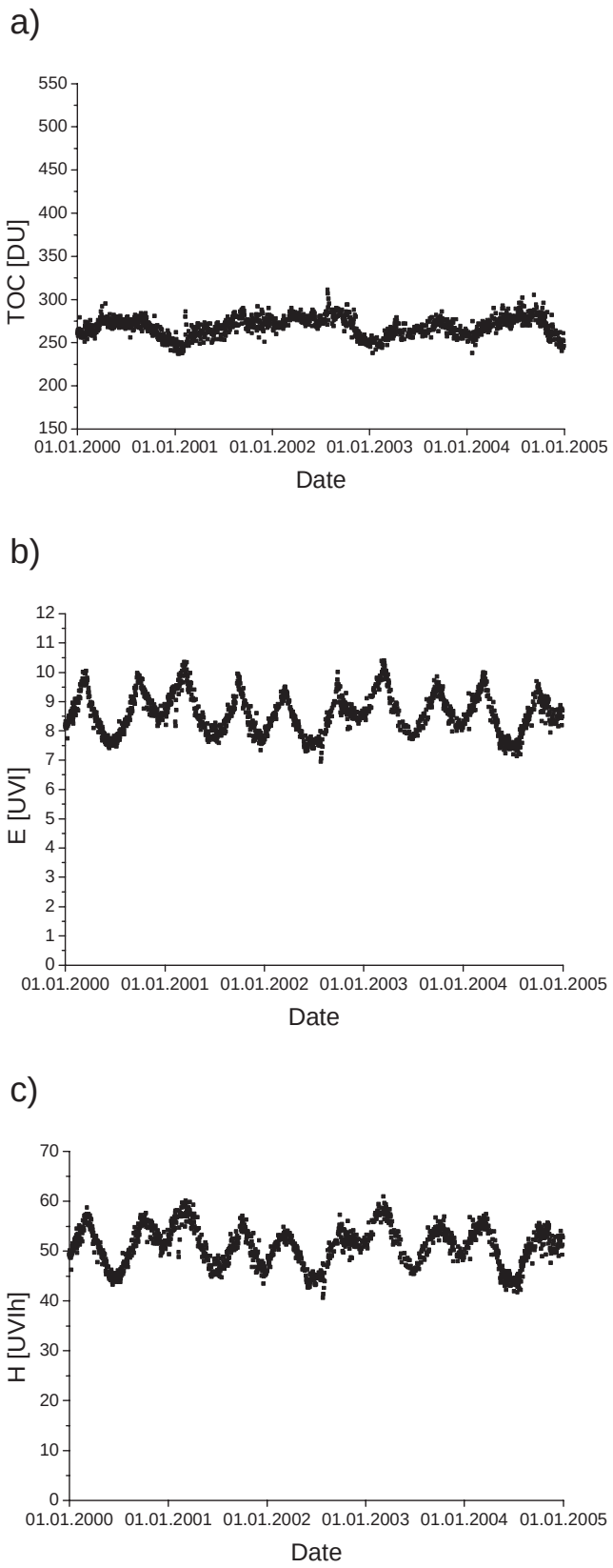


**Figure 5.** (a) Total ozone content of the atmosphere (TOC), (b) modeled erythemally effective irradiance at solar noon ($E$) and (c) daily dose ($H$) for the location of 0.0°S, 36.6°E (near Nairobi, Kenya) under clear skies.

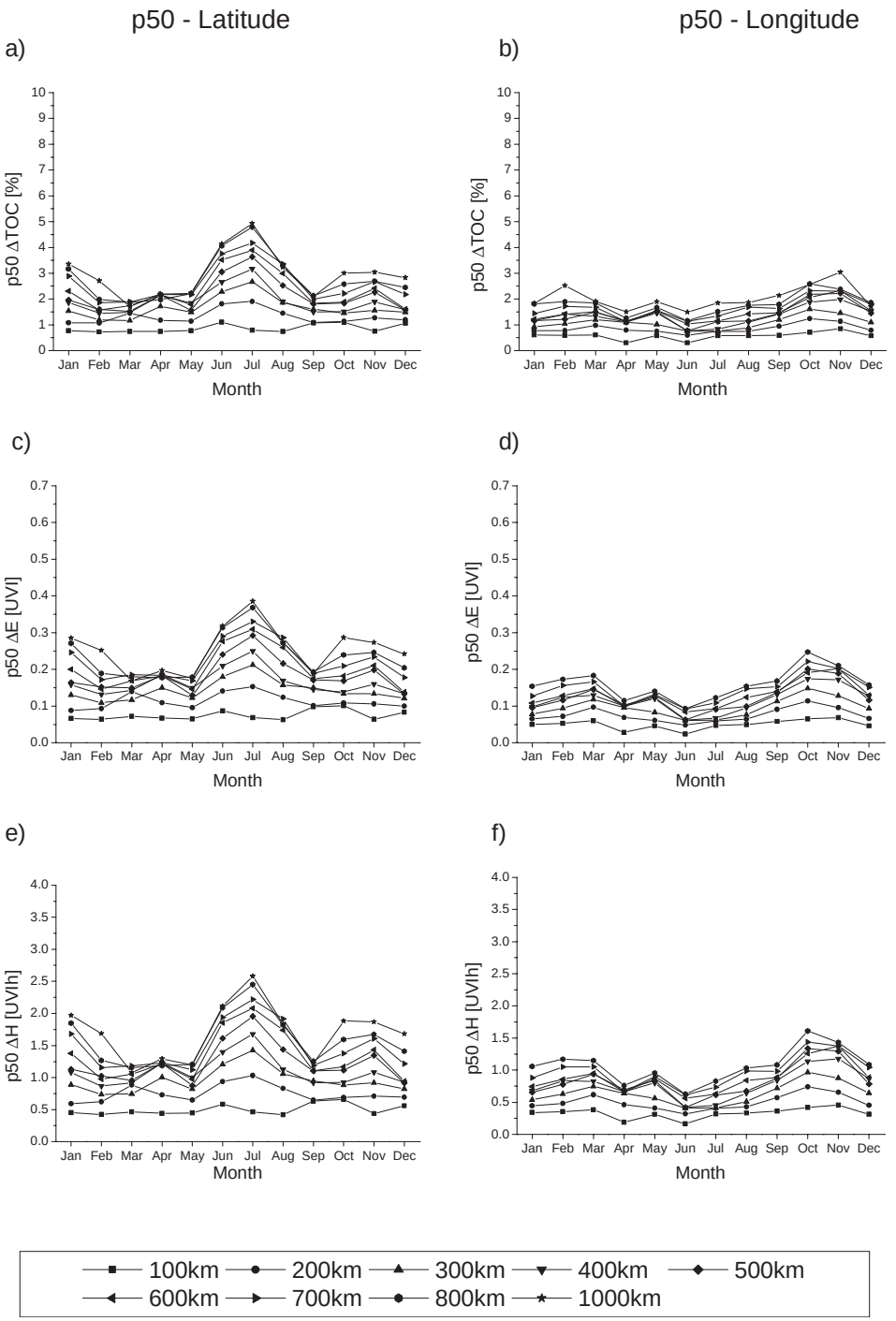


**Figure 6.** Fiftieth percentiles for absolute amount of differences in total ozone p50ΔTOC (a, b), irradiance at solar noon p50Δ*E* (c, d) and daily dose p50Δ*H* (e, f) for the region from 5°S to 5°N and from 26°E to 38°E for certain spatial distances in latitude (left panels) and in longitude (right panels).

All percentiles in irradiance (Figs. 2c,d, 3c,d and 4c,d) reveal a clear annual cycle related to solar elevation. However, the influence of TOC is quite obvious especially in the first months of the year and the few months after the summer solstice (August, September). The p100 values in irradiance (Fig. 4c,d) are strongly influenced by TOC, especially for longer distances.

Within the first 100 km the p50 values are below 0.1 UVI and are below 0.5 UVI even for distances of 1000 km. Gaps in TOC up to 200 km do not cause a p95 value of 0.5 UVI; a p95 of 1 UVI is caused by distances of 1000 km in June.

All percentile values in daily dose (Figs. 2e,f, 3e,f and 4e,f) are related to the length of the day with obvious features caused by TOC, especially in August. Within the first 100 km the p50 values are below 0.75 and 3.5 UVIh for distances of 1000 km. For distances shorter than 100 km the p95 value is below 2.5 UVIh and does not overstep 10 UVIh within distances of 1000 km.

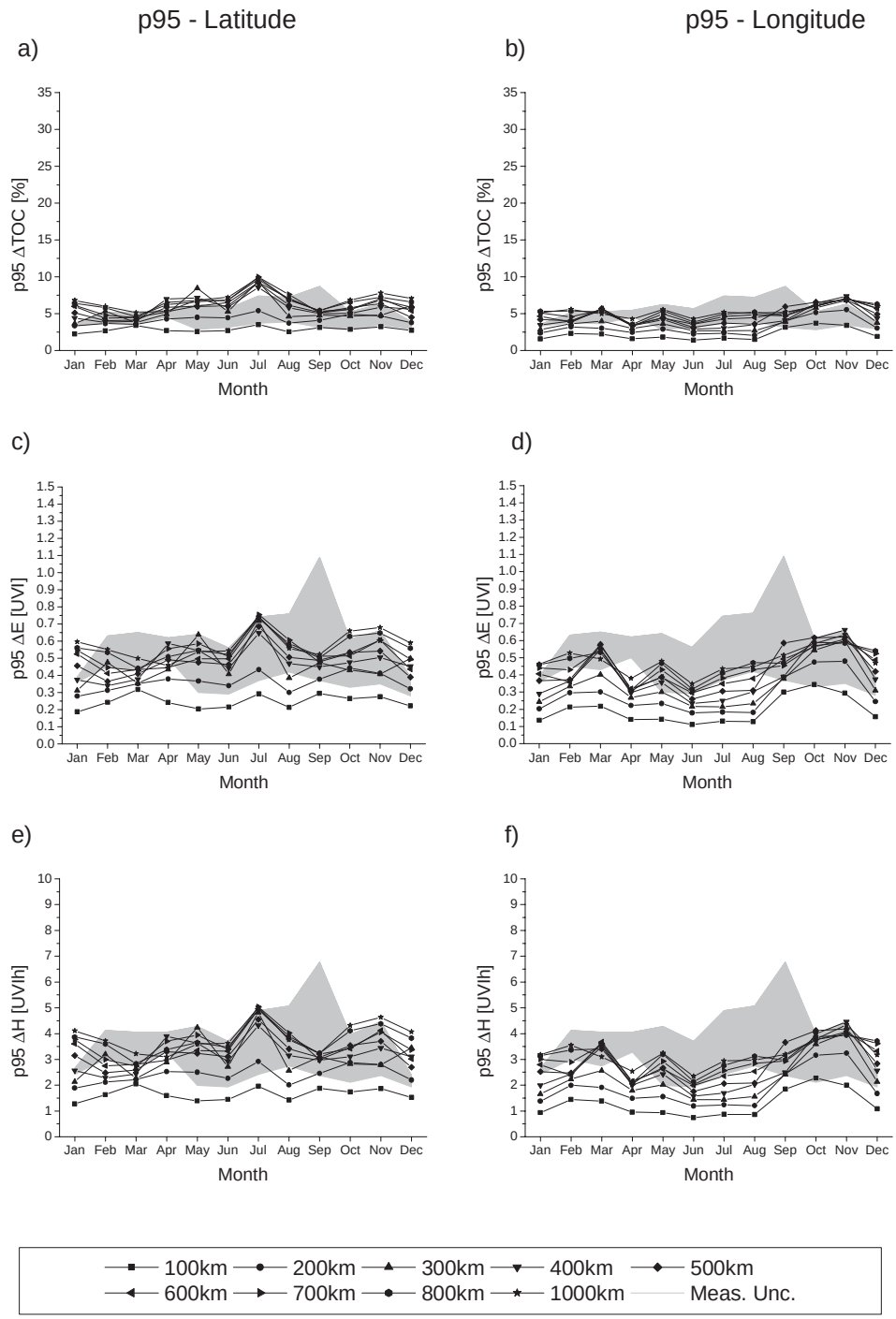


**Figure 7.** Ninety-fifth percentiles for absolute amount of differences in total ozone p95ΔTOC (a, b), irradiance at solar noon p95Δ*E* (c, d) and daily dose p95Δ*H* (e, f) for the region from 5°S to 5°N and from 26°E to 38°E for certain spatial distances in latitude (left panels) and in longitude (right panels). The gray areas indicate the p95 of uncertainties of TOC measurements and the corresponding p95 for irradiance and daily dose as given in Schmalwieser *et al.* (16).

### Influence of spatial total ozone variability at the equator

At the equator the TOC does not vary much during the year and lies between 230 and 310 DU (Fig. 5a). This range is on the order of changes that can easily occur within a few days at 50°N.

As photochemistry is the dominating process in the tropics, spatial variability of TOC is mainly a function of the solar zenith angle, *i.e.* latitudinal. However, wave disturbances like Kelvin waves may create some spatial variability (latitudinal and longitudinal) on time scales of some days. The change in solar zenith angle at noon is within $\pm 23°$. Therefore, clear sky irradiance at solar noon (Fig. 5b) varies by 3 UVI during the year exhibiting two peaks (March and September) around 10.5 UVI. Similar to this, the daily dose (Fig. 5c) undergoes smooth changes within 45 and 65 UVIh.

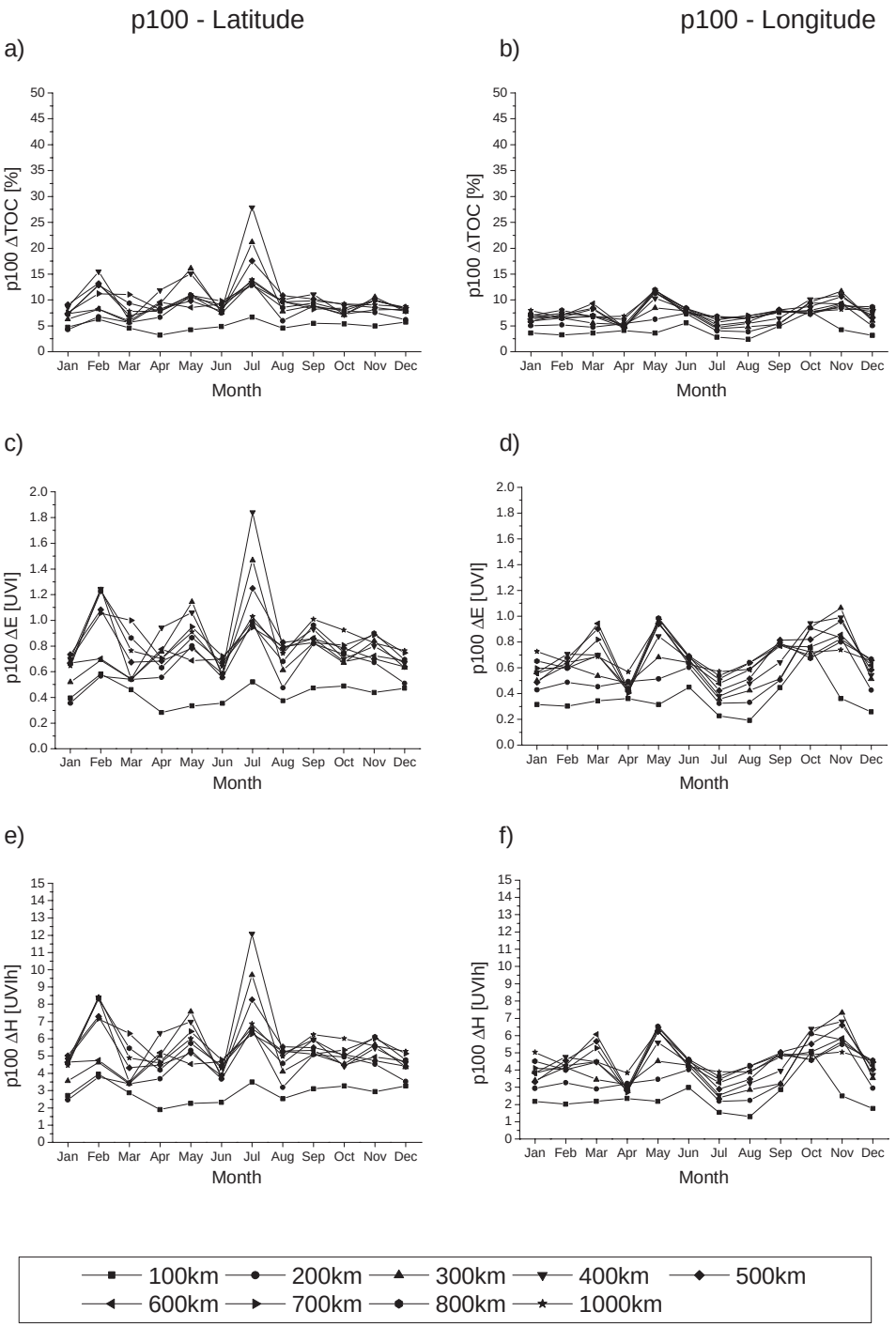


**Figure 8.** Hundredth percentiles for absolute amount of differences in total ozone p100ΔTOC (a, b), irradiance at solar noon p100Δ*E* (c, d) and daily dose p100Δ*H* (e, f) for the region from 5°S to 5°N and from 26°E to 38°E for certain spatial distances in latitude (left panels) and in longitude (right panels).

The p50 values of differences in TOC are characterized by a different pattern in latitude (Fig. 6a) and longitude (Fig. 6b). In longitude there is only a slight annual cycle with high values around October and November. In latitude, however, a peak develops with increasing distance between June and August, where the highest values have more than doubled compared with the lowest p50 values found in March. This peak is also obvious in p50 for irradiance (Fig. 6c) and daily dose (Fig. 6e). The variability of TOC dominates these annual courses and neither a dependency of the annual course from solar elevation nor from the length of the day is evident. This peak occurs in every single year and can thus not be attributed to one extreme event. This enhanced latitudinal gradient around July can also be seen in the zonal averaged TOC distribution (*e.g.* 27).

The annual patterns of the investigated quantities at p95 levels (Fig. 7) are similar to those of p50. The peak from June

to August is weaker than in the p50 values. Values do not increase much with distance going up to 0.8 UVI and 5 UVIh, respectively, for distances of 1000 km.

The p95 values for differences in irradiance in longitude indicate a smooth annual cycle with maxima around October and November. The values are slightly lower than those for latitudinal distances.

The increase in the p100 levels of differences (Fig. 8) in TOC with distance is only obvious within the first 200 km. For larger distances almost no increase can be found. Additionally, the annual pattern as evident in the p50 and p95 values is weaker. For gaps up to 100 km the p100 values for irradiance are below 0.5 UVI and below 4 UVIh for the daily dose.

**Influence of spatial total ozone variability at 30°S**

At 30°S the TOC ranges between 225 and 375 DU. A clear annual cycle can be seen (Fig. 9a) with low values around the winter solstice (June) and high values in spring. The spatial variability still follows photochemical processes similar to that in the tropics. Some spatial variability of TOC on time scales of days can be induced by displacements of the subtropical barrier and the episodic advection of air masses from the tropics or mid-latitudes. The erythemally effective irradiance at solar noon under clear sky (Fig. 9b) is within 2 and 10 UVI. Daily dose (Fig. 9c) varies within 10 and 65 UVIh during the year.

The p50 of differences for TOC as a function of/depending on distance reveals very different patterns in latitude and longitude (Fig. 10a,b). For latitudinal effects a strong annual cycle develops with distance. The highest p50 values are found in August and September, the lowest in March. The pattern of p50 in TOC for latitudinal gaps can be seen as well in the p50 of irradiance (Fig. 10c,d) and daily dose (Fig. 10e,f). The influence of solar elevation and the length of the day weaken the TOC pattern but the highest values can be still seen around September.

The weak pattern of p50 in TOC for longitudinal gaps almost vanishes when changing to irradiance and daily dose. The p50 value reaches up to 0.5 UVI and 2.5 UVIh only during a few months for latitudinal gaps larger than 600 km. For longitudinal gaps the p50 are all below 0.5 UVI and 2.5 UVIh within 1000 km.

The patterns of the p95 levels are similar to those evident for the p50 levels. The p95 levels for TOC (Fig. 11a,b) show an almost linear ascent with increasing distances of up to 600 km. Depending on the time of the year the increase is larger (around August) or smaller (around February). With that, the almost constant course for 100 km changes to a clear annual cycle for 1000 km. The spatial variability in longitude is less apparent.

The peak of TOC variability for larger distances around August is not outweighted by solar elevation and is therefore also obvious in the p95 for irradiance (Fig. 11c,d). For p95 in daily dose (Fig. 11e,f) the length of the day weakens this peak further but only to a certain extent.

In longitude the influence of distance is lower than that in latitude for distances larger than 300 km. Contrary to the p95 levels in latitude the p95 levels in longitude stay below 1 UVI. The patterns of p95 in daily dose are similar to those in

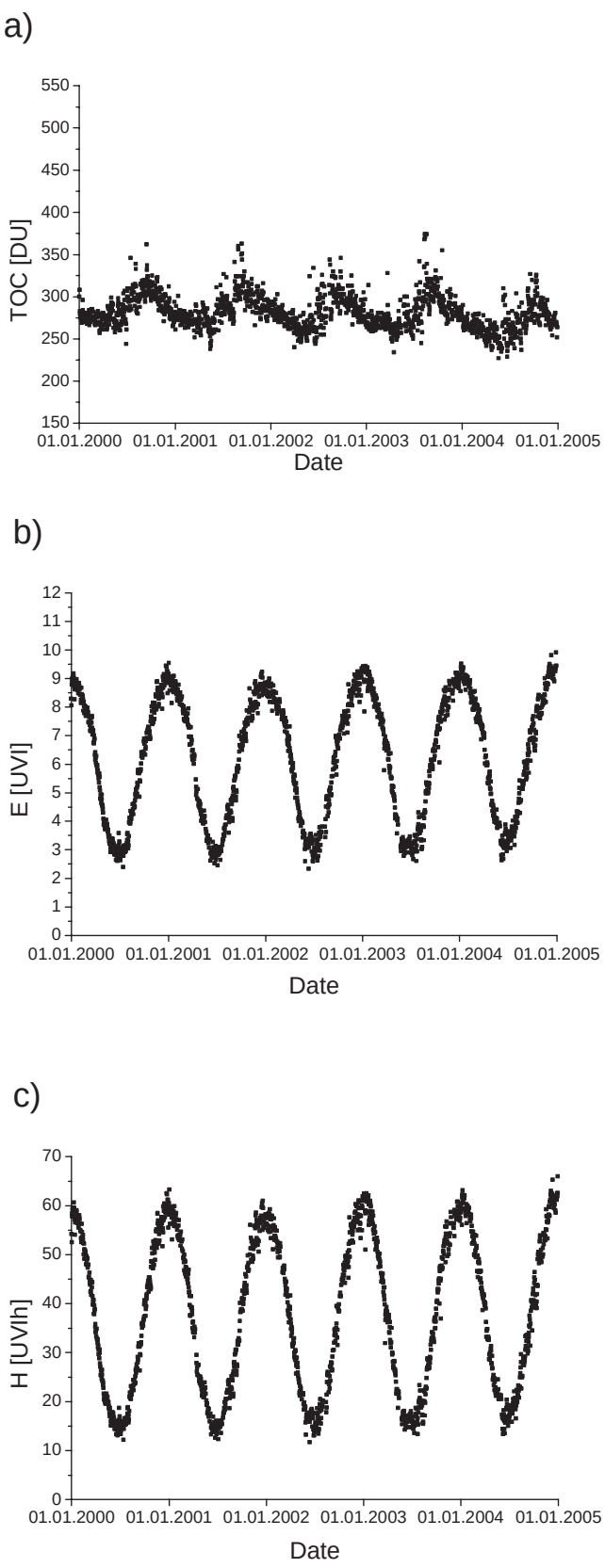


**Figure 9.** (a) Total ozone content of the atmosphere (TOC), (b) modeled erythemally effective irradiance at solar noon (*E*) and (c) daily dose (*H*) for the location of 30.0°S, 18.1°E (near Springbok South Africa) under clear skies.

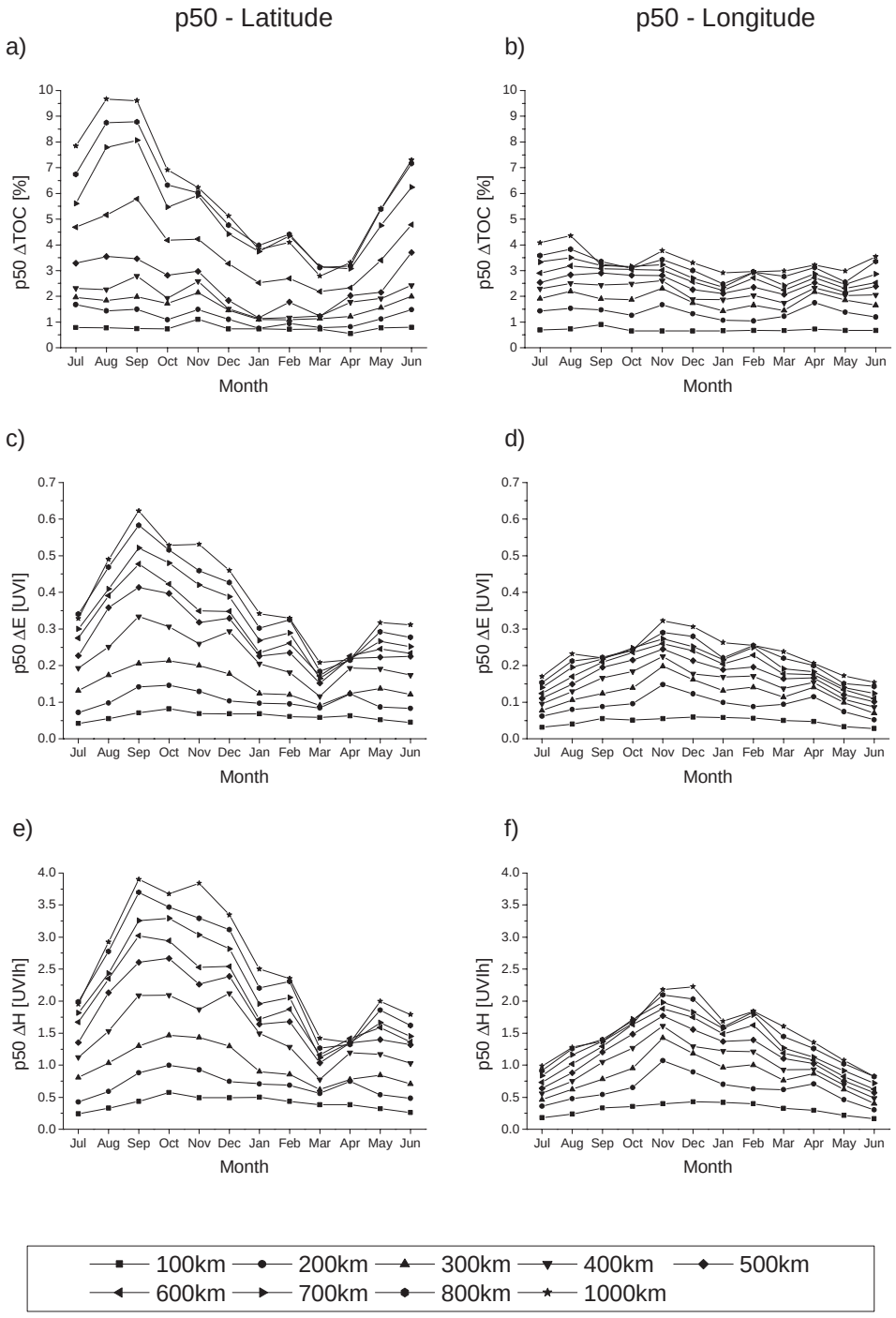


**Figure 10.** Fiftieth percentiles for absolute amount of differences in total ozone p50ΔTOC (a, b), irradiance at solar noon p50Δ*E* (c, d) and daily dose p50Δ*H* (e, f) for the region from 30°S to 19°S and 16°E to 28°E for certain spatial distances in latitude (left panels) and in longitude (right panels).

irradiance but higher values are shifted to summer solstice (December).

The pattern of the p100 in TOC (Fig. 12a,b) is similar to those of the p50 and p95 but weaker. The annual pattern in TOC can be seen to a certain extent in the p100 for irradiance (Fig. 12c,d) and daily dose (Fig. 12e,f).

A value of 0.5 UVI and 5 UVIh is exceeded in half of the year for a distance of 100 km. Within 1000 km a value of 2 UVI is not exceeded.

In daily dose the highest p100 (Fig. 12e,f) for distances of 1000 km reach 14 UVIh in latitudinal direction and only 10 UVIh in longitudinal direction.

## DISCUSSION

In this paper we have estimated the influence of spatial variability and data gaps in TOC on (calculated) clear sky erythemally effective UV radiation with special emphasis on

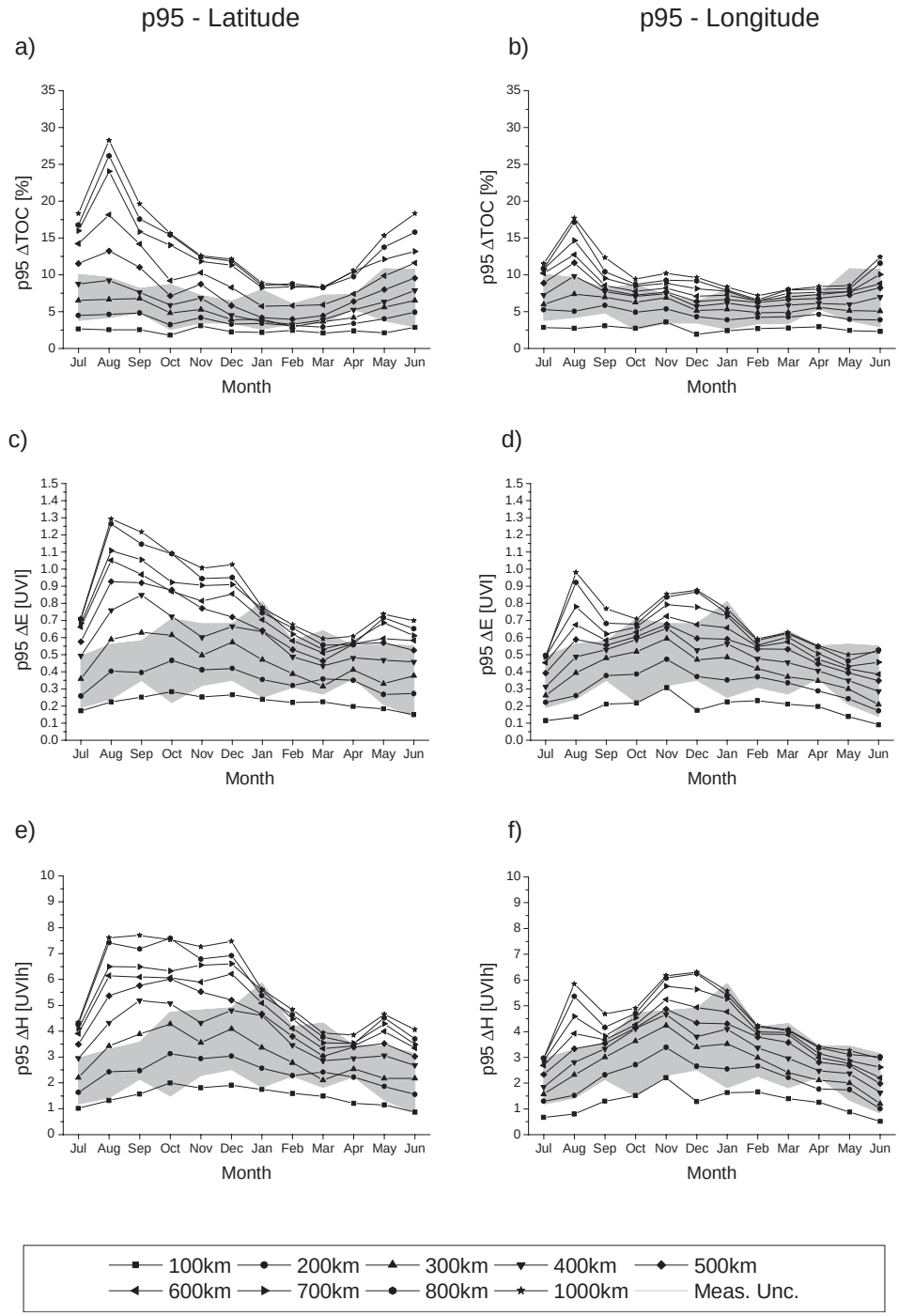


**Figure 11.** Ninety-fifth percentiles for absolute amount of differences in total ozone p95ΔTOC (a, b), irradiance at solar noon p95Δ*E* (c, d) and daily dose p95Δ*H* (e, f) for the region from 30°S to 19°S and 16°E to 28°E for certain spatial distances in latitude (left panels) and in longitude (right panels). The gray areas indicate the p95 of uncertainties of TOC measurements and the corresponding p95 for irradiance and daily dose as given in Schmalwieser *et al*. (16).

the UV Index and sun protection. It is proposed that the UV Index should be given as integer (3,4). For this, one could use a value of 0.5 and 1 UVI as limit value for inaccuracy. For radiant exposure—in our case the daily dose—one could use an equivalent to the minimal erythemal dose (MED) for melano-compromised (fair-skinned) persons (Fitzpatrick skin Types I and II) (4,38) and its multiples as limit values for accuracy. Expressed in units of UV Index hours 1 MED is close to 2.5 UVIh.

Considering these limit values an application-related estimation of the maximum size of spatial gaps in TOC can be made. For this, the p95 of absolute differences can be chosen as the measure of uncertainty because it indicates the error which occurs on one day in a month.

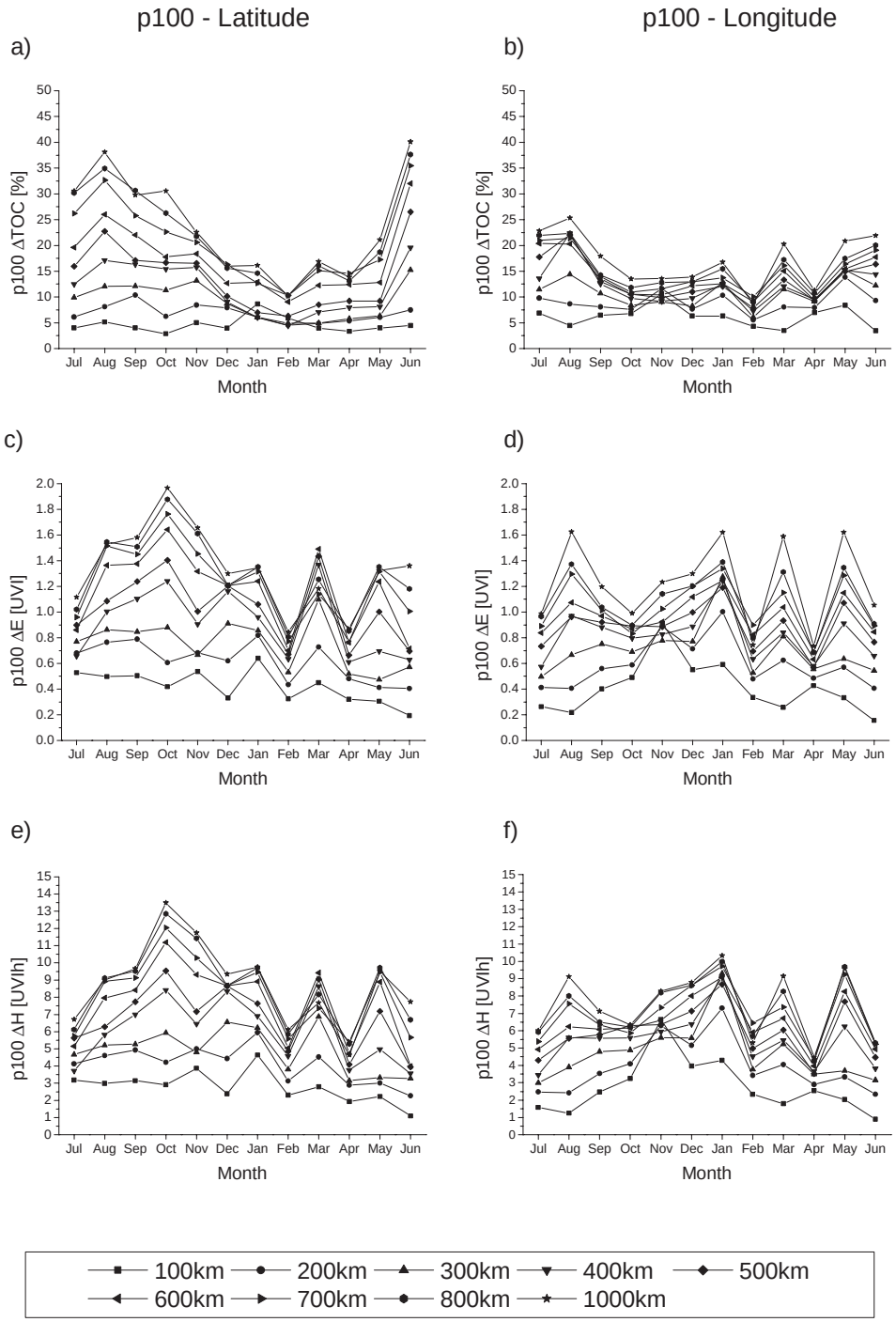


**Figure 12.** Hundredth percentiles for absolute amount of differences in total ozone p100ΔTOC (a, b), irradiance at solar noon p100Δ*E* (c, d) and daily dose p100Δ*H* (e, f) for the region from 30°S to 19°S and 16°E to 28°E for certain spatial distances in latitude (left panels) and in longitude (right panels).

At first glance, one could expect that the uncertainty of the erythemally effective radiation resulting from gaps in TOC is highest where the erythemally effective irradiance is highest. However, the results of this study show that the uncertainties are even somewhat higher at mid-latitudes than in the tropics. This results from the fact that at higher latitudes the spatial variability of TOC is highest. The increase in variability is more effective than the decrease in irradiance level. For the erythemally effective irradiance at 50°N an uncertainty (p95) of 0.5 UVI has to be taken into account when gaps in TOC of 200 km are present or invariability of the same distance is assumed. The uncertainty resulting from distances of 1000 km peaks up to 1 UVI. The uncertainties in longitude and latitude are similar. At 30°S gaps can be as large as 300 km to cause an uncertainty of 0.5 UVI. Depending on direction a p95 of 1 UVI is caused by TOC gaps of 600 km (latitude) and 1000 km (longitude). At the equator one has to take into account an uncertainty of 0.5 UVI from missing or invariable

TOC values within 300 km. Contrary to the other locations an uncertainty of 1 UVI is not reached by distances of up to 1000 km.

For the daily dose we found that at 50°N uncertainties of 2.5 UVIh result from gaps or distances in TOC of 100 km, 5 UVIh from distances of 300 km and 7.5 UVIh from distances of 700 to 800 km. At 30° the uncertainties in latitudinal direction are similar; gaps of 100 km may result in a p95 of 2.5 UVIh, of 400 km in 5 UVIh and of 1000 km in 7.5 UVIh. In longitudinal direction 7.5 UVIh are not reached even when gaps are as large as 1000 km. At the equator the influence of gaps in TOC does not increase much with size. A p95 of 2.5 UVIh is caused by missing TOC up to 200 km and 5 UVIh are not exceeded by gaps up to 1000 km.

In general, the results of this study show that a spatial resolution of approximately 100 km enables calculations of the erythemally effective irradiance with an accuracy higher than 0.5 UVI and 2.5 UVIh for skin Type 1.

In a recent study (16) the influence of uncertainties in TOC to the erythemally effective UV radiation was quantified. The p95 of absolute differences resulting from measurement uncertainties in TOC, maximum daily irradiance and daily dose are taken from this study and added to Figs. 3, 7 and 11 as gray shaded areas (data from TOVS are excluded). Their lower limits are at the level of those p95 which would result from a spatial gap of 100 or 200 km. The level of the upper limits of uncertainty differs quite significantly between the different locations. At 50°N they are comparable to distances of 400–500 km, at 30°S to distances of 500 and 600 km and at the equator they are larger than uncertainties from distances of 1000 km. The annual courses of the uncertainties from measurement uncertainties and from spatial variability may differ significantly for certain months of the year.

In order to reduce the uncertainty of the erythemally effective irradiance and eventually to improve UV index calculation we conclude that the spatial variability of TOC has to be considered especially for the mid-latitudes where high gradients on smaller spatial scales occur. Data gaps can be avoided and spatial ozone variability better taken into account by means of data assimilation procedures where total ozone measurements are assimilated into global chemistry-transport-models driven by meteorological fields (*e.g.* 39,40). This results in synoptic TOC distributions which build a basis for improving the derivation of erythemally effective irradiance, daily dose and the UV index.

In a follow-up paper the influence of the temporal variability to the erythemally effective irradiance and daily dose will be studied.

## REFERENCES


1. Thieden, E., P. A. Philipsen, J. Sandby-Moller, J. Heydenreich and H. C. Wulf (2004) Proportion of lifetime UV dose received by children, teenagers and adults based on time-stamped personal dosimetry. *J. Invest. Dermatol.* **123**, 1147–1150.
2. Schauberger, G., G. Keck and A. Cabaj (1992) Trend analysis of solar ultraviolet exposure of the Austrian population caused by holiday patterns since 1969. *Photodermatol. Photoimmunol. Photomed.* **9**, 72–77.
3. International Commission on Non-Ionizing Radiation Protection (1995) *Global Solar UV-Index—WHO/WMO/INCIRP Recommendation*. INCIRP publication No.1/95. ICNIRP, Oberschleissheim, Germany.
4. World Health Organization (2002) *Global Solar UV Index: A Practical User Guide*. WHO, Geneva, Switzerland.
5. Commission Internationale de l'Eclairage (2003) *International Standard Global Solar UV Index*. CIE Standard S 013:2003. CIE, Vienna, Austria.
6. European Commission (2006) *Measurements and Assessment of Personal Exposure to Incoherent Optical Radiation—Part 3: UV-Radiation Emitted by the Sun*. European Pre-Standard, prEN 14255-3:2006, Brussels, Belgium.
7. Vanicek, K., Z. Lytinska, T. Frei and A. Schmalwieser (2000) *UV Index for the Public*. Publication of the European Communities, Brussels, Belgium.
8. Schwander, H., P. Koepke and A. Ruggaber (1997) Uncertainties in modeled UV irradiances due to the limited accuracy and availability of input data. *J. Geophys. Res.* **102**, 9419–9429.
9. Weihs, P. and A. R. Webb (1996) Comparison of green and lowtran radiation schemes with a discrete ordinate method UV model. *Photochem. Photobiol.* **64**, 642–648.
10. Kylling, A., A. F. Bais, M. Blumthaler, J. Schreder, C. S. Zerefos and E. Kosmidis (1998) Effect of aerosols on solar UV irradiance during photochemical activity and solar ultraviolet radiation campaign. *J. Geophys. Res.* **103**, 26051–26060.
11. Koepke, P., A. Bais, D. Balis, M. Buchwitz, H. de Backer, X. de Cabo, P. Eckert, P. Eriksen, D. Gillotay, T. Koskela, B. Lapeta, Z. Litynska, J. Lorente, B. Mayer, A. Renaud, A. Ruggaber, G. Schauberger, G. Seckmeyer, P. Seifert, A. Schmalwieser, H. Schwander, K. Vanicek and M. Weber (1998) Comparison of models used for UV index calculations. *Photochem. Photobiol.* **67**, 657–662.
12. De Backer, H., P. Koepke, A. Bais, X. de Cabo, T. Frei, D. Gillotay, Ch. Haite, A. Heikkilä, A. Kazantzidis, T. Koskela, E. Kyrö, B. Lapeta, J. Lorente, K. Masson, B. Mayer, H. Plets, A. Redondas, A. Renaud, G. Schauberger, A. Schmalwieser, H. Schwander and K. Vanicek (2001) Comparison of measured and modelled UV indices for the assessment of health risks. *Meteor. Appl.* **8**, 267–277.
13. Schmalwieser, A. W., G. Schauberger, M. Janouch, M. Nunez, T. Koskela, D. Berger, G. Karamanian, P. Prosek and K. Laska (2005) Global validation of a forecast model for irradiance of the solar, erythemally effective UV radiation. *Opt. Eng.* **40**, 3040–3050.
14. Staiger, H. and P. Koepke (2005) UV index forecasting on a global scale. *Meteorol. Z.* **14**, 259–270.
15. Schmalwieser, A. W., G. Schauberger, M. Janouch, M. Nunez, T. Koskela, D. Berger and G. Karamanian (2005) Global forecast model to predict the daily dose of the solar erythemally effective UV radiation. *Photochem. Photobiol.* **81**, 154–162.
16. Schmalwieser, A. W., G. Schauberger, T. Erbertseder, M. Janouch, G. J. R. Coetzee and P. Weihs (2007) Sensitivity of erythemally effective UV irradiance and daily exposure to uncertainties in measured total ozone. *Photochem. Photobiol.* **83**, 433–434.
17. Bodecker, G. E., J. C. Scot, K. Kreher and R. L. McKenzie (2001) Global ozone trends in potential vorticity coordinates using TOMS and GOME intercompared against the Dobson network: 1978–1998. *J. Geophys. Res.* **106**, 23029–23042.
18. Kneiszys, F. X., G. P. Anderson, E. P. Sheetle, W. O. Gallery, L. W. Abreu, J. E. Selby, J. H. Chetwynd and S. A. Clough (1988) *User's Guide to LOWTRAN 7*. AFGL Tech. Rep., AFGL-TR-88-0177, Air Force Geophys Lab, Bedford, MA.
19. Krzyscin, J. W. (2000) Impact of the ozone profile on the surface UV radiation: Analysis of the Umkehr and UV measurements at Belsk (52°N, 21°E), Poland. *J. Geophys. Res.* **105**, 5009–5015.
20. Schmalwieser, A. W., G. Schauberger, P. Weihs, R. Stubi, M. Janouch, G. J. R. Coetzee and S. Simic (2003) Preprocessing of total ozone content as an input parameter to UV Index forecast calculations. *J. Geophys. Res* **108**, 4176–4189.
21. Holton, J. R. (1992) *An Introduction to Dynamic Meteorology*. Academic Press, San Diego.
22. Brasseur, G. P., J. J. Orlando and G. S. Tyndall (1999) *Atmospheric Chemistry and Global Change*. Oxford University Press, New York.
23. Solomon, S. (1990) Progress towards a quantitative understanding of Antarctic ozone depletion. *Nature* **347**, 34–37.

24. Metham, A. R. (1937) The correlation of the amount of ozone with other characteristics of the atmosphere. *Quart. J. Roy. Meteor. Soc.* **63**, 289–307.
25. Dobson, G. M. B., A. W. Brewer and B. M. Ceiling (1946) Meteorology of the lower stratosphere. *Proc. R. Soc. London Her. A.* **236**, 187–193.
26. Reed, R. J. (1950) The role of vertical motions in ozone-weather relationships. *J. Meteor.* **7**, 263–267.
27. Fortuin, J. P. and H. Kelder (1998) An ozone climatology based on ozonesonde and satellite measurements. *J. Geophys. Res.* **103**, 31709–31734.
28. McPeters, R. D., P. K. Bhartia, A. J. Krueger, J. R. Herman, C. G. Wellemeyer, C. J. Seftor, G. Jaross, O. Torres, L. Moy, G. Labow, W. Byerly, S. L. Taylor, T. Swissler and R. P. Cebula (1998) *Earth Probe Total Ozone Mapping Spectrometer (TOMS) Data Products User's Guide*. NASA Reference Publication, Greenbelt, MD.
29. National Aeronautic and Space Agency. Available at: ftp://jwockey.gscf.nasa.gov/pub/eptoms/. Accessed on 7 January 2008.
30. National Aeronautic and Space Agency. Available at: http://toms.gsfc.nasa.gov/etoms/. Accessed on 7 January 2008.
31. National Aeronautic and Space Agency (2006) *Earth Observing System Aura*. Goddard Space Flight Center, Greenbelt, MD. Available at: http://aura.gsfc.nasa.gov/images/outreach/Aura_Brochure.pdf.
32. Diffey, B. L. (1977) The calculation of the spectral distribution of natural ultraviolet radiation under clear day conditions. *Phys. Med. Biol.* **22**, 309–316.
33. Bener, P. (1972) *Approximate Values of Intensity of Natural Radiation for Different Amounts of Atmospheric Ozone*. Eur. Res. Off., US Army, London, UK.
34. Schmalwieser, A. W. and G. Schauberger (2000) Validation of the Austrian forecast model for solar, biologically-effective ultraviolet radiation—UV Index for Vienna, Austria. *J. Geophys. Res.* **105**, 26661–26668.
35. Commission Internationale de l'Eclairage (1987) A reference action spectrum for ultraviolet-induced erythema in human skin. *CIE J.* **6**, 17–22.
36. Saxebøl, G. (2000) UVH—A proposal for a practical unit for biological effective dose for ultraviolet radiation exposure. *Radiat. Prot. Dosimetry* **88**, 261.
37. Commission Internationale de l'Eclairage (1998) *Erythema Reference Action Spectrum and Standard Erythema Dose*. CIE S007E-1998. CIE, Vienna, Austria.
38. Fitzpatrick, T. B., M. A. Pathak, L. C. Harber, M. Seiji and A. Kukita (1974) *Sunlight and Man*. University of Tokyo Press, Tokyo, Japan.
39. Eskes, H., P. van Velthoven, P. Valks and H. Kelder (2003) Assimilation of GOME total ozone satellite observations in a three-dimensional tracer transport model. *Q. J. R. Met. Soc.* **129**, 166–3.
40. Baier, F., T. Erbertseder, O. Morgenstern, M. Bittner and G. Brasseur (2005) Assimilation of MIPAS observations using a three-dimensional chemical-transport model. *Q. J. R. Met. Soc.* **131**, 3529–3542.

## 2.4 Publikation 4:

# Sensitivity of Erythemally Effective UV Irradiance and Daily Exposure to Temporal Variability in Total Ozone

Alois W. Schmalwieser, Thilo Erbertseder, Günther Schauberger, Philipp Weihs

Photochemistry and Photobiology, accepted for publication (9. Juni 2008)

Online verfügbar seit 27. August 2008
http://www.blackwell-synergy.com/toc/php/0/0
DOI: 10.1111/j.1751-1097.2008.00431.x
http://www3.interscience.wiley.com/journal/120121002/issue

Photochemistry and Photobiology, 20**, **: *–*

# Sensitivity of Erythemally Effective UV Irradiance and Daily Exposure to Temporal Variability in Total Ozone

**Alois W. Schmalwieser*[1], Thilo Erbertseder[2], Günther Schauberger[1] and Philipp Weihs[3]**

[1]Institute of Medical Physics and Biostatistics, University of Veterinary Medicine, Vienna, Austria
[2]Deutsches Fernerkundungsdatenzentrum, Deutsches Zentrum für Luft- und Raumfahrt, Oberpfaffenhofen, Germany
[3]Institute of Meteorology, University of Natural Resources and Applied Life Sciences, Vienna, Austria

**Received 18 January 2008, accepted 9 June 2008, DOI: 10.1111/j.1751-1097.2008.00431.x**

## ABSTRACT

**The provision of information to the public about current levels of the erythemally effective UV radiation is an important issue in health care. The quality of promoted values is therefore of special importance. The atmospheric parameter which affects the erythemally effective UV radiation under clear sky most is the total ozone content of the atmosphere. In this paper we examined the sensitivity of the erythemally effective irradiance and daily radiant exposure to the temporal variability of total ozone on time scales from 1 to 15 days. The results show that the sensitivity is highest for the first 24 h. Larger time scales do not exhibit a similar influence. Total ozone measurements of the previous day may already cause uncertainties higher than 0.5 UV index (UVI) independent of the geolocation. For comparison, a temporal persistence of 15 days may cause uncertainties of 1.2 UVI at 50°N, 1 UVI at 30°S and less than 1 UVI at the equator. The results of this study allow finding the necessary temporal resolution of total ozone values when a certain accuracy for the UVI or for the purpose of sun protection is required. The results are compared with those of two preceding studies where we quantified the influence of measurement uncertainties and spatial total ozone variability to the erythemally effective irradiance at noon and to the daily dose. We conclude that temporal variability of total ozone is the most critical issue, but also measurement uncertainties do have a noticeable influence on the erythemally effective radiation.**

## INTRODUCTION

Sun care nowadays is an important issue in health care. Information for the public about the current intensity of UV radiation may therefore be very helpful. The quality of published values is a critical issue and it is essential to know the accuracy of the promoted values. As evident from several studies (*e.g.* 1,2) the total ozone column (TOC) of the atmosphere is the most critical input parameter for calculations of the UV radiation under clear sky (cloud and aerosol free) conditions. In turn, uncertainties in TOC influence the accuracy of calculated values.

*Corresponding author email: alois.schmalwieser@vu-wien.ac.at (Alois W. Schmalwieser)


Uncertainties in TOC values result from limited accuracy of the intrinsic measurements, from limited spatial coverage and limited temporal availability, *i.e.* resolution. The magnitude of these uncertainties depends on a variety of parameters like measuring technique, ozone retrieval scheme, atmospheric dynamics, solar zenith angle and others.

In a previous paper we studied the effects of the intrinsic uncertainties of TOC measurements to calculated values of the erythemally effective irradiance at noon and daily radiant exposure (3). In a follow-up paper we examined the effects of uncertainties due to limited spatial resolution of TOC measurements (4). In this paper we investigate the influence of the temporal total ozone variability on time scales from 1 to 15 days on the erythemally effective UV irradiance at solar noon and daily exposure under clear sky conditions. We aim at quantifying the influence of total ozone data with a limited temporal resolution or temporal lags and the effect of assuming persistency of total ozone.

The temporal variability of TOC is caused by a variety of phenomena on a broad spectrum of temporal and spatial scales. Generally, ozone distribution is determined by photochemical production, transport and destruction. A strong annual or semiannual cycle builds the most obvious pattern in the temporal course of TOC on both hemispheres. The annual cycle reaches its maximum in the winter and spring months and its minimum in the autumn months. The amplitude depends strongly on latitude. In the tropics the semi annual cycle is most obvious and corresponds clearly to solar elevation.

For periods up to 15 days, however, phenomena that affect TOC at subsynoptic and synoptic scales are most important. These subsynoptic and synoptic fluctuations, the classical weather–ozone relations, amount up to 10% of the total column in the tropics and up to 30% in middle and high latitudes. These fluctuations are known since the pioneering work of Dobson (5,6), Meetham (7) and Reed (8). Depending on geolocation, these fluctuations can change the TOC amount by more than 100 DU within 24 h and hence govern the short-term variability of TOC. Short-time fluctuations of TOC for a time span of 2 days around the globe were estimated by Schmalwieser *et al.* (9) using correlation analysis. It was shown that low correlation coefficients are found at mid and high latitudes, and that the coefficients increase toward higher and lower latitudes.

To a much lower extent, but for the sake of completeness, contributions to the temporal variability of TOC within 15 days result from the quasi-biennial oscillation (QBO), regional El Niño/La Niña effects, volcanic eruptions and the solar activity cycles.

Changes in solar activity affect the ozone forming UV irradiance. The 11-year solar cycle (*e.g.* 10–12) may cause variations in TOC of the order of 4% relative to a long-term mean. The TOC reaches maximum values near sunspot maxima and can be identified best at the tropics. The 27-day solar rotation is seen as similar change (*e.g.* 11,13) of the order of a few percent. The amplitude of the QBO signal in TOC (14) depends on latitude and season and can reach up to 8% of the annual mean (*e.g.* 13,15,16).

Effects from the El Niño/La Niña Southern Oscillation occur on a time scale from 3 to 7 years (*e.g.* 17), and exhibit a duration from 7 to 8 months. Its effect on TOC variability shows zonal asymmetry and may cause a reduction in TOC of the order of −4%. Large volcanic eruptions can lead to significant radiative/chemical and dynamical changes which may lead to declines as large as −5% (*e.g.* 18) over a period of a few years. Finally, the North Atlantic Oscillation and the Arctic Oscillation (*e.g.* 19) induce clear signatures on synoptic scale fluctuations of TOC over the Euro-Atlantic sector (20,21) and higher latitudes, respectively, and may be responsible for the enhanced appearance of ozone miniholes (22).

In this paper we investigate the sensitivity of the erythemally effective irradiance and daily radiant exposure to short-term fluctuations of TOC on time scales up to 15 days depending on the season. The sensitivity to temporal variability can also be interpreted as the constraint of accuracy due to a limited temporal resolution, availability or the uncertainty which may arise from assuming persistency. The study is carried out aiming at sun care and public health. For this, the values of the erythemally effective irradiance are expressed in units of the UV Index (UVI) as proposed by several organizations (23–27). In case of the daily dose, UVI hours (UVIH) are used as unit following a suggestion of Saxebøl (28). Regarding radiation protection and health care we use the 95th percentile (p95) as the measure of relevance for the analysis.

Additionally, this study allows to estimate the necessary properties of TOC if a certain accuracy of the UVI or of a recommendation for sun protection, like the sun protection factor, is required.

## MATERIALS AND METHODS

The uncertainties in the erythemally effective UV radiation from a restricted temporal resolution are estimated by analyzing the differences resulting from temporally shifted TOC time series as input parameter. Differences due to lags in TOC between 1 day and 15 days were calculated and analyzed.

*TOC data.* In order to be consistent with two related preceding papers (3,4), the TOC data have been taken from the Total Ozone Mapping Spectrometer (TOMS) on board NASA's Earth Probe satellite (EPTOMS) for this study, too. TOMS measures incident solar radiation and backscattered ultraviolet sunlight at six near-UV wavelengths and TOC values are retrieved from these measurements (29,30). The measurements are taken close to solar noon. We use the gridded level-3 near-real time data. These data are given on a 1° latitude by 1.25° longitude grid containing $180 \times 288$ grid points at global coverage. We apply gathered near-real time data, which were processed by TOMS Version 7.

The analysis is based on time series of EPTOMS total ozone observations at the following geolocations: 50.0°N and 15.6°E (Solar and Ozone Observatory at Hradec Kralove, Czech Republic); 0.0°N and 36.6°E (ozone observatory near Nairobi, Kenya); and 30.0°S and 18.1°E (ozone observatory near Springbok, South Africa). To be consistent with the related earlier work we have included all available observations between 1 January 2000 and 31 December 2004. The ongoing problems in calibration of EPTOMS in 2004 did not affect our analysis. This was proved by analyzing the statistical parameters for each single year (see below).

*Uncertainty analysis.* In order to quantify the influence of temporal variability in TOC data on the erythemally effective radiation, we performed model calculations with a fast spectral UV radiation model. This model was developed by some of us (31) improving the suggestion of Diffey (32). It uses the data base from Bener (33) which was obtained from spectral measurements made over several years at Davos (46°48′N, 9°49′E, 1590 m a.s.l.) for parameterization. The model setup is similar to that used in the two related previous papers. A more detailed description of the model can be found in Schmalwieser *et al.* (34).

The erythemally effective irradiance is gained by using the CIE (Commission Internationale de l'Eclairage) action spectrum of the erythema (35) for weighting followed by the integration over the whole spectral range and expressed in units of the UVI where 1 UVI corresponds to 0.025 $W_{eff}\ m^{-2}$. The daily radiant exposure (or daily dose) is gained by integrating the daily course of the effective irradiance from sunrise to sunset and is expressed in units of UVIh following a suggestion of Saxebøl (28) where 1 UVIh corresponds to 90 $J\ m^{-2}$ (0.9 SED) (36).

The model was validated with respect to the erythemally effective UV radiation by comparison with other models (37–39) and comparison with measurements made at four different continents for irradiance (35) and daily dose (40).

To be consistent with our two related previous papers an aerosol pure atmosphere and a cloud-free sky was assumed to point out the maximum influence as this is important for radiation protection. Therefore, the input parameters comprise date, time, geographical position, altitude and TOC.

The uncertainties in the erythemally effective radiation resulting from limitations in accuracy due to temporal lags were estimated by consecutively inputting temporally shifted time series of TOC to the model. First, the erythemally effective irradiance was calculated for a certain location and a certain day with the temporally correct TOC value. It was then calculated by using time series of TOC shifted between 1 and 15 days. For each day of the 5 year period such a time series was calculated. Finally, the absolute differences between the current value and the shifted time series were calculated for each day of the 5 year period.

Differences in TOC are derived similarly. Differences are calculated between the current value and the shifted time series. Additionally the differences were set in relation to the current value and expressed in percentage.

The statistical analysis of the obtained differences was carried out by using the p95 of absolute differences for each month of the year as the main indicator. The p95 value indicates the difference or uncertainty that is exceeded at one day of the month. The statistical analysis is completed using the 50th percentile (p50) and the 100th percentile (p100). The p50 value denotes the median, *i.e.* the difference that is exceeded on 50% of the days. The p100 values quantifies the highest difference found over the 5 year period for a given month. The analysis is performed separately for daily maximum irradiance (solar noon), daily dose under clear sky conditions and TOC.

## RESULTS

### Influence of temporal total ozone variability at 50°N

At 50°N (Hradec Kralove, Czech Republic) the TOC exhibits high temporal variability throughout the year with values from 200 to 500 DU. Significant changes by more than 100 DU within 24 h can be observed. Solar height at noon varies

between 17° in winter and 63° in summer. With these, the erythemally effective irradiance at solar noon under clear sky varies from 0.5 UVI (winter) to 7 UVI (summer). The length of the day undergoes large changes of more than 8 h. The daily dose under clear sky may be below 2 UVIh in winter and can exceed 50 UVIh near the summer solstice. Visualizations of TOC values, erythemally effective irradiance at noon and daily dose can be found in Schmalwieser *et al.* ([3] 1997–1999) and Schmalwieser *et al.* ([4] 2000–2004).

The temporal variability analysis of TOC at the p50 and p95 level (Figs. 1a and 2a) shows a clear annual cycle with higher values during late winter/early spring and lower values during

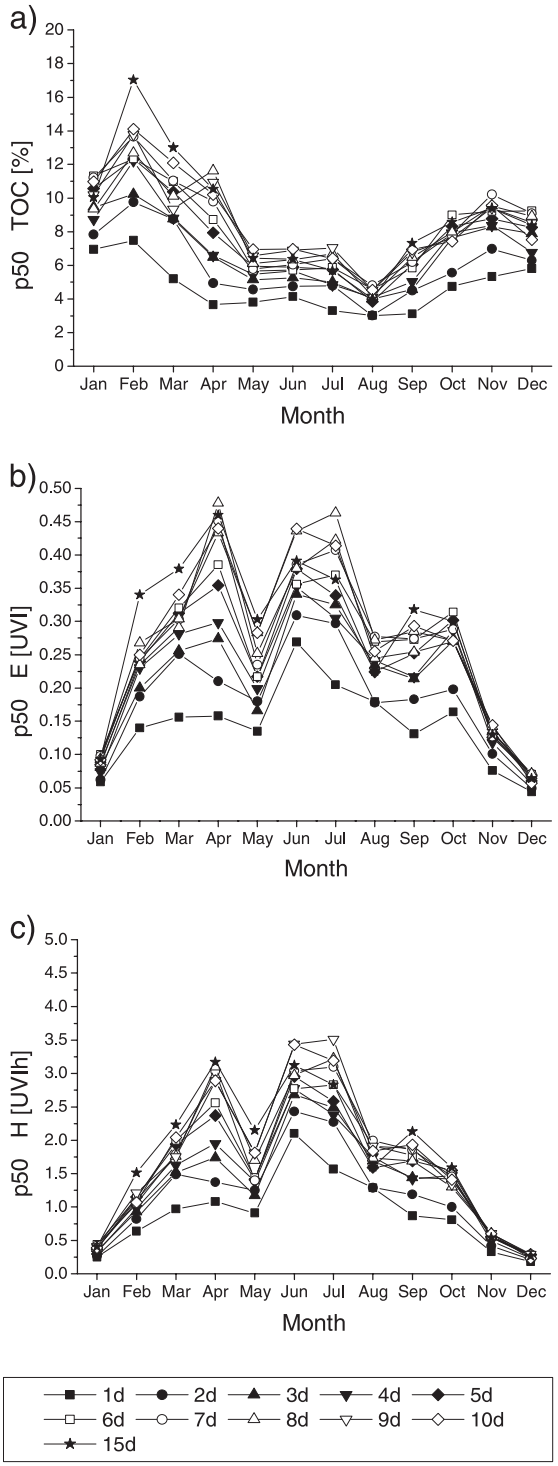


**Figure 1.** Fiftieth percentiles for absolute differences in total ozone p50ΔTOC (a), irradiance at solar noon p50Δ*E* (b) and daily dose p50Δ*H* (c) at 50.0°N, 15.6°E (near Hradec Kralove, Czech Republic) under clear skies for certain temporal lags up to 15 days.

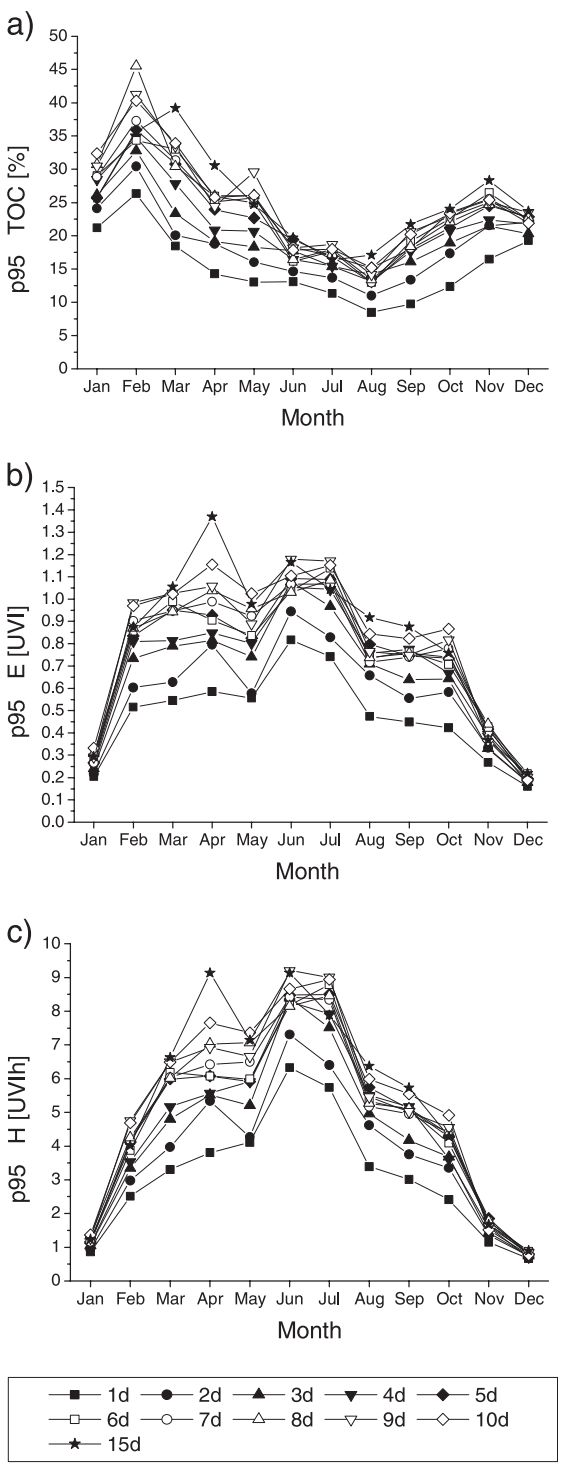


**Figure 2.** Ninety-fifth percentiles for absolute differences in total ozone p95ΔTOC (a), irradiance at solar noon p95Δ*E* (b) and daily dose p95Δ*H* (c) at 50.0°N, 15.6°E (near Hradec Kralove, Czech Republic) under clear skies for certain temporal lags up to 15 days.

summer. Only for the shorter time lags there is a clear relationship between the p50 or p95 value and the lag. The longest lags do not necessarily cause the highest uncertainty values. The increase in the differences is rather low as the values for a lag of 15 days are approximately twice as high as for a lag of 1 day only. The highest monthly differences in TOC (p100) due to time lags found within the 5 year period (Fig. 3a) show a clear annual course but only a weak relationship between their magnitude and the underlying time lag. Similar to the above, they are highest in spring and lowest in summer. From one day to another TOC may vary by 15% in summer and 40% in spring. Within a week changes up to 70% can be observed in spring which corresponds to more than 100 DU.

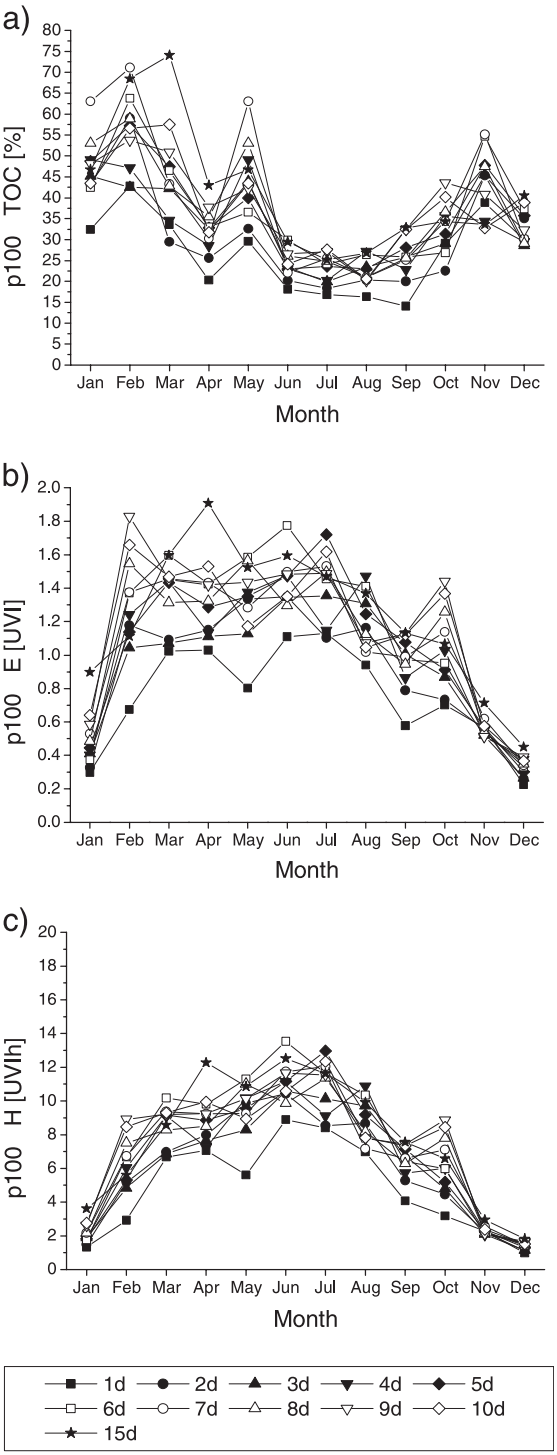


**Figure 3.** Hundredth percentiles for absolute differences in total ozone p100ΔTOC (a), irradiance at solar noon p100Δ$E$ (b) and daily dose p100Δ$H$ (c) at 50.0°N, 15.6°E (near Hradec Kralove, Czech Republic) under clear skies for certain temporal lags up to 15 days.

The p50 values of the erythemally effective irradiance at noon exhibit a dual pattern (Fig. 1b). During spring the pattern is dominated by the higher temporal variability of TOC due to high dynamic activity in the atmosphere. An influence from solar height cannot be seen. From May to August the pattern is dominated by the annual course of solar height. Late summer and fall are then again strongly influenced by the increasing dynamic activity and the influence of solar height becomes invisible again. The changes from variability as main influence to solar height and vice versa become obvious by the relatively low values in for May and August. Further, the pattern changes with progressing time lag. For longer temporal delays the increase is much lower than within the first day. The annual behavior of p95 (Fig. 2b) and p100 (Fig. 3b) is similar but the influence of high variability in late winter and spring (February–May) becomes stronger. The p100 values are almost constant from February to August at a level of 1 UVI for a lag of 24 h. In the p95 the corresponding values are above 0.5 UVI from February to July.

In the absolute differences for the daily dose (Figs. 1c, 2c and 3c) the duality is still evident but the length of the day dominates the pattern significantly.

### Influence of temporal total ozone variability at 30°S

At 30°S (near Springbok, South Africa) the TOC varies by 150 DU during the year where a clear annual cycle can be observed. The lowest values are around 225 DU and are measured near the winter solstice (June). The highest are observed in spring and are of the order of 375 DU. Day-to-day variability is up to 70 DU.

The erythemally effective irradiance at solar noon under clear skies is within 2 UVI (winter) and 10 UVI (summer). The daily dose undergoes annual changes from 10 to 65 UVIh. Visualizations of TOC values, erythemally effective irradiance and daily dose can be found in Schmalwieser *et al.* ([3] 1997–1999) and Schmalwieser *et al.* ([4] 2000–2004).

The p50 values of the absolute differences (Fig. 4a) caused by temporal variability of TOC reveal an annual course with highest values around August and lowest values around January and February. An increase in the p50 and p95 values with increasing lag can be detected up to lags of 3 or 4 days. In some cases there is a further increase with longer lags but there are also some months where longer lags cause lower differences. The relationship between the p100 value and the length of the lag is weaker than for the p50 and the p95 values. The highest values at certain months are induced even by a temporal lag of 6 (p50), 4 (p95) or 7 (p100) days.

The temporal variability in TOC influences the annual course of p50 for the erythemally effective irradiance (Fig. 4b). The highest values can be found in the months before the summer solstice (December), between August and November. A temporal lag of 1 day in TOC produces an uncertainty at the

p50 level between 0.12 UVI (May) and 0.25 UVI (November). The highest p50 values are 0.37 UVI in August from a lag of 6 days and 0.38 UVI in November from a lag of 15 days.

The length of the day weakens the influence of the temporal variability of TOC less and the highest values can still be found before the summer solstice (Fig. 4c). A temporal lag in TOC of 1 day results in a p50 of 0.75 UVIh in June and July and a value of 1.75 UVIh in November. The highest p50 value of all is found in November for a lag of 15 days. During most months, however, the highest p50 value is caused by shorter lags.

The p95 in the erythemally effective irradiance at noon (Fig. 5b) within the first 24 h goes up to 0.4 UVI in April and

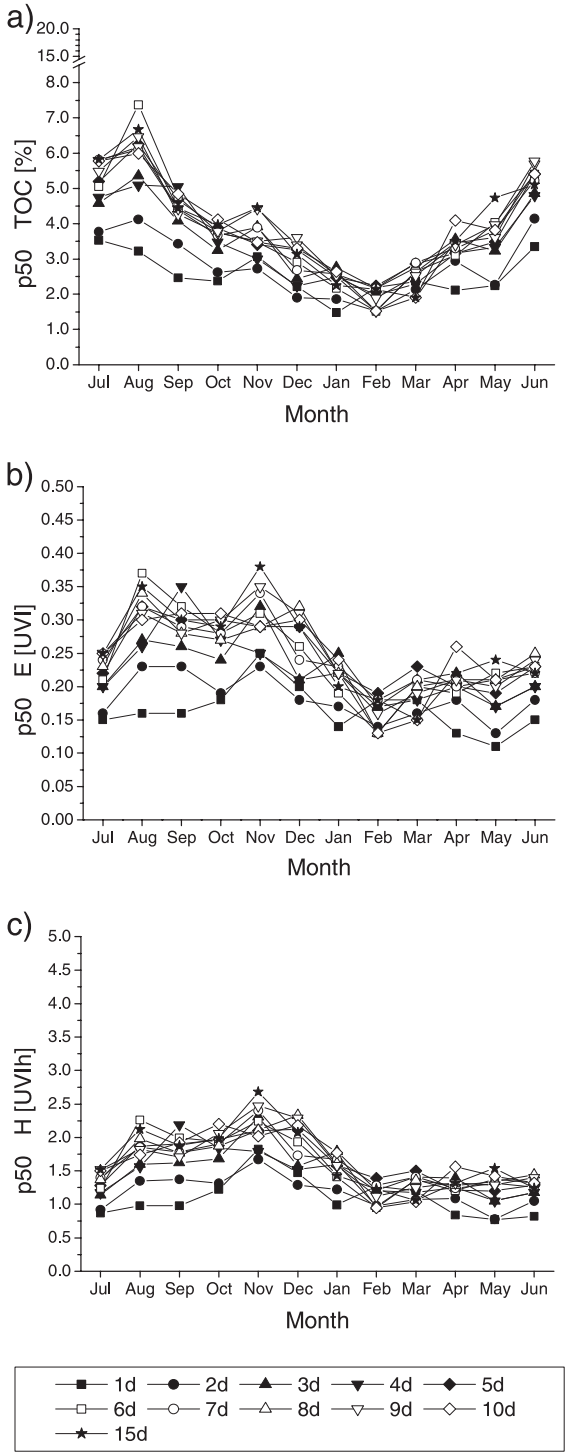


**Figure 4.** Fiftieth percentiles for absolute differences in total ozone p50ΔTOC (a), irradiance at solar noon p50Δ$E$ (b) and daily dose p50Δ$H$ (c) at 30.0°S, 18.1°E (near Springbok, South Africa) under clear skies for certain temporal lags up to 15 days.

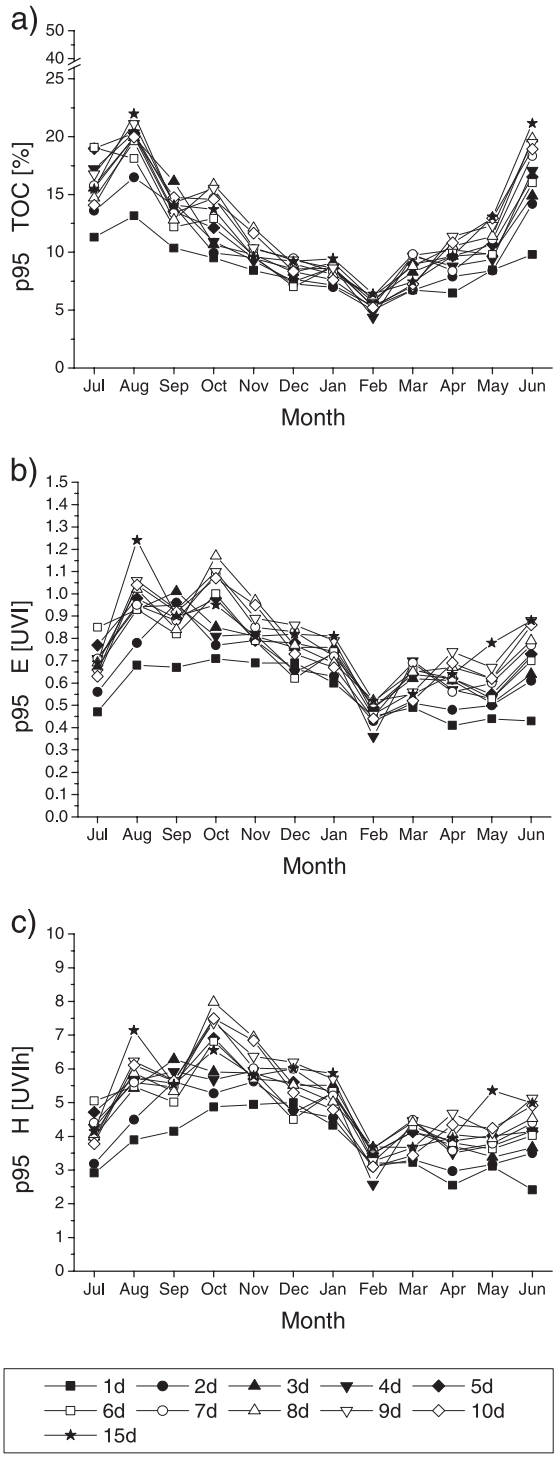


**Figure 5.** Ninety-fifth percentiles for absolute differences in total ozone p95ΔTOC (a), irradiance at solar noon p95Δ$E$ (b) and daily dose p95Δ$H$ (c) at 30.0°S, 18.1°E (near Springbok, South Africa) under clear skies for certain temporal lags up to 15 days.

0.7 UVI in October. For the daily radiant exposure (Fig. 5c) the values are within 2.5 UVIh (June) and 5 UVIh (December). Except for September, the highest p95 values are caused by lags longer than 8 days. The annual pattern of the p95 in irradiance as well as in daily dose peaks obviously before the summer solstice and is therefore much more influenced by the temporal variability of TOC than the p50 values are.

For the erythemally effective irradiance at noon the p100 values (Fig. 6b) do not show a clear annual course and only the shortest lag gives the lowest p100 values. They are between 0.6 and 1.2 UVI with no tendency for a certain season. The highest p100 around 1.8 UVI are seen in October and November and are caused by lags in TOC of 10 or 15 days. However, lags of 3 or 4 days may cause p100 values around 1.6 UVI.

A lag of 1 day causes p100 values between 4.5 UVIh (April) and 8 UVIh (November) as can be seen from Fig. 6c. As in the case of irradiance, temporal lags of 3 days may cause as high p100 values than lags of 10 or 15 days.

### Influence of temporal total ozone variability at the equator

At the equator (Nairobi, Kenya) the TOC changes by less than 100 DU during the year, *i.e.* between 220 and 300 DU. This amplitude is of the order of changes that can occur within a day at 50°N. Day-to-day variations in TOC can be as high as 40 DU. Further, the change in solar zenith angle at noon is within $\pm 23°$. Therefore, irradiance at solar noon varies by only 3 UVI units during the year having one maximum in March and one in September around 10.5 UVI. Accordingly, the daily dose undergoes smooth changes within 45 and 65 UVIh. Visualizations of TOC values, erythemally effective irradiance and daily dose can be found in Schmalwieser *et al.* ([3] 1997–1999) and Schmalwieser *et al.* ([4] 2000–2004).

For the differences in TOC at Nairobi (Fig. 7a) no relationship between the length of the temporal lag and the p50 value can be found. The annual course of p50 does not exhibit an obvious pattern. Values are between 1.0% and 3.25% with a slight tendency to be highest in November.

For the erythemally effective irradiance at noon the p50 values (Fig. 7b) caused by temporal lags in TOC the annual course is very similar to that of TOC as solar height at noon does not change much during the year. Values range from 0.10 UVI to just above 0.25 UVI. The same characteristic is exhibited by the p50 in daily exposure (Fig. 7c). The p50 values are within 0.6 and 1.9 UVIh.

A relationship between the temporal distance and the p95 value is slightly distinguishable for the absolute differences in TOC (Fig. 8a). The lowest values of 3.5% are found for a lag of 2 days in June and September. The highest values of 9.5% are caused by a temporal lag of 7 days in November.

The p95 values for irradiance (Fig. 8b) and daily dose (Fig. 8c) show a smooth annual course. Similar to that at the other locations, the increase in p95 is highest within the first 24 h, but on the contrary there is almost no further increase in the p95 values with increasing temporal lag. For a lag of 1 day the p95 oscillates around a value of 0.55 UVI or 3.5 UVIh. For lags of 10 days the p95 values are of the order of 0.65 UVI or 4 UVIh.

For the differences in TOC at the p100 level (Fig. 9a) a relationship to the temporal distance is slightly noticeable but not for each month of the year.

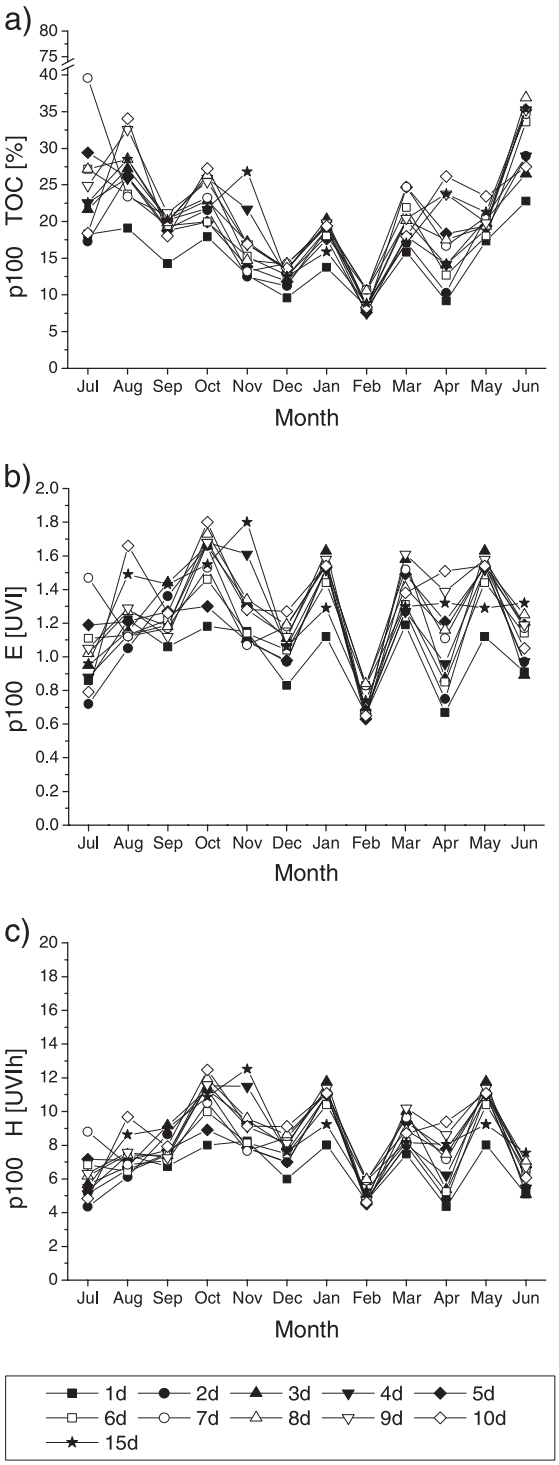


**Figure 6.** Hundredth percentiles for absolute differences in total ozone p100ΔTOC (a), irradiance at solar noon p100Δ*E* (b) and daily dose p100Δ*H* (c) at 30.0°S, 18.1°E (near Springbok, South Africa) under clear skies for certain temporal lags up to 15 days.

For irradiance at noon the p100 (Fig. 9b) is between 0.5 and 1.5 UVI, hence a lag of 1 day may result in a value above 1 UVI (January).

The p100 values for daily dose (Fig. 9c) are all above 2.5 UVIh and a lag of 1 day may result in a value of 9 UVIh (January). For the others the p100 values may go up to 11 UVIh.

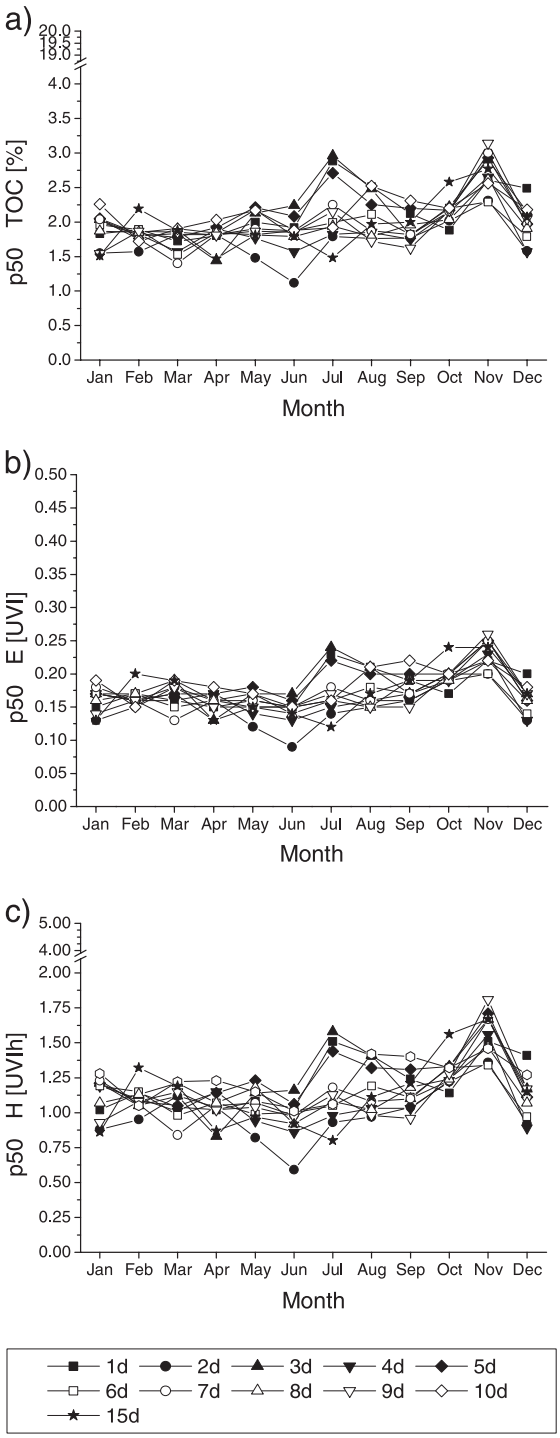


**Figure 7.** Fiftieth percentiles for absolute differences in total ozone p50ΔTOC (a), irradiance at solar noon p50Δ*E* (b) and daily dose p50Δ*H* (c) at 0.0°S, 36.6°E (near Nairobi, Kenya) under clear skies for certain temporal lags up to 15 days.

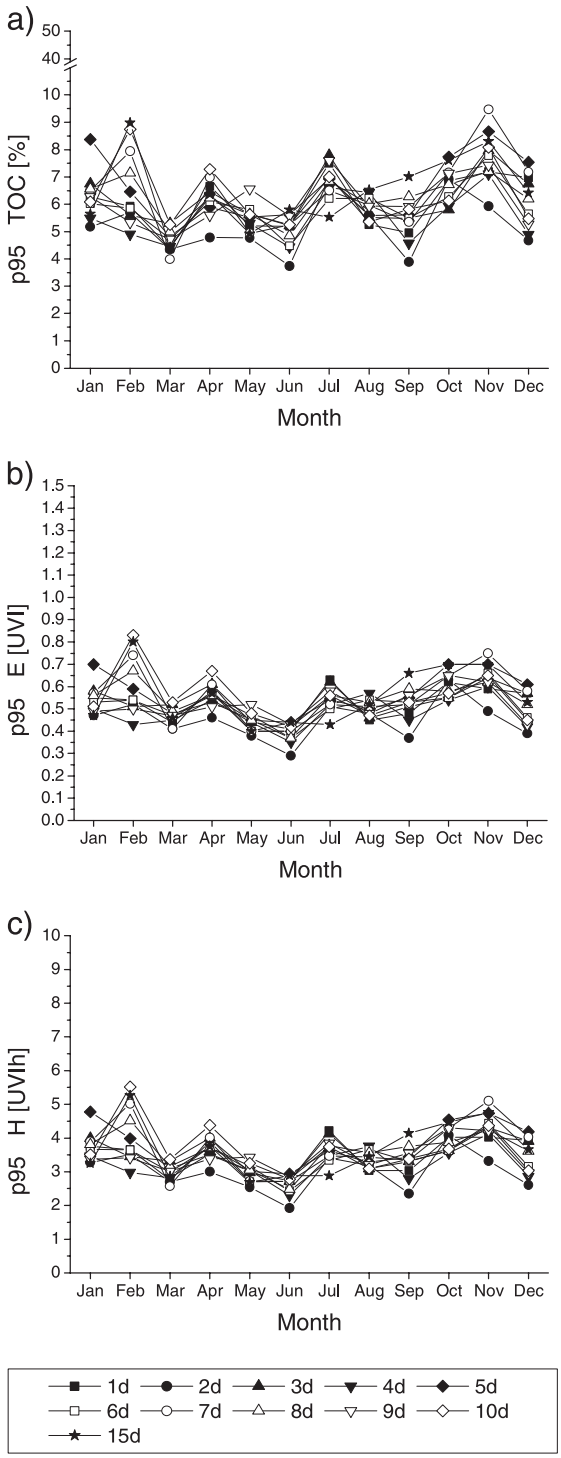


**Figure 8.** Ninety-fifth percentiles for absolute differences in total ozone p95ΔTOC (a), irradiance at solar noon p95Δ*E* (b) and daily dose p95Δ*H* (c) at 0.0°S, 36.6°E (near Nairobi, Kenya) under clear skies for certain temporal lags up to 15 days.

## DISCUSSION

The accuracy of calculations of the erythemally effective UV radiation (*E*) is strongly limited by the temporal and spatial availability and resolution as well as the accuracy of measured TOC values. In this paper we have studied the influence of temporal variability of TOC on the erythemally effective UV radiation. We have quantified the uncertainties which are introduced when using TOC values with a certain temporal delay, the influence of time lags and the effect of assuming temporal persistency of TOC for periods up to 15 days.

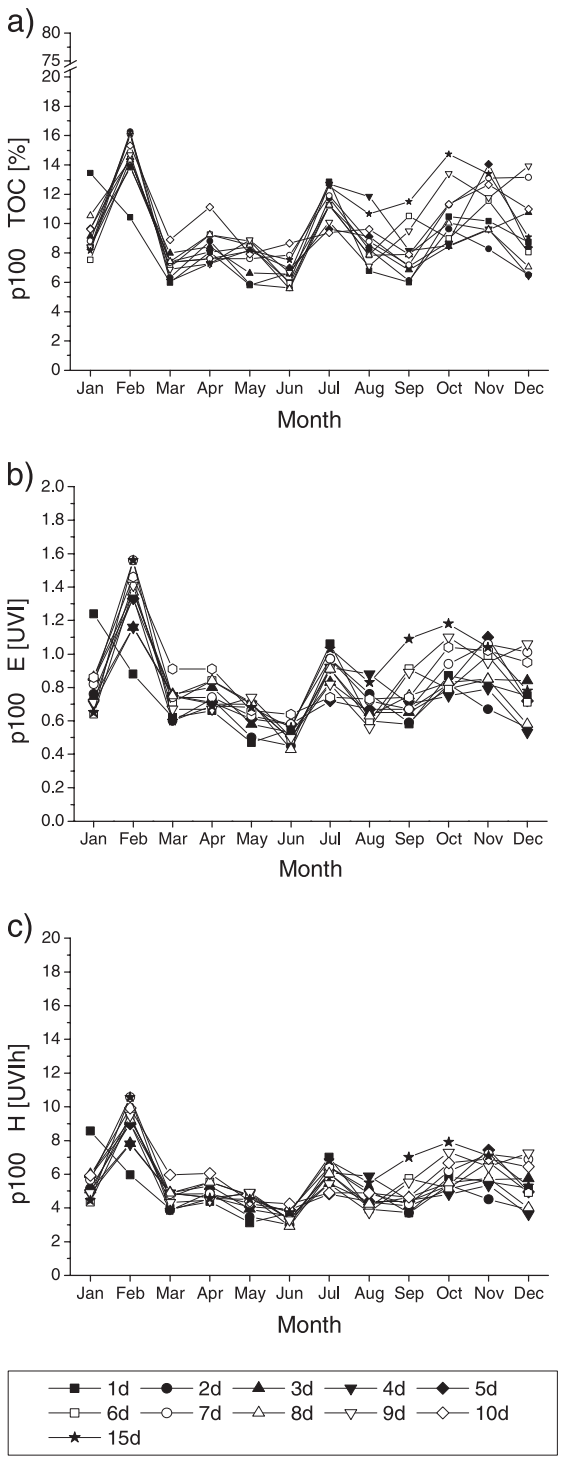


**Figure 9.** Hundredth percentiles for absolute differences in total ozone p100ΔTOC (a), irradiance at solar noon p100Δ$E$ (b) and daily dose p100Δ$H$ (c) at 0.0°S, 36.6°E (near Nairobi, Kenya) under clear skies for certain temporal lags up to 15 days.

As in two related preceding papers, where we estimated the influence of measurement uncertainties and uncertainties due to spatial variability of TOC, we performed this analysis with special emphasis on the UVI and sun protection. When promoting the UVI as integer one can use values of 0.5 and 1 UVI as thresholds for inaccuracy. Accordingly, an equivalent to the minimal erythema dose (MED) for melano-compromised (fair-skinned) persons (Fitzpatrick skin Type I and II) (24,41) and its manifolds can be used as threshold for radiant exposure (daily dose) ($H$). Expressed in units of UVIh, 1 MED is close to 2.5 UVIh and denotes a difference in the sun protection factor of 1.

The study enables to estimate the maximum length of lags/gaps in TOC time series in order to stay below a certain threshold of accuracy for a quantity related to sun protection. For this, we have chosen the p95 of the absolute differences as an indicator of uncertainty as it indicates the error that is reached on 1 day in a month.

At first glance one could expect increasing differences with increasing time lags in TOC or persistency of TOC. Thus, the most surprising outcome of our analysis is that the influence of time lags does not increase much with lag length. At each geolocation and for all percentiles the uncertainty due to temporal variability is relatively highest within the first 24 h. For longer lags the further increase is much lower and even vanishing. The explanation is quite simple; the classical ozone–weather relationship resulting in large day-to-day variations in TOC is the dominating factor for periods up to 15 days.

At 50°N an uncertainty of 0.5 UVI for $E$ and 2.5 UVIh for $H$ is exceeded at least during 6 months a year at the p95 level. For $E$ a lag of 5 days can cause a difference of 1 UVI in June and July; but for time lags of 15 days the maximum remains below 1.2 UVI at the p95 level. For $H$ the uncertainties stay below 10 UVIh. However, a lag of 1 day may result already in 5 UVIh.

At 30°S an uncertainty of at least 0.5 UVI for $E$ and 2.5 UVIh for $H$ has to be taken into account throughout the year by a lag of 1 day only. For $E$ an uncertainty $>1$ UVI only occurs in August and October caused by lags longer than 7 days. For $H$ the highest p95 values reach 7.5 UVIh for an 8-day lag.

At the equator temporal lags in TOC may result in uncertainties for $E$ between 0.3 and 0.8 UVI. A clear relationship with respect to the length of the lag or a seasonal dependence cannot be inferred. The corresponding values for $H$ vary from 2.5 to 5 UVIh.

To sum up, the temporal variability of TOC is highest at 50° and decreases with latitude. A lag or gap of 1 day in TOC measurements may cause an uncertainty of more than 0.5 UVI for $E$ and 2.5 UVIh for $H$ at all locations. Therefore, an uncertainty of 1 UVI for $E$ and 5 UVIh for $H$ should be taken into account. For temporal lags up to 15 days uncertainties stay below 1.5 UVI and 10 UVIh.

If we compare these results with the findings of a previous study on the influence of total ozone measurement uncertainties to the erythemally effective radiation (13), we can infer that at 50°N the impact of a time lag of 1 day is higher than the influence of measurement uncertainties (Fig. 10). The same can be concluded for 30°S (Fig. 11). At the equator, however, the influence of measurement uncertainties can be slightly lower or higher (Fig. 12) than that of a 1-day lag or gap.

In any case, a certain contribution of the observed variability within the first 24 h comes from measurement uncertainties. However, there is a noticeable difference between the annual courses of the p95 values from measurement uncertainties and from time lags. At 50° the difference is most

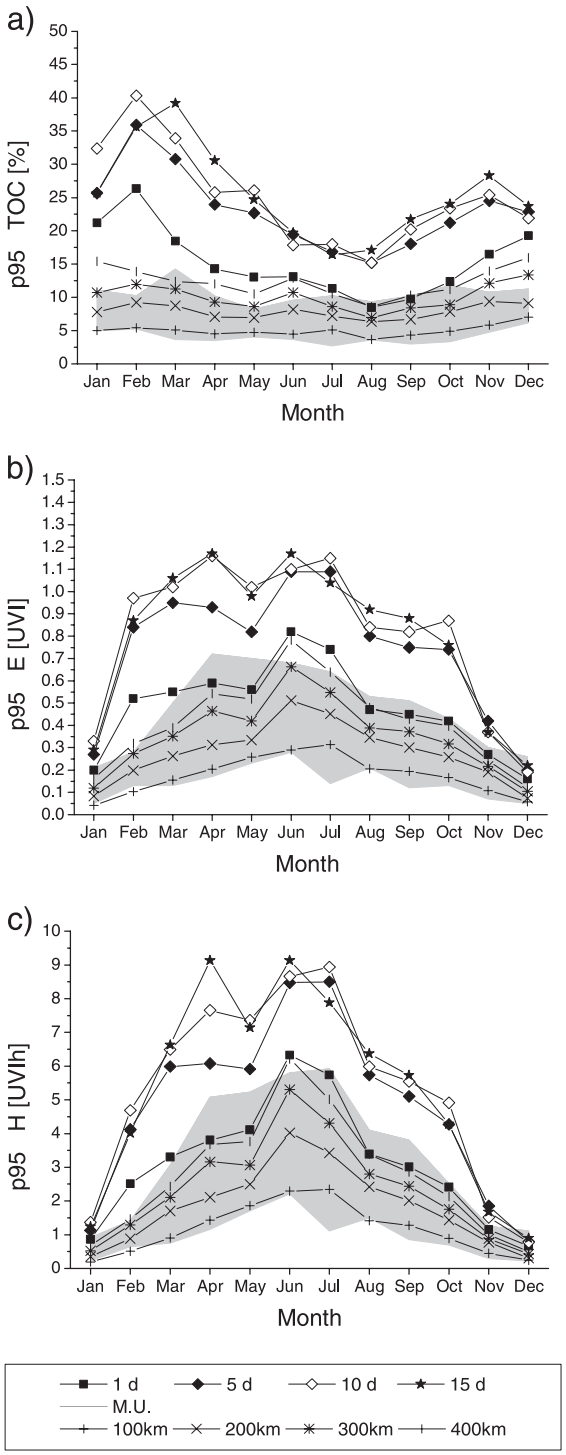


**Figure 10.** Ninety-fifth percentiles for absolute differences in total ozone p95ΔTOC (a), for irradiance at solar noon p95Δ*E* (b) and for daily dose p95Δ*H* (c) at 50.0°N, 15.6°E for certain temporal lags up to 15 days. The gray area indicates the measuring uncertainties of TOC and their influence on the erythemally effective UV radiation after Schmalwieser *et al.* (3). Shown are also the p95 values caused by the spatial (latitudinal) variability in TOC after Schmalwieser *et al.* (4).

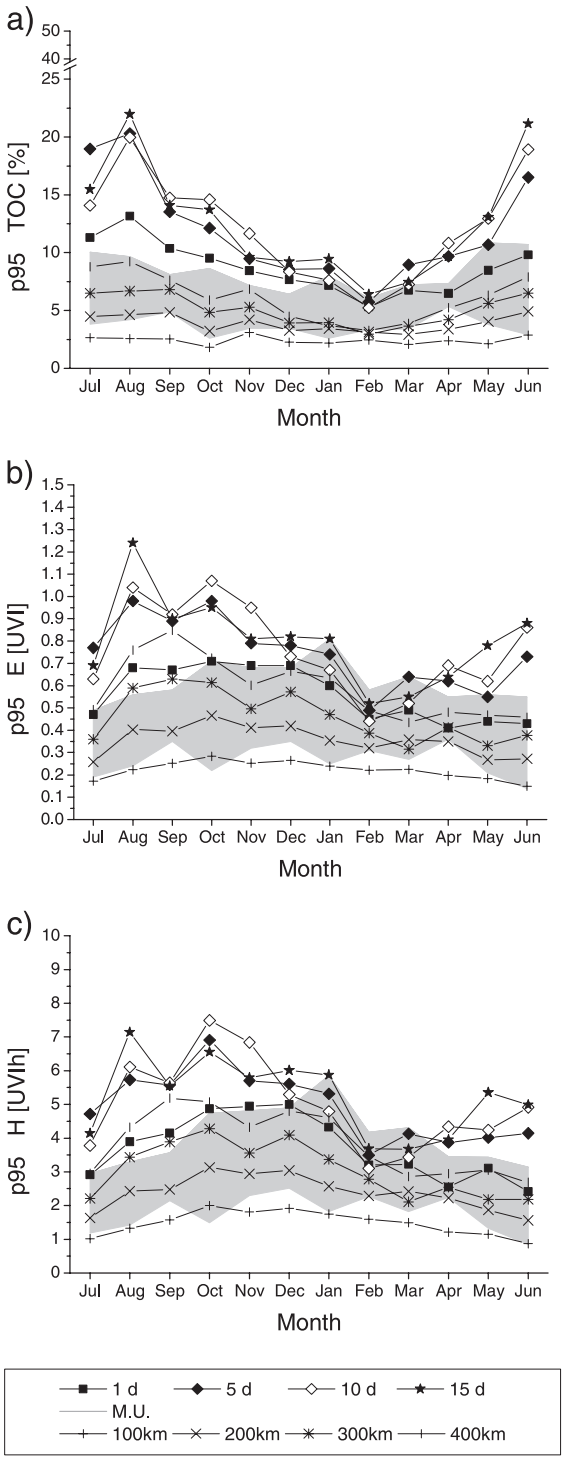


**Figure 11.** Ninety-fifth percentiles for absolute differences in total ozone p95ΔTOC (a), for irradiance at solar noon p95Δ*E* (b) and for daily dose p95Δ*H* (c) at 30.0°S, 18.1°E for certain temporal lags up to 15 days. The gray area indicates the measuring uncertainties of TOC and their influence on the erythemally effective UV radiation after Schmalwieser *et al.* (3). Shown are also the p95 values caused by the spatial (latitudinal) variability in TOC after Schmalwieser *et al.* (4).

obvious during the first months of the year. The p95 values in TOC caused by time lags are two times higher than those in summer. The annual course of measurement uncertainties remains relatively smooth. The difference in the annual courses is similar at 30°S. At the equator one can rather suspect the difference in the annual patterns.

In another preceding paper (4) we examined the influence of spatial variability in TOC values. At 50°N the p95 values due

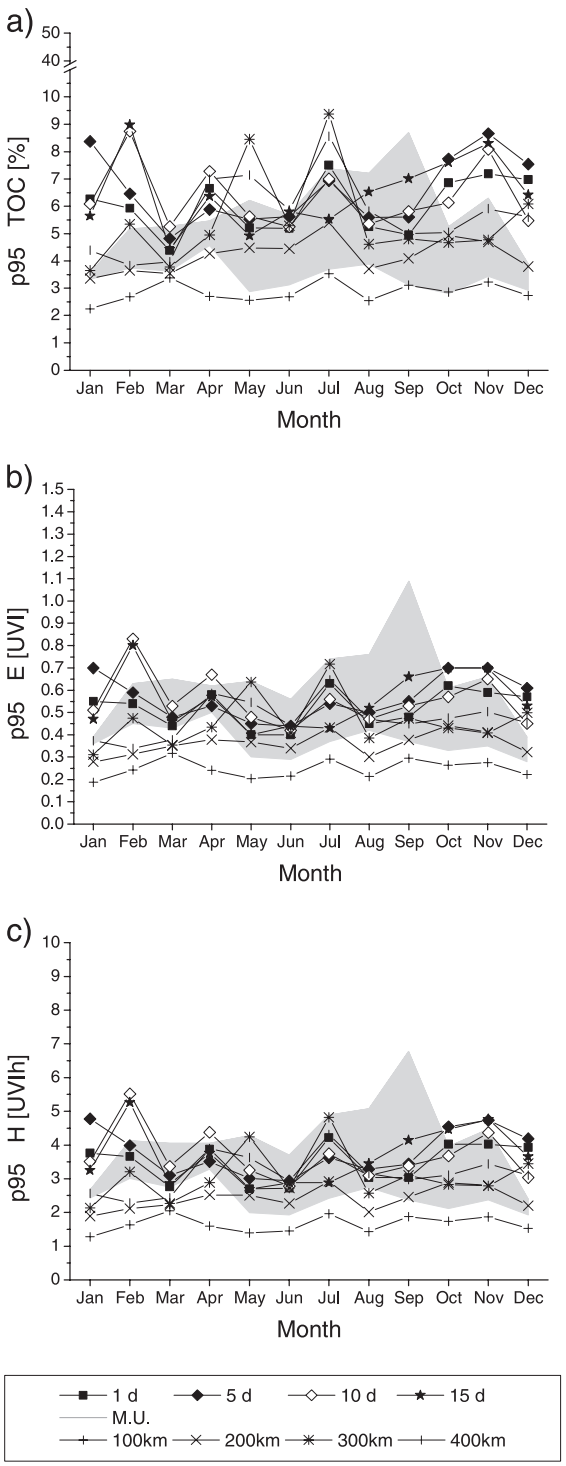


**Figure 12.** Ninety-fifth percentiles for absolute differences in total ozone p95ΔTOC (a), for irradiance at solar noon p95Δ*E* (b) and for daily dose p95Δ*H* (c) at 0.0°S, 36.6° for certain temporal lags up to 15 days. The gray area indicates the measuring uncertainties of TOC and their influence on the erythemally effective UV radiation after Schmalwieser *et al.* (3). Shown are also the p95 values caused by the spatial (latitudinal) variability in TOC after Schmalwieser *et al.* (4).

to a delay in TOC availability of 1 day is comparable with p95 values that are caused by spatial distances (latitude) between 400 and 500 km (Fig. 10). At 30°S a time lag of 1 day is comparable with spatial gaps of 300–400 km (Fig. 11). At the equator a delay of 1 day causes comparable p95 values as a gap of 200–300 km (Fig. 12).

From these sensitivity studies on spatial, temporal and measurement uncertainties it becomes evident that the most critical parameter for the accuracy of calculated UVI and daily dose values is the temporal resolution. Measurement uncertainties have a remarkable influence on the accuracy, too. The influence of a spatial resolution of 100 km (approximately 1° × 1°) is clearly smaller than that of the two others.

In order to minimize uncertainties by temporal total ozone variability for proposed and published UV values for the next day, forecasting of total ozone is crucial. Total ozone forecasts can be derived on a global basis by assimilating total ozone observations from satellites (*e.g.* EPTOMS or the Global Ozone Monitoring Experiment 2 aboard MetOp) into global chemistry transport models (42,43). The daily resulting total ozone analysis can then be used as the initial condition for the forecasting procedure driven by temperature- and windfields (*e.g.* from the European Center for Medium Range Weather Forecast).

## REFERENCES

1. Weihs, P. and A. R. Webb (1996) Comparison of Green and Lowtran radiation schemes with a discrete ordinate method UV model. *Photochem. Photobiol.* **64**, 642–648.
2. Schwander, H., P. Koepke and A. Ruggaber (1997) Uncertainties in modeled UV irradiances due to the limited accuracy and availability of input data. *J. Geophys. Res.* **102**, 9419–9429.
3. Schmalwieser, A. W., G. Schauberger, T. Erbertseder, M. Janouch, G. J. R. Coetzee and P. Weihs (2007a) Sensitivity of erythemally effective UV irradiance and daily exposure to uncertainties in measured total ozone. *Photochem. Photobiol.* **83**, 434–444.
4. Schmalwieser, A. W., T. Erbertseder, G. Schauberger and P. Weihs (2008) Sensitivity of erythemally effective UV irradiance and daily exposure to spatial gaps in total ozone measurements. *Photochem. Photobiol.* (in press).
5. Dobson, G. M. B. and D. N. Harrison (1926) Measurements of the amount of ozone in the earth's atmosphere and its relation to other geophysical conditions. *Proc. R. Soc. Meteorol. Lond. A* **110**, 660–693.
6. Dobson, G. M. B., A. W. Brewer and B. M. Cwilong (1946) Meteorology of the lower stratosphere. *Proc. R. Meteorol. Soc. Lond.* **185**, 144–175.
7. Meetham, A. R. (1937) The correlation of the amount of ozone with other characteristics of the atmosphere. *Quart. J. R. Meteorol. Soc.* **63**, 289–307.
8. Reed, R. J. (1950) The role of vertical motions in ozone-weather relationship. *J. Atmos. Sci.* **7**, 263–267.
9. Schmalwieser, A. W., G. Schauberger, P. Weihs, R. Stubi, M. Janouch, G. J. R. Coetzee and S. Simic (2003) Preprocessing of total ozone content as an input parameter to UV Index forecast calculations. *J. Geophys. Res.* **108**, 4176–4189.
10. Haigh, J. (1996) The impact of solar variability on climate. *Science* **272**, 981–984.
11. Zerefos, C. S., K. Tourpali, B. R. Bojkov, D. S. Balis, B. Rognerud and I. S. A. Isaksen (1997) Solar activity-total column ozone relationships: Observations and model studies with heterogeneous chemistry. *J. Geophys. Res.* **102**, 1561–1569.
12. Labitzke, K., J. Austin, N. Butchart, J. Knight, M. Takahashi, M. Nakamoto, T. Nagashima, J. Haigh and V. Williams (2002) The global signal of the 11-year solar cycle in the stratosphere: Observations and models. *J. Atmos. Solar Terr. Phys.* **64**, 203–210.
13. Zerefos, C. S., A. Bais, I. C. Ziomas and B. R. Bojkov (1992) On the relative importance of Quasi-Biennial Oscillation and El Nino Southern Oscillation in the revised Dobson Total Ozone records. *J. Geophys. Res.* **100**, 10135–10144.

14. Funk, J. P. and G. L. Garnham (1962) Australian ozone observations and a suggested 24-month cycle. *Tellus* **14**, 378–382.
15. Bojkov, R. D. and V. E. Fioletov (1995) Estimating the global ozone characteristics during the last 30 years. *J. Geophys. Res.* **100**, 16537–16551.
16. Kane, R. P., Y. Sahai and N. R. Teixeira (1998) Latitude dependence of the quasi-biennial oscillation and quasi-triennial oscillation characteristics of total ozone measured by TOMS. *J. Geophys. Res.* **103**, 8477–8490.
17. Hasebe, F. (1980) A global analysis of the fluctuation of total ozone. II. Non-stationary annual oscillation, quasi-biennial oscillation and long-term variations in total ozone. *J. Meteorol. Soc. Jpn* **58**, 104–110.
18. Angell, J. K. (1997) Estimated impacts of Agung, El Chichon, and Pinatubo volcanic eruptions on global and regional total ozone after adjustment for the QBO. *Geophys. Res. Lett.* **24**, 647–650.
19. Nikulin, G. N. and R. P. Repinskaya (2001) Modulation of total ozone anomalies in the midlatitude Northern Hemisphere by the arctic oscillation. *Atm. Oceanic Phys.* **37**, 633–643.
20. Schnadt, C. and M. Dameris (2003) Relationship between North Atlantic Oscillation changes and stratospheric ozone recovery in the Northern Hemisphere in a chemistry-climate model. *Geophys. Res. Lett.* **30**(9), 1487, doi: 10.1029/2003GL017006.
21. Appenzeller, C., A. K. Weiss and J. Staehelin (2000) North Atlantic Oscillation modulates total ozone winter trends. *Geophys. Res. Lett.* **27**, 1134–1138.
22. Orsolini, Y. J. and V. Limpasuvan (2001) The North Atlantic Oscillation and the occurrence of ozone miniholes. *Geophys. Res. Lett.* **28**, 4099–4102.
23. International Commission on Non-Ionizing Radiation Protection (1995) *Global Solar UV Index—WHO/WMO/INCIRP Recommendation*. INCIRP publication No. 1/95. ICNIRP, Oberschleissheim, Germany.
24. World Health Organization (2002) *Global Solar UV Index: A Practical User Guide*. WHO, Geneva, Switzerland.
25. Commission Internationale de l'Eclairage (2003) *International Standard Global Solar UV Index*. CIE Standard S 013:2003. CIE, Vienna, Austria.
26. Vanicek, K., Z. Lytinska, T. Frei and A. Schmalwieser (2000) *UV Index for the Public*. Publication of the European Communities, Brussels, Belgium.
27. European Commission (2006) *Measurements and Assessment of Personal Exposure to Incoherent Optical Radiation—Part 3: UV-Radiation Emitted by the Sun*. European Pre-Standard prEN 14255-3:2006. European Commission, Brussels, Belgium.
28. Saxebøl, G. (2000) UVH—A proposal for a practical unit for biological effective dose for ultraviolet radiation exposure. *Radiat. Prot. Dosimetry* **88**, 261.
29. McPeters, R. D., P. K. Bhartia, A. J. Krueger, J. R. Herman, C. G. Wellemeyer, C. J. Seftor, G. Jaross, O. Torres, L. Moy, G. Labow, W. Byerly, S. L. Taylor, T. Swissler and R. P. Cebula (1998) *Earth Probe Total Ozone Mapping Spectrometer (TOMS) Data Products User's Guide*. NASA Reference Publication. NASA, Greenbelt, MD.
30. Wellemeyer, C. G., P. K. Bhartia, S. L. Taylor, W. Qin and C. Ahn (2004) Version 8 Total Ozone Mapping Spectrometer (TOMS) Algorithm. Available at: http://macuv.gsfc.nasa.gov/doc/toms_algor.pdf. Accessed on 4 August 2008.
31. Schauberger, G., A. W. Schmalwieser, F. Rubel, Y. Wang and G. Keck (1997) UV-index: operationelle Prognose der solaren, biologisch-effektiven Ultraviolett-Strahlung in Österreich. *Z. Med. Phys.* **7**, 153–160.
32. Diffey, B. L. (1977) The calculation of the spectral distribution of natural ultraviolet radiation under clear day conditions. *Phys. Med. Biol.* **22**, 309–316.
33. Bener, P. (1972) *Approximate Values of Intensity of Natural Radiation for Different Amounts of Atmospheric Ozone*. Eur. Res. Off., US Army, London, UK.
34. Schmalwieser, A. W., G. Schauberger, M. Januch, M. Nunez, T. Koskela, D. Berger, G. Karamanian, P. Prosek and K. Laska (2002) Global validation of a forecast model for irradiance of the solar, erythemally effective UV radiation. *Opt. Eng.* **40**, 3040–3050.
35. Commission Internationale de l'Eclairage (1987) A reference action spectrum for ultraviolet induced erythema in human skin. *CIE J.* **6**, 17–22.
36. Commission Internationale de l'Eclairage (1998) *Erythema Reference Action Spectrum and Standard Erythema Dose*. CIE S007E-1998. CIE, Vienna, Austria.
37. Koepke, P., A. Bais, D. Balis, M. Buchwitz, H. de Backer, X. de Cabo, P. Eckert, P. Eriksen, D. Gillotay, T. Koskela, B. Lapeta, Z. Litynska, J. Lorente, B. Mayer, A. Renaud, A. Ruggaber, G. Schauberger, G. Seckmeyer, P. Seifert, A. Schmalwieser, H. Schwander, K. Vanicek and M. Weber (1998) Comparison of models used for UV index calculations. *Photochem. Photobiol.* **67**, 657–662.
38. Schmalwieser, A. W. and G. Schauberger (2000) Validation of the Austrian forecast model for solar, biologically-effective ultraviolet radiation-UV index for Vienna. *Austria. J. Geophys. Res.* **105**, 26661–26668.
39. De Backer, H., P. Koepke, A. Bais, X. de Cabo, T. Frei, D. Gillotay, Ch. Haite, A. Heikkilä, A. Kazantzidis, T. Koskela, E. Kyrö, B. Lapeta, J. Lorente, K. Masson, B. Mayer, H. Plets, A. Redondas, A. Renaud, G. Schauberger, A. Schmalwieser, H. Schwander and K. Vanicek (2001) Comparison of measured and modelled UV indices for the assessment of health risks. *Meteor. Appl.* **8**, 267–277.
40. Schmalwieser, A. W., G. Schauberger, M. Janouch, M. Nunez, T. Koskela, D. Berger and G. Karamanian (2005) Global forecast model to predict the daily dose of the solar erythemally effective UV radiation. *Photochem. Photobiol.* **81**, 154–162.
41. Fitzpatrick, T. B., M. A. Pathak, L. C. Harber, M. Seiji and A. Kukita (1974) *Sunlight and Man*. University of Tokyo Press, Tokyo, Japan.
42. Eskes, H., P. van Velthoven, P. Valks and H. Kelder (2003) Assimilation of GOME total ozone satellite observations in a three-dimensional tracer transport model. *Q. J. R. Met. Soc.* **129**, 1663.
43. Baier, F., T. Erbertseder, O. Morgenstern, M. Bittner and G. Brasseur (2005) Assimilation of MIPAS observations using a three-dimensional chemical-transport model. *Q. J. R. Met. Soc*, **131**, 3529–3542.

# 3. Anhang

## 3.1 Curriculum vitae

**Personalien**

| | |
|---|---|
| Titel: | Mag.rer.nat. |
| Vor- Nachname: | Alois Wolfgang Schmalwieser |
| SVNR.: | 3057 27 02 67 |
| Geburtstag: | 27.Februar 1967 |
| Geburtsort: | Grieskirchen, Oberösterreich |
| Staatsbürgerschaft: | Österreich |
| Wohnort: | Himbergerstrasse 6,<br>A-2482 Münchendorf<br>02259/87062<br>alois.schmalwieser@vu-wien.ac.at |
| Familienstand: | Verheiratet seit Sept. 2000 mit Esther S. Schmalwieser (geb. Neves) |
| Kinder: | Susanne Sophie Schmalwieser (16.4.2001),<br>Veronika Theresia Schmalwieser (15.4.2005) |

**Schulbildung**
1973-1977: Volksschule Gaspoltshofen, OÖ
1977-1981: Hauptschule Gaspoltshofen, OÖ
1981-1987: HTBLA I für Hochbau Linz, OÖ

**Präsenzdienst**
1988: Wehrdienst (9 Monate), PzStB3, NTI-Komp., Spratzern/St.Pölten, NÖ

**Studium**
1988: Immatrikulation an der Universität Wien, Studium der Astronomie
2000: Sponsion zum Magister rer.nat., Diplomarbeit: Computersimulation von grundlegenden Eigenschaften nichtradial pulsierender Sterne am Beispiel der Delta-Scuti-Variablen
2004-2008: Doktoratsstudium der Landwirtschaft an der Universität für Bodenkultur

**Berufstätigkeit**
1986-1993: Zeitweise beschäftigt bei der Firma GEA-Happel KG (Klima- und Wärmerückgewinnungsanlagen): Detailkonstruktion und Programmierung technischer Anwendersoftware (Auslegungsprogramme).
1994-1995: Mitarbeit am Whole Earth Telescope Kampagne XCOV13: Datenreduktion (Filtern nicht relevanter Strahlungsinformation) und Frequenzanalyse.
1995-2008: Dienstvertrag am Institut für Medizinische Physik und Biostatistik der Veterinärmedizinischen Universität Wien: Weltweite Prognose der biologischwirksamen solaren UV-Strahlung, Entwicklung eines Sonnenschutz-Nowcast-Systems, Real-Time Datenmonitoring, Strahlungsmessung im UV und optischen Bereich inklusiver

biologischer Bewertung, Kalibrierung verschiedenster Strahlungsmessgeräte, Wasserdesinfektion mit UV-Strahlung,…

**Lehre**

1994-1996: Betreuung von Studierenden im Astronomischen Praktikum (Institut für Astronomie)

2004-dato: Übungen aus Biophysik,
Übungen aus Medizinsicher Physik,
Grundlagen epidemiologische Modelle

**International Aktivitäten**

1998-2002: Teilnehmer an der COST Action 713: "UVB-Forecasting"

2004-dato: Leiter Arbeitsgruppe 3 (Biologisch effektive UV-Strahlung) der COST Action 726: „Long term changes and climatology of UV radiation over Europe"

2007-dato: Reporter Status CIE (Commission Internationale de l'Eclairage): Biologische Wirkungsspektren

## 3.2 Danksagung

Mein Dank gilt A.Univ.-Prof. Dr. Phillip Weihs für die Betreuung meiner Dissertation.

Weiters gilt mein Dank A.Univ.-Prof. Dr. Günther Schauberger (Institut für Medizinische Physik und Biostatistik, Veterinärmedizinische Universität Wien) unter dessen Leitung ich mich in das Gebiet der biologisch wirksamen UV-Strahlung einarbeiten und weiter entwickeln konnte.

Mein Dank geht natürlich auch an die Koautoren der Artikel: Dr. Michal Janouch (Solar and Ozone Observatory Hradec Kralove, Czech Hydrometeorological Institute, Tschechien), Dr. Gerrie J.R. Coetzee (South African Weather Service, Pretoria, Rep. Südafrika), Dr. Rene Stubi (Aerological Station Payerne, MeteoSwiss, Payerne, Schweiz) und Dr. Stana Simic (Inst. für Meteorologie, Universität für Bodenkultur, Wien). Besonderen Dank an Dr. Thilo Erbertseder (Deutsches Fernerkundungsdatenzentrum der DLR, Oberpfaffenhofen, Deutschland) dessen fachliche Kompetenz sehr zur Qualität der Artikel beigetragen hat und der sich auch um die Verbesserung der sprachlichen Qualität der Artikel ebenfalls sehr bemüht hat.

Die Idee zu den, in dieser kumulativen Dissertation verwendeten Artikeln entstand nach einem Gespräch mit Dr. Peter Köpke (Institut für Meteorologie, Universität München, Deutschland) im Umfeld eines Management Commeetee Meeting der COST Action 713. Aus der Zusammenarbeit mit ihm im Rahmen der COST Action 713 und 726 konnte ich viele wertvolle Erfahrungen sammeln.

# 3.3 Bestätigung der Publikation

**Publikation 4**

09-Jun-2008

Dear Mr. Schmalwieser:

It is a pleasure to accept your manuscript entitled "Sensitivity of Erythemally Effective UV Irradiance and Daily Exposure to Temporal Variability in Total Ozone" in its current form for publication in Photochemistry and Photobiology.

Please note that your galley proofs will be sent via email within approximately 5 weeks of this letter. Please add the following address to your "accept" or "white list" to avoid the proofs being marked as spam. The address is: spseproof@sps.co.in

The galley proof serves as your opportunity to review and make corrections to your article during the production process. You will work with the proofreader, who will incorporate any alterations you may have along with any minor changes (spelling, grammar). We are pleased to announced that PHP is an online early publication. Shortly after we receive your corrections the article appears online. They are considered published and cannot be altered prior to print. Corrections after the articles appear online can only be made in the form of a “correction line” added to the text, or a separately published erratum at the discretion of the editor.

Thank you for your fine contribution. On behalf of the Editors of Photochemistry and Photobiology, we look forward to your continued contributions to the Journal.

Sincerely,
Dr. David Sliney
Associate Editor, Photochemistry and Photobiology
david.sliney@att.net